

FOR REFERENCE

NOT TO BE TAKEN FROM THIS ROOM

TEMPORARY EXCAVATIONS IN SOFT CLAY

by

K. S. CEVIK

B.Sc.C.E., B.U., 1984

*Submitted to the Institute for
Graduate Studies in Science and
Engineering in Partial Fulfillment
Of the Requirements for the Degree
Of Master of Science in Civil Engg.*

Bogazici University Library



39001100313959

14

*Boğaziçi University
April, 1986*

TEMPORARY EXCAVATIONS IN SOFT CLAY

by

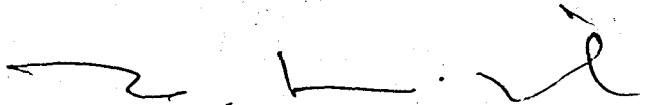
Kamil Şevket Cevik

APPROVED BY:

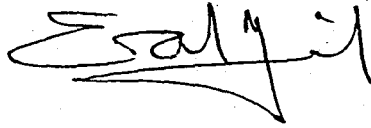
NAME

SIGNATURE

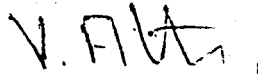
Prof. Turan DURGUNOĞLU
(Thesis Supervisor)



Erol GÜLER



Vural ALTIN



APPROVAL DATE:

6/6/1986

TEMPORARY EXCAVATIONS IN SOFT CLAY

ABSTRACT

The objectives of this thesis were to analyse procedures for finite element analysis of temporary excavations in clayey soils, to review some case studies and to obtain some reliable solutions for practical problems.

The procedures developed involve the use of incremental finite element analyses with non linear, stress-dependent, inelastic soil behavior. The soil stress-strain parameters required for these analyses may be determined from the results of triaxial compression tests. The properties of the interface elements are expressed in terms of a nonlinear, stress-dependent, stress-displacement relationship.

Some classical methods are also reviewed in order to establish the basis for the required study.

Application of the analytical procedures developed to some specific case studies showed that the procedures gave results in good agreement with the results of extensive instrumentation programs on these structures.



YUMUŞAK KİLDE GEÇİCİ KAZILAR

ÖZET

Bu tezin amaçları: sonlu elemanlar metodu ile killi zeminlerdeki geçici kazıların yöntemlerini analiz etmek, daha önceden yapılmış problemleri tekrar gözden geçirmek ve bu türdeki kazılar için güvenilir sonuçlar elde etmektir.

Kullanılan yöntemler, lineer olmayan, gerilmelere bağımlı, elastik olmayan zemin davranışlarını sonlu elemanlar metoduyla inceler. Analizler için gerekli olan zemin değişkenleri üçeşenli basınç testlerinin sonuçlarından elde edilebilir. Ara bağlayıcı elemanların özellikleride lineer olmayan, gerilmelere bağımlı gerilme-deplasman bağlantılarıyla ifade edilmiştir.

Bazı klasik metodlarda, çalışmaların temelini oluşturmak için tekrar gözden geçirilmiştir.

Geliştirilen analitik yöntemlerin bazı belirli geçmiş çalışmalara uygulanması göstermiştir ki, kullanılan yöntemlerle elde edilen sonuçlar bu çalışmalardaki yoğun arazi ölçümleriyle izlenen sonuçlarla tam bir uyum içindedir.

ACKNOWLEDGEMENTS

I am grateful to the following for helping me to prepare this thesis:

OTAK Corp. for their co-operation

Prof. Erol Manas, Head of Computer Engg. Dept., for given me the permission to work in Ege Univ.

Yasemin Ertan and Resat for their help

Special thanks to Prof. Turan Durgunoğlu for all his efforts to help me accomplish this thesis, his understanding and friendship.

TABLE OF CONTENTS

	<u>PAGE</u>
LIST OF FIGURES	iii
LIST OF TABLES	vi
LIST OF SYMBOLS	vii
CHAPTER 1 INTRODUCTION	1
CHAPTER 2 STRESS-STRAIN BEHAVIOR OF SOILS	
2.1 Introduction	3
2.2 Analytical Formulations for the Stress-Strain Behavior of Foundation Soils	3
2.3 Stress-Strain Parameters	8
2.4 Summary	15
CHAPTER 3 LOAD-DEFORMATION BEHAVIOR OF INTERFACE ELEMENTS	1
3.1 Introduction	20
3.2 Hyperbolic Formulation for Shear Stiffness	21
3.3 Summary	27
CHAPTER 4 FINITE ELEMENT METHOD	
4.1 Introduction	28
4.2 Incremental Finite Element Techniques	29
4.3 Incremental Excavation	30
4.4 Incremental Water Pressure Loading	36
4.5 Number of Increments Required to Simulate Excavation	40
4.6 Anchor Installation	44
4.7 Summary	45
CHAPTER 5 CLASSICAL METHODS IN DESIGN OF FLEXIBLE EARTH RETAINING STRUCTURES	
5.1 Introduction	46
5.2 Behavior of Flexible Earth Retaining Structures	46

5.3	Design of Sheet Pile Retaining Walls	47
5.4	Braced Cuts	50
5.5	Tied-Back Cuts	56
5.6	Anchored Bulkheads	65
5.7	Summary	75
CHAPTER 6	CASE HISTORY STUDIES	
6.1	Introduction	76
6.2	Design and Observation of a Tied-Back Wall	76
6.3	Temporary Excavations in Varved Clay	96
6.4	Summary	106
CHAPTER 7	FACTORS AFFECTING TEMPORARY EXCAVATIONS IN CLAY	
7.1	Introduction	109
7.2	Effect of Method of Excavation Simulation	109
7.3	Effect of Soil Modeling Procedure	113
7.4	Problems in Selecting Soil Model Parameters for Design	115
7.5	Problems Introduced by Construction Variables	116
7.6	Summary	118
CHAPTER 8	CONCLUSION	
REFERENCES		122
APPENDIX A	FINITE ELEMENT MESH DESIGN	123

LIST OF FIGURES

<u>FIGURE NO.</u>		<u>PAGE</u>
1	Typical stress-strain curves for cyclic loading of a soil sample	4
2	Typical hyperbolic stress-strain curve and transformed linear hyperbolic plot	5
3	Typical results from one-dimensional consolidation test	12
4	Correction to be applied to tangent modulus to obtain initial tangent modulus	13
5	Definition of incremental coefficient of lateral earth pressure and coefficient of lateral earth pressure	14
6	Incremental coefficient of lateral earth pressure	16
7	Effect of shape of unloading curve on tangent modulus values	17
8	Modes of behavior of interface element	22
9	Hyperbolic representation of the variation of shear stress with relative displacement	25
10	Transformed linear hyperbolic plots for interface tests	26
11	Arbitrary quadrilateral element and boundary stress distribution	32
12	Example of boundary stress reversal for arbitrary slope	35
13	Comparison of results from one-step and three-steps excavation sequences	37
14	Arbitrary quadrilateral element and boundary water pressure distribution	39
15	Example of water pressure loading on pervious soil element	41
16	Values of errors in simulation of small layer excavation for $n:0.3, 0.5, 0.7, 0.9, \text{ and } 1.1$	43
17	Typical patterns of deformation of vertical walls	49

18	Earth pressure on cantilever sheet piling	49b
19	Initial earth pressure for design of cantilever sheet piling entirely on cohesive soil	49b
20	Types of steel sheet piles commonly used for bracing sides of deep excavations	51
21	Cross sections through typical bracing in deep excavations	51
22	Typical bracing in deep wide excavations	53
23	Bearing capacity factors for foundations on clay	53
24	Diagram illustrating method of calculating strut loads from apparent pressure diagram	55
25	Apparent pressure diagrams for calculating loads in struts of braced cuts	55
26	a-Geometry of kicker block for inclined strut b-Bearing capacity factors for kicker block in saturated clay c-Simplified diagram of forces acting on sheeting in raker system	57
27	One of several tieback systems for supporting vertical sides of open cut	59
28	Limits beyond which the anchorages of tiebacks must be located to avoid general failure	59
29	Reported tied-back wall settlements	64
30	Anchored bulkhead-structural schemes	66
31	Placement of the tie rod	66
32	Construction sequences: a-backfilled bulkhead: and b-dredged bulkhead "Heredity" effect	69
33	a-Large-scale model bulkhead deflection b-Bending moment, c-lateral pressures	69
34	Design schemes	74
35	Site plan	78
36	Soil profile	80
37	Triaxial compression test data	81
38	Finite element mesh-design studies	84
39	Computed boundary displacements	85
40	Distribution of lateral soil stress	87
41	Observed boundary deflections	88
42	Tieback load data	90

43	Finite element mesh-Post construction analysis	91
44	Predicted and observed lateral wall movements	93
45	Distribution of lateral soil stress	94
46	Tied-back excavation-Hartford	98
47	Sheeting and bracing-Bowline Point	98
48	Undrained strength versus depth-Hartford	98
49	Finite element mesh for two-tier excavation Hartford	100
50	Predicted and observed displacements for two-tier excavation-Hartford	102
51	Earth pressure design analysis for two-tier excavation-Hartford	102
52	Finite element mesh-Bowline Point	104
53	Geometry and sequence-Bowline Point	105
54	Computed and observed displacements-Bowline Point	105
55	Predicted failure zones-South wall for Bowline Point	107
56	Determining boundary stresses for excavation by interpolation	110
57	Predicted movements using different excavation simulation procedures	112
58	Comparison of observed excavation deflections to values predicted using a nonlinear elastic model and an elasto-plastic model	114
59	Predicted wall deflections, Hartford excavation showing effect of construction changes on prediction	117

LIST OF TABLES

<u>TABLE NO.</u>		<u>PAGE</u>
1	<i>K and n values for clayey soils</i>	19
2	<i>Description of tied-back walls with observed behavior</i>	62
3	<i>Reported methods of calculating prestress loads</i>	62
4	<i>Reported tied-back wall movements</i>	63
5	<i>Imprical values of K_M and K_R</i>	72
6	<i>Factors of safety</i>	72
7	<i>Strut loads at end of construction, case no.3</i>	107
8	<i>Stiffness values for interface element under inactive and active conditions</i>	125

LIST OF SYMBOLS

<u>Symbol</u>	<u>Meaning</u>
a	reciprocal of initial tangent modulus or initial tangent stiffness
$a_1, a_2 \dots$	interpolation coefficients
a_v	rate of change of void ratio with change in pressure
b	reciprocal of ultimate principal stress difference or ultimate shear stress on an interface
c	cohesion
c'	effective cohesion
D	correction factor to determine initial tangent modulus from tangent modulus from consolidation test
e_0	initial void ratio
E	young's modulus
E_i	initial tangent modulus
E_t	tangent modulus
E_{ur}	unloading-reloading modulus
k_n	normal stiffness, interface element
k_s	shear stiffness, interface element
k_{st}	tangent shear stiffness, interface element
k_{si}	initial tangent shear stiffness, interface element
K_j	coefficient of proportionality between interface initial shear stiffness and power function of interface normal stress
K_m	coefficient of proportionality between interface initial shear stiffness and power function of minor principal stress
K_0	coefficient of lateral earth pressure at rest
K_{ur}	coefficient of proportionality between unloading-reloading modulus and power function of minor principal stress
n	exponent for stress-dependent modulus relationship
$O.C.R.$	overconsolidation ratio
P_a	atmospheric pressure
R_f	correlation factor
R_x	horizontal nodal force

R_y	vertical nodal force
x	horizontal coordinate
y	vertical coordinate
α	coefficient of linear thermal expansion
δ	angle of wall friction
Δ_n	relative normal displacement
Δ_s	relative shear displacement
Δu	change in pore pressure
ϵ_x	horizontal strain
ϵ_y	vertical strain
γ	unit weight
γ_w	unit weight of water
$\bar{\gamma}_{xy}$	shearing strain
ν	poisson's ratio
ϕ	angle of internal friction
σ_1	major principal stress
σ_1'	effective major principal stress
σ_3	minor principal stress
σ_3'	effective minor principal stress
$(\sigma_1 - \sigma_3)'_f$	principal stress difference at failure
σ_x	horizontal stress
σ_y	vertical stress
$(\sigma_1 - \sigma_3)'_{ult}$	maximum principal stress difference predicted by hyperbolic stress-strain relationship
τ	shear stress
τ_f	shear stress at failure for interface element
τ_{xy}	shear stress on x-y plane
τ_{ult}	shear stress at failure predicted by hyperbolic load-displacement curve for interface element

CHAPTER 1

INTRODUCTION

Design of a temporary excavation such as braced, tied-back, etc. in an urban area requires a knowledge of the movements expected to be caused by the excavation in surrounding areas. Traditionally, prediction of the movements in such cases has been made purely on the basis of experience. However, the finite element technique gives us a tool which has the capabilities to allow analytical movement predictions to be made. Although some studies which have been reported previously suggest that the finite element method can be used to make suitable predictions of temporary excavation behavior, the state-of-the-art in this area is not well established, and the available literature often is conflicting and confusing as to how such an analysis should be performed and whether or not it will provide reliable predictions.

On the analytical side, it is possible to find a number of different methods used to simulate excavation effects and various constitutive models employed to simulate soil behavior but the question of how much the various solution techniques affect the predicted behavior has not been answered. On the practical side, the engineer will find authorities often pointing out that during temporary excavations, the analytical predictions are subject to distrust because, (1) it is difficult to define soil strength and deformation parameters, and (2) construction sequence, which affects behavior significantly, is often subject to change during construction, after analysis is usually complete.

Thus, on the basis of both analytical and practical considerations, questions can be raised as to how the finite element method should be applied to temporary excavations and how reliable the predicted results are. It is the purpose of this thesis to deal with these questions specifically as addressed to excavations in clays, and to provide a reliable use of the finite element method in analysis of temporary excavations. The results of case history studies have been very useful and experiences learned from them have become a guide line for this investigation.

CHAPTER 2

STRESS-STRAIN BEHAVIOR OF FOUNDATION SOILS

2.1 INTRODUCTION

The stress-strain behavior of any type of soil depends mainly on the factors such as; density, water content, structure, drainage conditions, strain conditions, duration of loading, stress history, confining pressure, stress level.

In many cases laboratory tests on selected soil specimens give good results to simulate the field conditions. When appropriate testing procedures are used the stress-strain relation obtained in the laboratory could represent the actual response of the soil in the field. It is found that the soil behavior over a wide range of stresses is non-linear, inelastic and dependent upon the magnitude of confining pressure. In this chapter, a simplified stress-strain relationship is described which takes into account the nonlinearity, stress-dependency and inelasticity of soil behavior proposed by Clough. (Figure 1)

2.2 ANALYTICAL FORMULATIONS FOR THE STRESS-STRAIN

BEHAVIOR OF FOUNDATION SOILS

Duncan and Chang (1969) have employed two relationships, in their formulation of stress-strain behavior of a soil, the first one is a non-linear, stress dependent behavior during primary loading and the second is the same behavior during unloading and reloading.

Primary loading

This behavior is simulated by Kandner (1963) by the relation:

$$\sigma_1 - \sigma_3 = \frac{\epsilon}{a + b\epsilon} \quad (2.1)$$

in which $\sigma_1 - \sigma_3$ is the principal stress difference: ϵ is the axial strain: and a and b are constants.

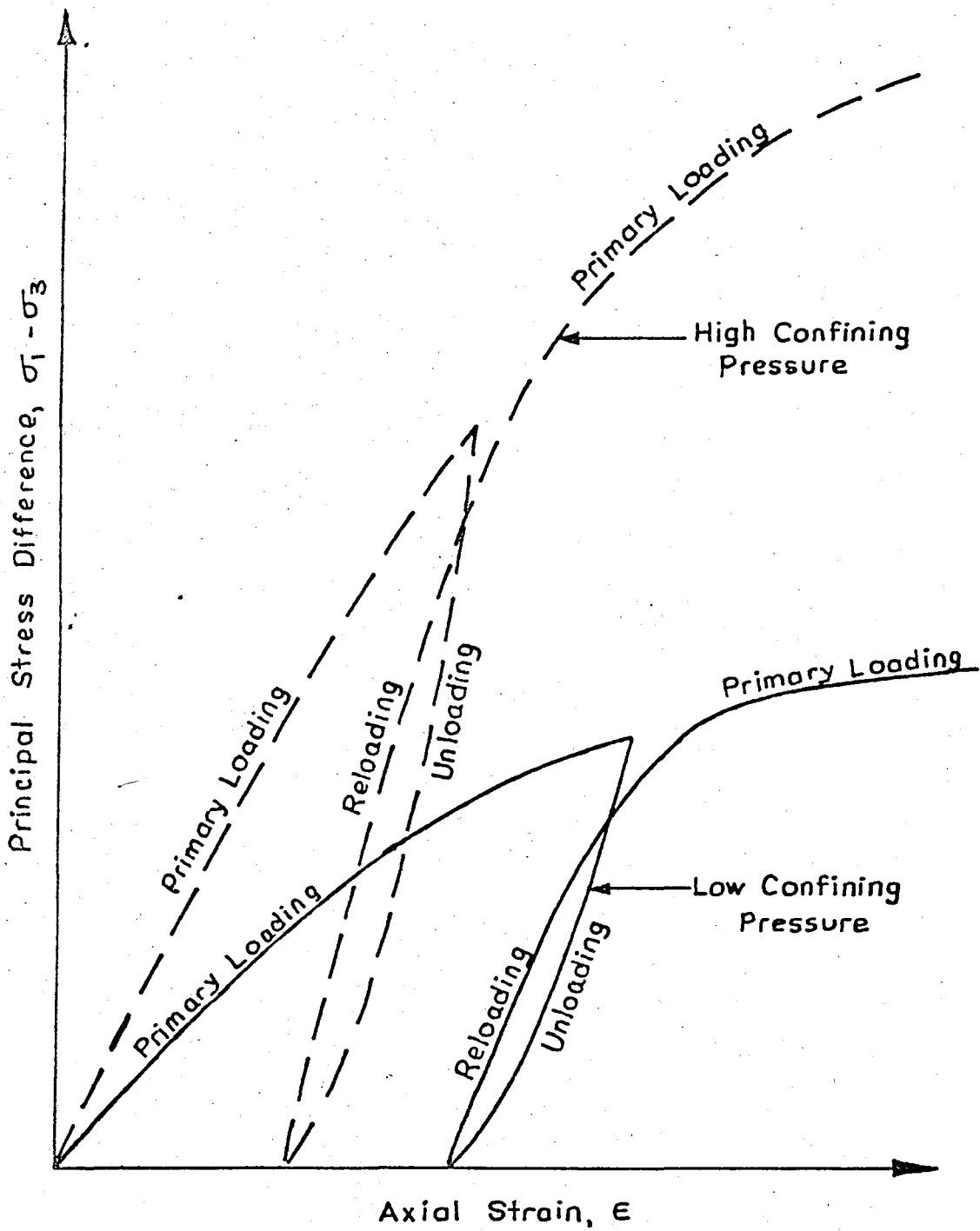
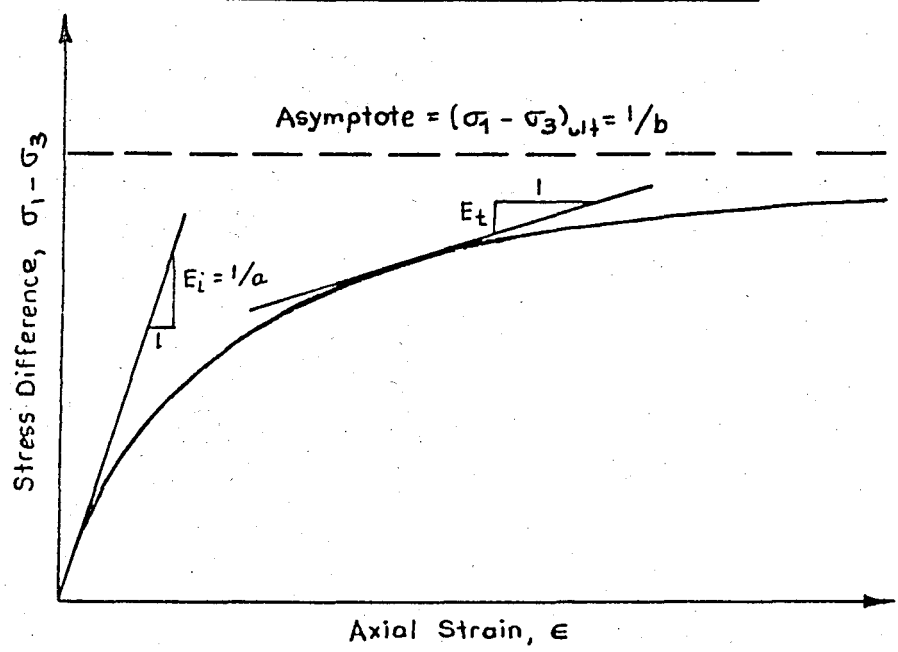


Figure 1. Typical Stress-Strain Curves For Cyclic Loading of a soil Sample (after Clough, 1969).

Typical Hyperbolic Stress-Strain Curve



Transformed Linear Hyperbolic Plot

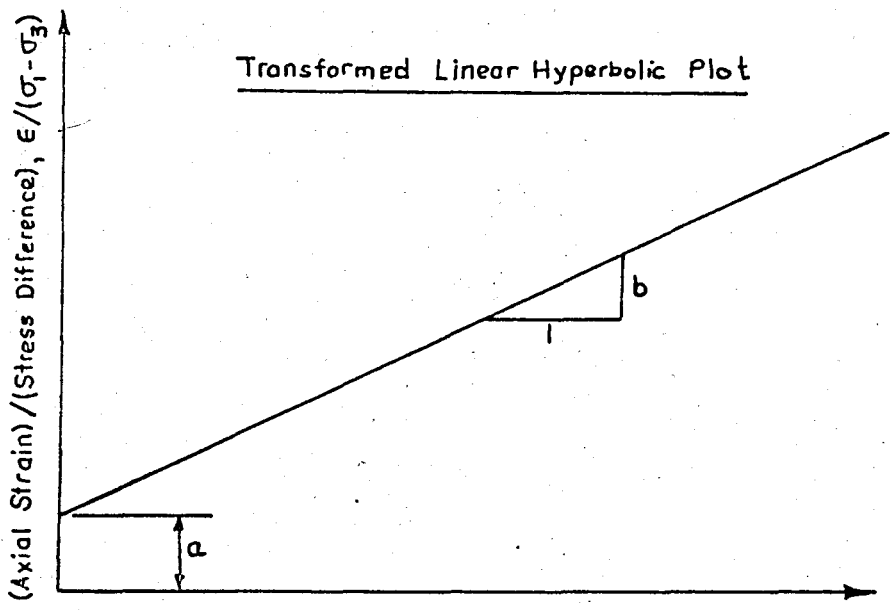


Figure 2. Typical Hyperbolic Stress-Strain Curve and Transformed Linear Hyperbolic Plot (after Kondner, 1969).

Equation (1) may be rearranged in the form:

$$\frac{\epsilon}{\sigma_1 - \sigma_3} = a + b\epsilon \quad (2.2)$$

in which the intercept at $\epsilon \neq 0$, a , is the reciprocal of the initial tangent modulus and the slope, b , is the reciprocal of the asymptote of the hyperbolic curve, $(\sigma_1 - \sigma_3)_{ult}$ (Figure 2).

At this stage, it could be defined an empirically determined "failure ratio," R_f , as:

$$R_f = \frac{(\sigma_1 - \sigma_3)_f}{(\sigma_1 - \sigma_3)_{ult}} \quad (2.3)$$

Kulhawy (1969) has shown that R_f is commonly about 0.85 for many soils.

Duncan and Chang (1969) have differentiated Equation (2.1) and they have obtained an expression for the tangent modulus:

$$\epsilon_t = 1 - \left[\frac{R_f (\sigma_1 - \sigma_3)}{(\sigma_1 - \sigma_3)_f} \right]^2 \cdot \epsilon_i \quad (2.4)$$

in which $(\sigma_1 - \sigma_3) / (\sigma_1 - \sigma_3)_f$ is the stress level which can be defined, in terms of ϕ and c as:

$$\frac{\sigma_1 - \sigma_3}{(\sigma_1 - \sigma_3)_f} = \frac{\sigma_1 - \sigma_3}{\sigma_3 \{ \tan^2(45 + \phi/2) \} + 2c \tan(45 + \phi/2)} \quad (2.5)$$

By substituting the value of ϵ_i as:

$$\epsilon_i = K_m p_a \left(\frac{\sigma_3}{p_a} \right)^n \quad (2.6)$$

and rearranging Equation (2.4), the equation for ϵ_t was obtained as follows:

$$\epsilon_t = \left[1 - \frac{R_f (\sigma_1 - \sigma_3)}{(\sigma_1 - \sigma_3)_f} \right]^2 \cdot K_m p_a \left(\frac{\sigma_3}{p_a} \right)^n \quad (2.7)$$

Unloading

Duncan and Chang (1969) have defined an unloading and reloading modulus, ϵ_{ur} as:

$$E_{ur} = K_{ur} p_a \left(\frac{\sigma_3}{p_a} \right)^n \quad (2.8)$$

where : E_{ur} is the unloading modulus, K_{ur} and n are constants, for a given soil. This form of equation is the same as the one which was obtained for the initial tangent modulus. Holubec (1968) and Chang (1969) have shown that the exponent n is the same for Equation (2.6) and Equation (2.8), but the value of K_{ur} is greater than the value of K_m .

Procedure of Analysis

The stress-strain parameters in the formulation developed by Duncan and Chang (1969) are stress-dependent. This results that the modulus value of each element in a finite element mesh could be different. For a given increment, the modulus value is evaluated for each element in terms of existing stresses. Iteration may be required if the change in stresses within the increment are large relative to the stresses existing within the element prior to execution of the increment.

Duncan and Chang (1969) have developed a criterion to control the use of E_{ur} or E_t , based on the maximum previous value of $|\sigma_1 - \sigma_3|$. For any value of $\sigma_1 - \sigma_3$ less than the maximum previous value, the modulus E_{ur} is applicable, and for any value of $\sigma_1 - \sigma_3$ greater than the maximum previous value E_t is applicable.

Laboratory experiments reported by Duncan and Chang (1969) have shown that the proposed modulus relationships could predict the actual stress-strain behavior of the samples to high degree of accuracy.

Determination of Parameters from Direct Shear and One-Dimensional Consolidation Tests

For long term analyses, the stress-strain behavior of a soil should be determined under drained test conditions. Many clayey soils have a very low permeability.

A fully drained triaxial test on these soils takes a very long time, and it is not feasible. For practical reasons two laboratory tests in which drained conditions are employed

are used to determine soil parameters:

1-Direct Shear Tests: To determine ϕ and c'

2-Consolidation tests: for K_m and n

Direct Shear test. The results of these tests may be employed in the hyperbolic equation of Duncan and Chang (1969), such as these results provide the data to determine the Mohr Coulomb strength parameters, ϕ and c' .

One-Dimensional Compression Tests. The results of a one-dimensional consolidation test are shown in Figure 3. As shown in these figures, this is a plot of void ratio versus logarithm of effective axial pressure. This is mainly a stress-strain plot, because a change in void ratio represents a change in vertical strain, ϵ_v . Also in the consolidation test the lateral stress change at any stage of loading is defined by :

$$\sigma'_x = K_o p' \quad (2.9)$$

The value of K_o has been shown by Brooker and Ireland (1965) to vary with plasticity index and overconsolidation ratio.

2.3 STRESS-STRAIN PARAMETERS

1. Primary Loading.

During primary loading, the overconsolidation ratio is equal to unity, and the value of K_o is constant. For primary loading the confining pressure for a given axial stress is defined by:

$$\sigma'_3 = \sigma'_x = K_o p' = K_o \sigma'_1 \quad (2.10)$$

and the tangent modulus from a consolidation test for an increment of loading has been derived by (Chang (1969)) as,

$$\epsilon_x = \frac{1+e_o}{a_v} \left[1 - \frac{2v^2}{1-v} \right] \quad (2.11)$$

In which e_o is the initial void ratio, and a_v is the rate of change of void ratio with change in pressure, p' . By substituting $K_o = v/(1-v)$ in equation (2.11), it is possible to obtain:

$$\epsilon_x = \frac{1+e_o}{a_v} \cdot \left[1 - \frac{2K_o^2}{(1+K_o)} \right] \quad (2.12)$$

Values of K_o may be determined for any soil from the results of Brooker and Ireland (1965). Equation (2.11) defines a tangent modulus at the stress level corresponding to K_o stress conditions. However, it is also possible to obtain, values of initial tangent modulus from the values of tangent modulus calculated from one - dimensional compression test results. To find E_i from E_t , equation (2.4) is solved for E_i , giving:

$$E_i = E_t / \left[1 - \frac{R_f (\sigma_1 - \sigma_3)^2}{(\sigma_1 - \sigma_3)_f} \right]^2 \quad (2.13)$$

substituting for E_i from equation (2.12)

$$E_i = \frac{1+e_o}{a_v} \left[1 - \frac{2K_o^2}{(1+K_o)} \right] \div \left[1 - \frac{R_f (\sigma_1 - \sigma_3)}{(\sigma_1 - \sigma_3)_f} \right]^2 \quad (2.14)$$

The stress level during primary loading in a consolidation test is determined as follows:

$$\sigma'_3 = K_o \sigma'_1 \quad (2.15)$$

and

$$\sigma_1 - \sigma_3 = \sigma'_3 \left(\frac{1-K_o}{K_o} \right) \quad (2.16)$$

Substituting into the equation for stress level, equation (2.5) for $\sigma_1 - \sigma_3$,

$$\frac{\sigma_1 - \sigma_3}{(\sigma_1 - \sigma_3)_f} = \frac{\sigma'_3 \left(\frac{1-K_o}{K_o} \right)}{\sigma'_3 [\tan^2(45+\phi/2) - 1] + 2c' \tan(45+\phi/2)} \quad (2.17)$$

This expression may be simplified by simply taking c' equal to zero (during primary loading, for many normally consolidated soils this is the case), and the expression becomes :

$$(\sigma_1 - \sigma_3)_f = \frac{1-K_o}{K_o [\tan^2(45+\phi/2) - 1]} \quad (2.18)$$

It can be seen that the stress level in a consolidation test no longer depends upon the magnitude of σ'_3 , provided that c' equals to zero.

The initial tangent modulus can be defined by substituting equation (2.17) for stress level into equation (2.12), the result is:

$$\epsilon_i = \frac{\epsilon_t}{1 - \frac{R_f (1 - K_o)}{K_o \{ \tan^2 (45 + \phi'/2) - 1 \}}} \quad (2.19)$$

If the reciprocal of the denominator of equation (2.19) is denoted by D , this factor represents a correction to be applied to ϵ_t to obtain ϵ_i . Figure 4 shows curves for the correction, D for various values of ϕ' and K_o , assuming that $R_f = 0.85$. For the general case of a stress level of 0.5, the correction becomes:

$$\epsilon_i \cong 3 \epsilon_t \quad (2.20)$$

Thus, for most normally consolidated soils, the initial tangent modulus is about three times as large as the value of tangent modulus determined from a consolidation test.

(Clough has applied equation (2.19) to consolidation test results, and has found that the exponent, n , of the variation of ϵ_i with σ_3 is related to the curvature of the virgin curve of the e - $\log p'$ plot. His findings may be summarized as follows:

- "1. For an e - $\log p'$ curve which is concave downward, typical for silts and sands, n is less than one.
2. For a straight line virgin curve, n is equal to unity. The resulting K_m value under these condition is:

$$K_m = \frac{2.3 c (1 + e_o)}{C_c K_o} \quad (2.21)$$

where C_c is the compression index and C is a constant given by the equation:

$$C = \left[1 - \frac{2 K_o^2}{1 K_o} \right] \cdot \left[1 - \frac{R_f (\sigma_1 - \sigma_3)}{(\sigma_1 - \sigma_3)_f} \right]^2 \quad (2.22)$$

3. For an e - $\log p'$ curve which is concave upward, typical for sensitive clays, n is greater than one."

2. Unloading-Reloading. Clough has shown that determination of an unloading modulus value from the rebound curve of

a consolidation test differs from the procedure used for the primary loading modulus in the following ways:

"1. The incremental change in lateral stress is not related to the incremental change in axial stress by K_o , but by an incremental coefficient of lateral earth pressure, K_o^Δ , which is not equal to K_o^Δ .

2. The values of K_o and K_o^Δ increase with overconsolidation ratio throughout unloading."

The difference between K_o^Δ and K_o during unloading is illustrated in Figure 5. At point A, the slope of the tangent to the unloading curve is K_o^Δ , while the value of K_o is the slope of the secant line to the same point. These values are not equal because the unloading curve does extend on a straight line through the origin. In this case, the change in lateral stress is :

$$\Delta\sigma'_x = K_o^\Delta \Delta p' \quad (2.23)$$

and equation (2.12) can be rewritten as :

$$\epsilon_{ur} = \frac{1+e_o}{a_v} \left[1 - \frac{2(K_o^\Delta)^2}{(1+K_o^\Delta)} \right] \quad (2.24)$$

The values of K_o^Δ may be derived from Figure 6. This is a plot of K_o^Δ versus the plasticity index and it is also a function of the overconsolidation ratio (after Brooker and Ireland).

For an overconsolidation ratio of 16, the values for K_o^Δ and K_o are 1.0 and 1.8 respectively.

Although the value of unloading modulus has been assumed to be independent of stress level, the shape of the rebound curve actually varies somewhat with stress level and as a result the degree to which the modulus value depends on σ'_3 is somewhat exaggerated. (Lough has shown that by examining the behavior of a triaxial specimen in which the stress level is reduced while the confining pressure is held constant, the reason for the exaggeration comes from the method of calculation, as seen in Figure 7. At the upper portion of the

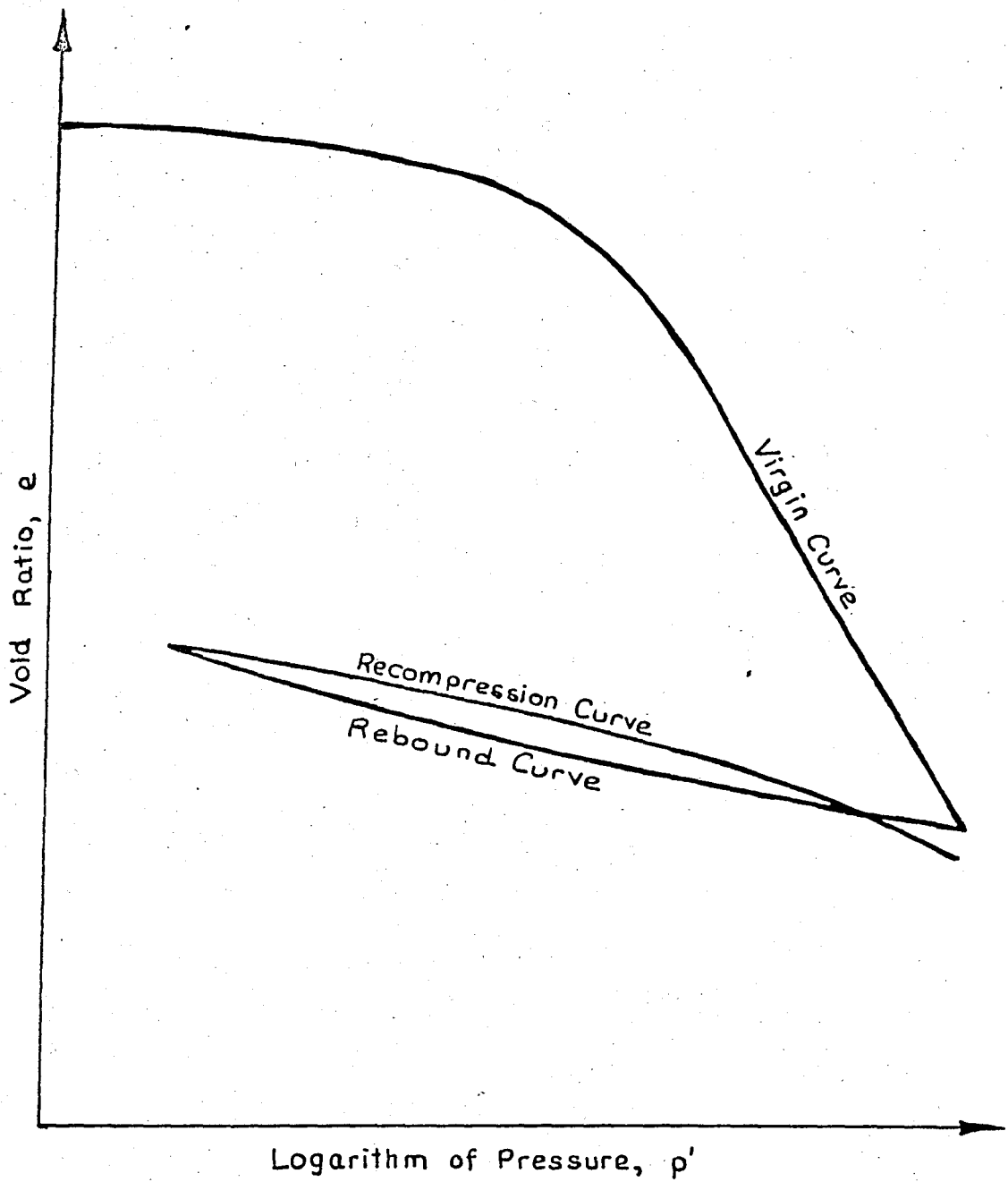


Figure 3. Typical Results From One-Dimensional Consolidation Test

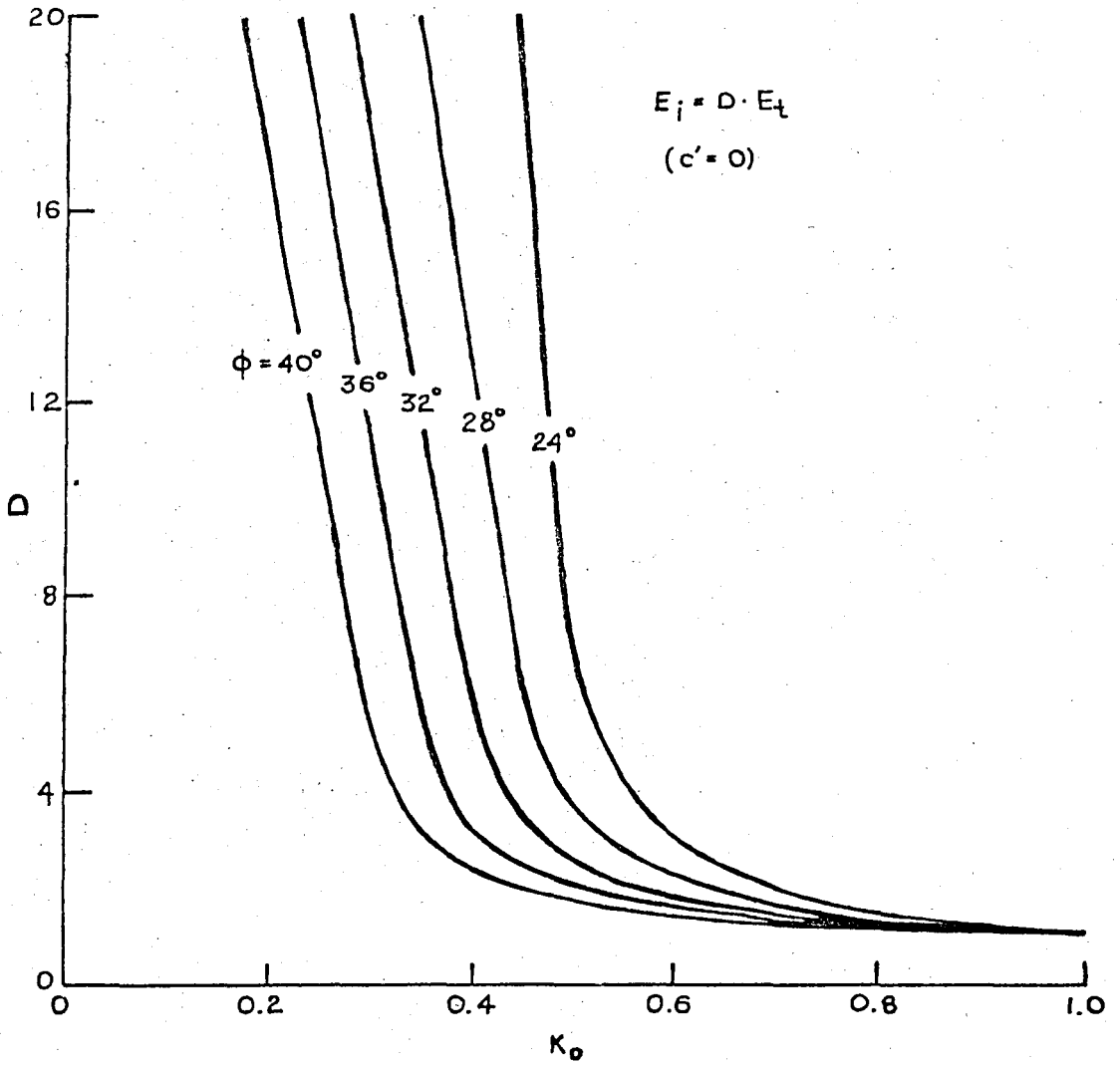


Figure 4. Correction to be Applied to Tangent Modulus to obtain Initial Tangent Modulus (after Clough, 1969).

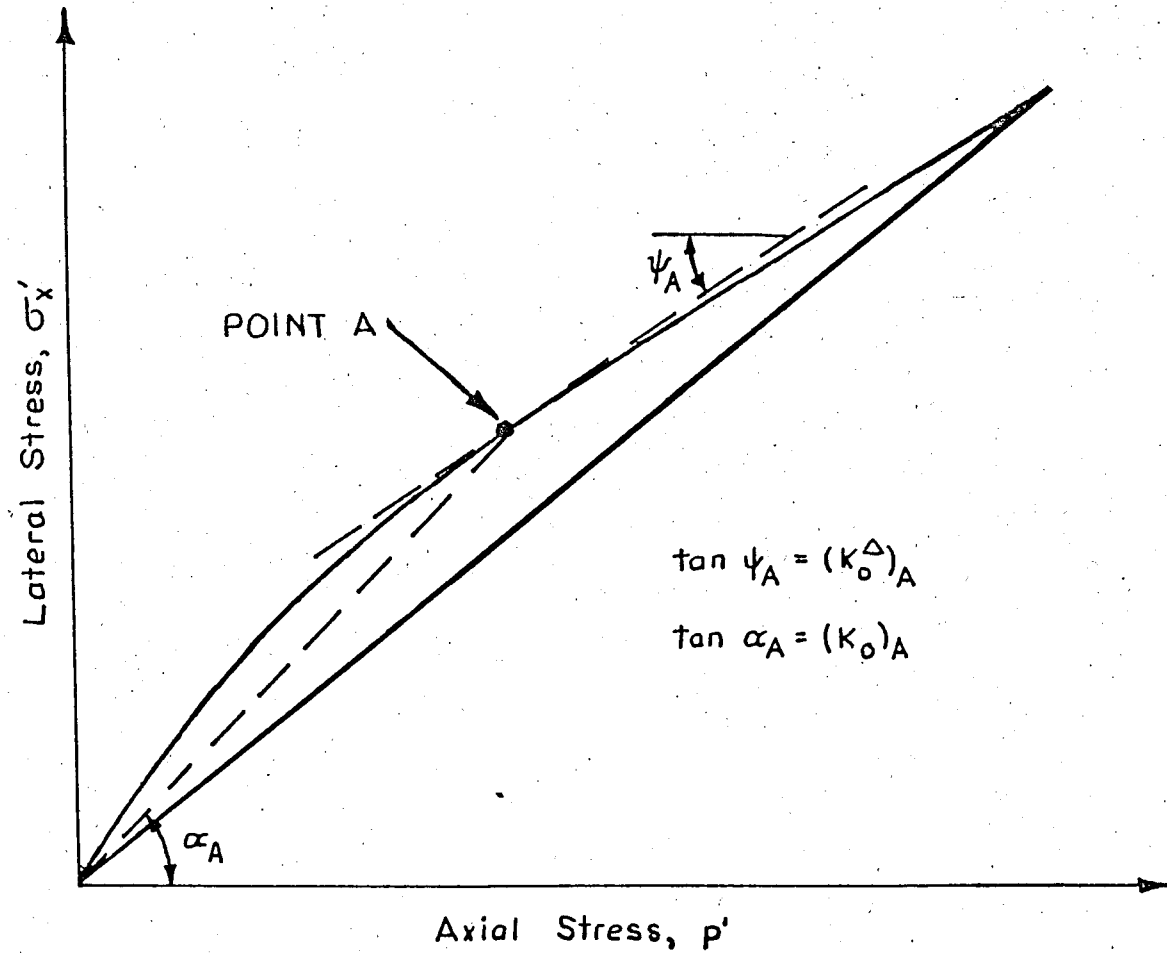


Figure 5. Definition of Incremental Coefficient of Lateral Earth Pressure and Coefficient of Lateral Earth Pressure (after Clough, 1969).

unloading stress-strain curve, the tangent modulus, E_1 , is larger than E_3 . In a consolidation test, the higher value of modulus, similar to E_1 , is determined from the initial portions of the rebound curve, where σ'_3 is the highest, and the lower value of modulus, similar to E_3 , is determined at the other end. Thus, a variation of E_{ur} with σ'_3 determined in this manner will exaggerate the effect of σ'_3 on E_{ur} .

It can be seen from Figure 7, E_2 is the most appropriate value to represent the unloading modulus. Also a modulus value may be determined from the rebound curve of an e - $\log p'$ plot by calculating a tangent modulus value using equation (2.24) at a vertical pressure equal to one-half of the original preconsolidation pressure. The variation of E_{ur} with σ_3 is established by assuming that the exponent, n , is the same for primary loading and unloading. And the relationship between E_{ur} and σ_3 , is completed by solving equation (2.8) for K_{ur} , as follows:

$$K_{ur} = \frac{E_{ur}}{p_a} \div \left(\frac{\sigma_3}{p_a} \right)^n \quad (2.25)$$

Thus, with the unloading modulus value determined by this procedure, the initial tangent modulus determined by equation (2.19), the ϕ' and c' values from the direct shear tests, and the analytical formulation of Duncan and Chang (1969), the stress-strain response of a soil may be established using consolidation and direct shear tests.

2.4 SUMMARY

In this chapter, the stress-strain behavior of soils was reviewed. A simplified stress-strain relationship was described and a general expression for E_x was obtained for primary loading and an unloading-reloading modulus, E_{ur} , was derived for unloading.

The analytical formulation of Duncan and Chang (1969) was explained and stress-strain parameters during primary

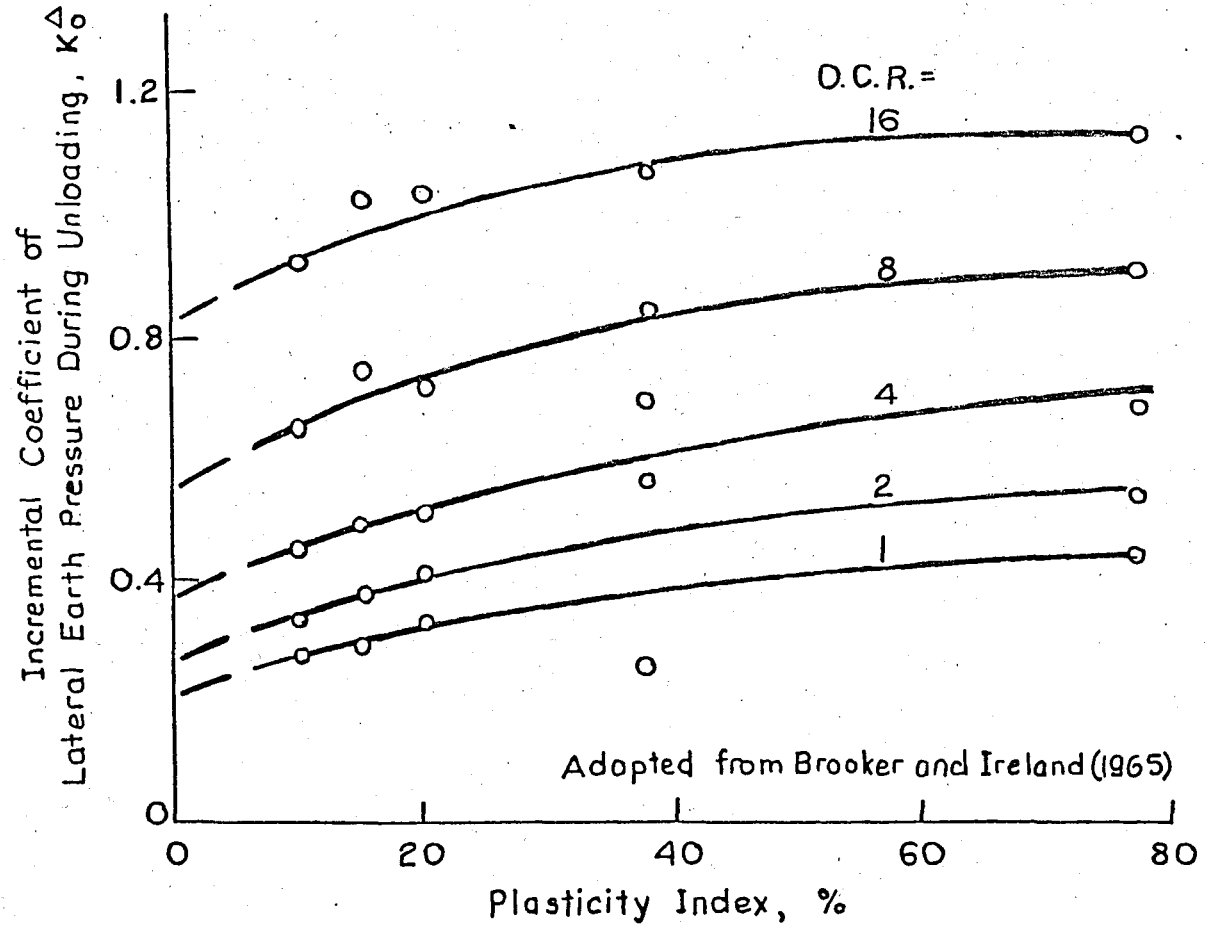


Figure 6. Incremental Coefficient of Lateral Earth Pressure (after Clough, 1969).

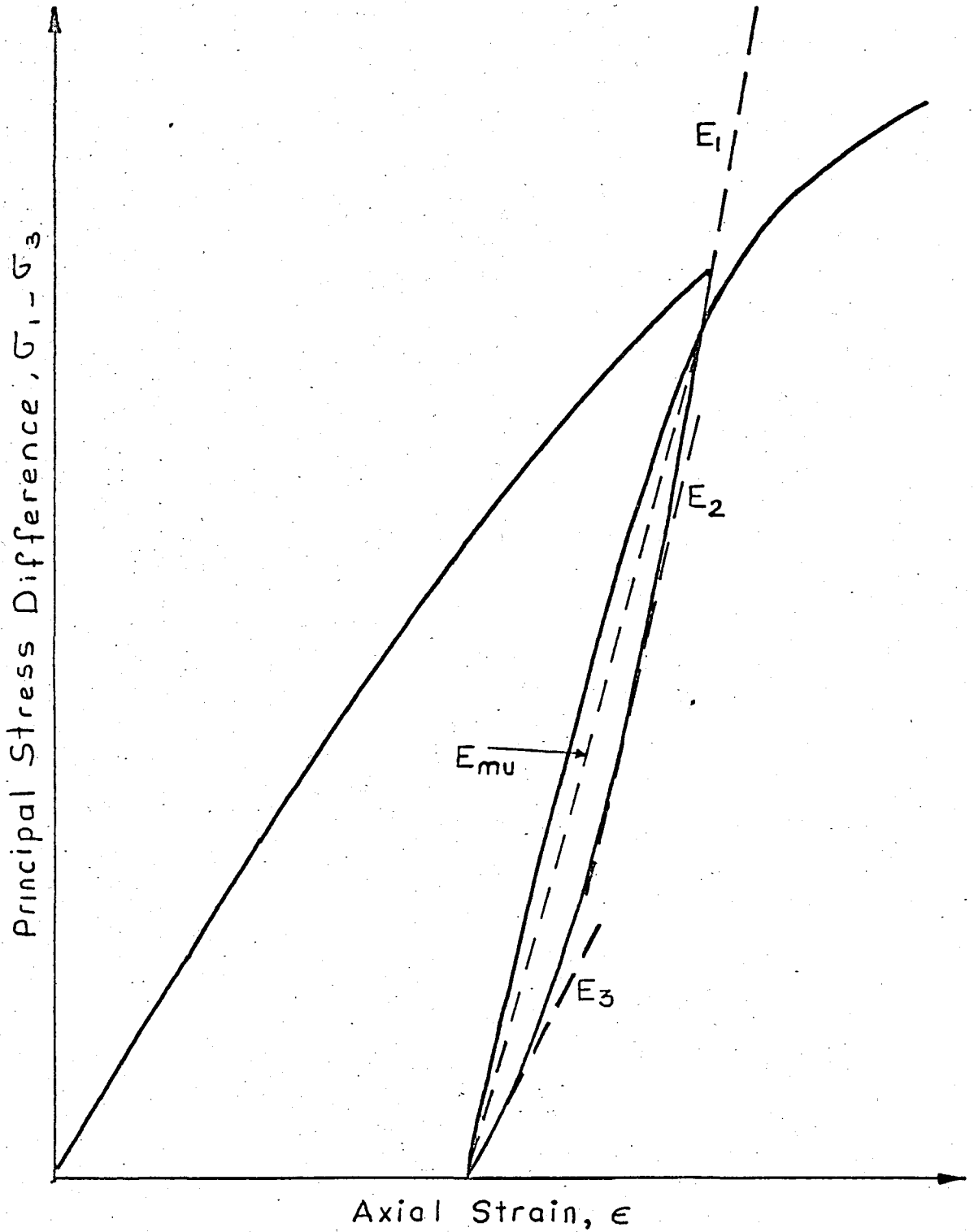


Figure 7. Effect of Shape of Unloading Curve on Tangent Modulus Values (after Clough, 1969).

loading and unloading-reloading were defined. To do this, some classical test procedures were proposed and the necessary parameters were chosen. It has been found that, the initial tangent modulus, the unloading modulus, the ϕ and c values were sufficient to simulate the stress-strain response of a soil.

Table 1.K and n values for clayey soils.

SOIL TYPE	C (tsp)	ϕ	K	N	R_f
Sandy Clay S ~ 60-90	0.74	6	23	0.32	0.61
	0.67	4	75	0.44	0.88
	0.91	18	280	0.60	0.93
	0.66	20	220	0.23	0.90
	1.30	8	140	0.20	0.84
	1.00	13	120	0.09	0.83
	0.80	2	47	0.33	0.82
	1.50	24	950	-0.15	0.90
Lean Clay S ~ 85-90	1.10	2	100	0.27	0.89
	0.99	1	160	0.54	0.97
	1.10	3	130	0.46	0.91
	1.00	16	110	0.94	0.91
	1.40	11	67	0.71	0.77
	1.00	9	37	0.37	0.65

CHAPTER 3

LOAD-DEFORMATION BEHAVIOR OF INTERFACE ELEMENTS

3.1 INTRODUCTION

In order to predict the relative displacements between the structural material and the foundation soils or for any other kinds of material, it was desired to develop techniques to represent a special type of element, so called the interface element.

Conventional finite element analysis require nodal point displacement compatibility and do not allow relative movement between adjacent elements, even where the material types are dissimilar. To allow for relative movements between adjacent two dimensional finite elements, Goodman, et. al., (1968) developed a one-dimensional element capable of undergoing relative displacements which connected the adjacent two-dimensional elements along the entire boundary between the elements. The stiffness of an interface element was first calculated by Goodman, et. al., (1968). It was assumed that both normal and shear displacements vary linearly along the length of the element.

The properties for the interface element consist of a normal stiffness, k_n , and a shear stiffness, k_s , which are related to the corresponding normal stress, σ_n , and shearing stress, T , acting on the element by the equations;

$$k_n \Delta_n = \sigma_n \quad (3.1)$$

$$k_s \Delta_s = T \quad (3.2)$$

where Δ_n is the average relative normal displacement across the element and Δ_s is the average relative shear displacement along the element. The units of σ_n and T are force/length² and the units of k_n and k_s are force/length³.

Figure 8 shows theoretically possible modes of behavior for an interface element. In the case of the combined and compressional mode, the two adjacent elements overlap, this occurs because compressive stresses require compressive

relative displacements across the interface element. For the purpose of analysis, the element is assumed to have zero thickness.

Shearing behavior of the interface element is the most important mode, as shown in Figure 8. The amount of the relative shear displacement and shear stress that develops on an interface element depends upon the shearing stiffness, k_s . With a small shearing stiffness, an interface element should be frictionless. In order to reflect the appropriate stress-displacement characteristics of the interface element, its properties must be properly chosen.

3.2 HYPERBOLIC FORMULATION FOR SHEAR STIFFNESS

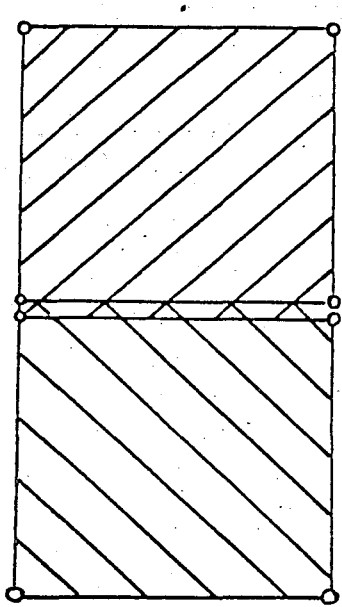
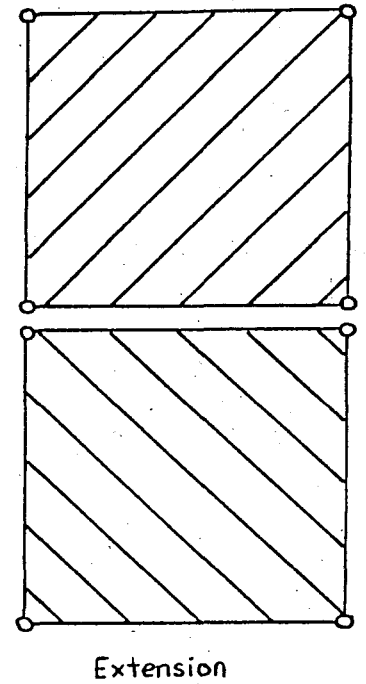
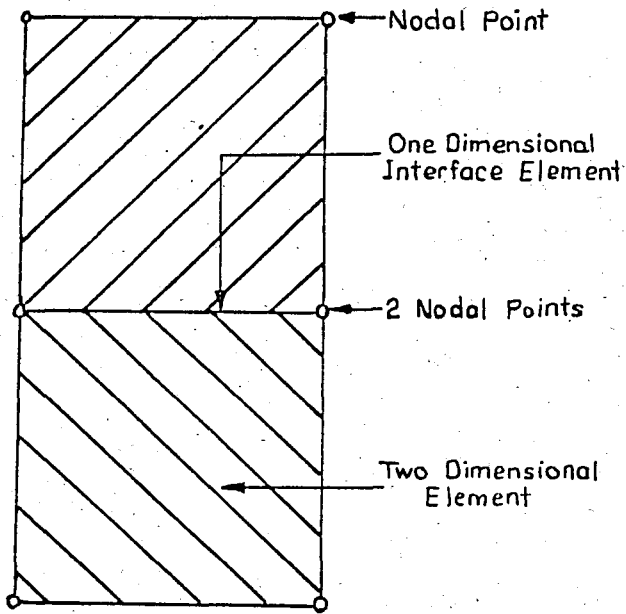
(Clough (1969)) has shown that the relation between the shear stress and relative displacement on the interface element was non-linear in form and dependent upon the normal stress on the interface. The influence of the interface friction in the incremental analysis must be correctly represented. Thus an analytical simulation of this behavior was desirable. The clear resemblance of the shear stress-relative displacement curves to the hyperbolic form for the stress-strain behavior of soils, suggested that a hyperbolic formulation might be appropriate for the interface characteristics as well. Figure 9 shows a typical shear stress-relative displacement curve for an interface element.

The hyperbolic shearing stress versus relative displacement curve is described by the following equation :

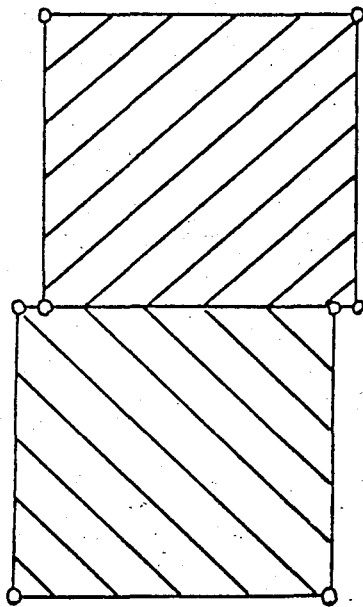
$$\tau = \frac{\Delta_s}{a + b\Delta_s} \quad (3.3)$$

where a and b are constants depending upon the roughness characteristics of the interface and the value of normal stress. Equation (3.3) may be rearranged into a linear form as follows :

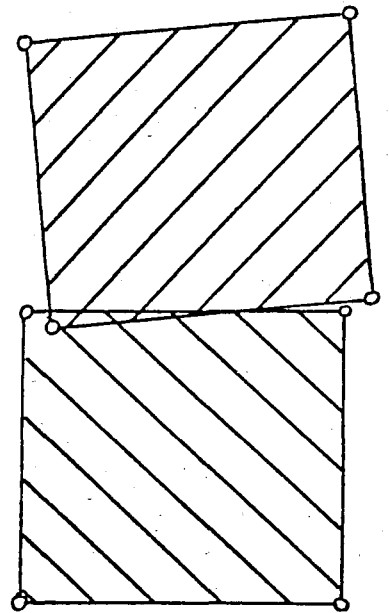
$$\frac{\Delta_s}{\tau} = a + b\Delta_s \quad (3.4)$$



Compression



Shear



Combined

Figure 8. Modes of Behavior of Interface Element (after Duncan and Goodman, 1968).

This is an equation of a straight line. The transformed linear hyperbolic plots for some typical interface tests are shown in Figure 10.

The constant a in equation (3.4) is related to the initial tangent stiffness by equation:

$$a = \frac{1}{k_{si}} \quad (3.5)$$

And by rearranging equation (3.4) into the form:

$$b = \frac{1}{\tau} - \frac{a}{\Delta_s} \quad (3.6)$$

It may be noted that as Δ_s becomes large τ approaches its asymptotic value, τ_{ult} , therefore:

$$b = \frac{1}{\tau_{ult}} \quad (3.7)$$

The relationship expressed by equations (3.5) and (3.7) may be used to determine k_{si} and τ_{ult} from the transformed linear hyperbolic plots in Figure 10, by evaluating a and b .

The tangent shear stiffness at any point on the hyperbolic curve may be found from equation (3.4) by determining the slope:

$$k_{st} = \frac{\partial \tau}{\partial \Delta_s} = \frac{a}{(a + b \Delta_s)^2} \quad (3.8)$$

By rearranging equation (3.3), an expression for Δ_s may be obtained:

$$\Delta_s = \frac{a \tau}{1 - b \tau} \quad (3.9)$$

Substituting the expressions for a and b from equations (3.5) and (3.7):

$$\Delta_s = \frac{(\tau_{ult}) \tau}{k_{si} (\tau_{ult} - \tau)} \quad (3.10)$$

Substituting the expressions for a , b and Δ_s from equations (3.5), (3.7) and (3.10), respectively, into equation (3.8)

For the tangent shear stiffness and simplifying, the following equation may be obtained:

$$k_{st} = k_{si} \left(1 - \frac{\tau}{\tau_{ult}} \right)^2 \quad (3.11)$$

The ratio between, the asymptotic value of shear stress at failure, τ_{ult} , and the actual shear stress at failure is defined as R_f . Its range varies from 0.84 to 0.95 with an average value of 0.88. Then, equation (3.11) could be altered as follows:

$$k_{st} = k_{si} \left(1 - \frac{R_f \tau}{\tau_f} \right)^2 \quad (3.12)$$

τ_f is a function of the normal stress on the interface, σ_n , according to the following relationship:

$$\tau_f = \sigma_n \tan \delta \quad (3.13)$$

Substituting this expression for τ_f in equation (3.12) k_{st} may be expressed as follows:

$$k_{st} = k_{si} \left(1 - \frac{R_f \tau}{\sigma_n \tan \delta} \right)^2 \quad (3.14)$$

It is possible to obtain a relationship between k_{si} and n by simply plotting the values of k_{si} versus σ_n on log-log scale. The resulting equation is:

$$k_{si} = K_j \gamma_w \left(\frac{\sigma_n}{p_a} \right)^n \quad (3.15)$$

In which K_j and n are experimentally determined constants and γ_w is the unit weight of water.

By substituting equation (3.15) for k_{si} into equation (3.14) for k_{st} , the following expression could be obtained:

$$k_{st} = K_j \gamma_w \left(\frac{\sigma_n}{p_a} \right)^n \left(1 - \frac{R_f \tau}{\sigma_n \tan \delta} \right)^2 \quad (3.16)$$

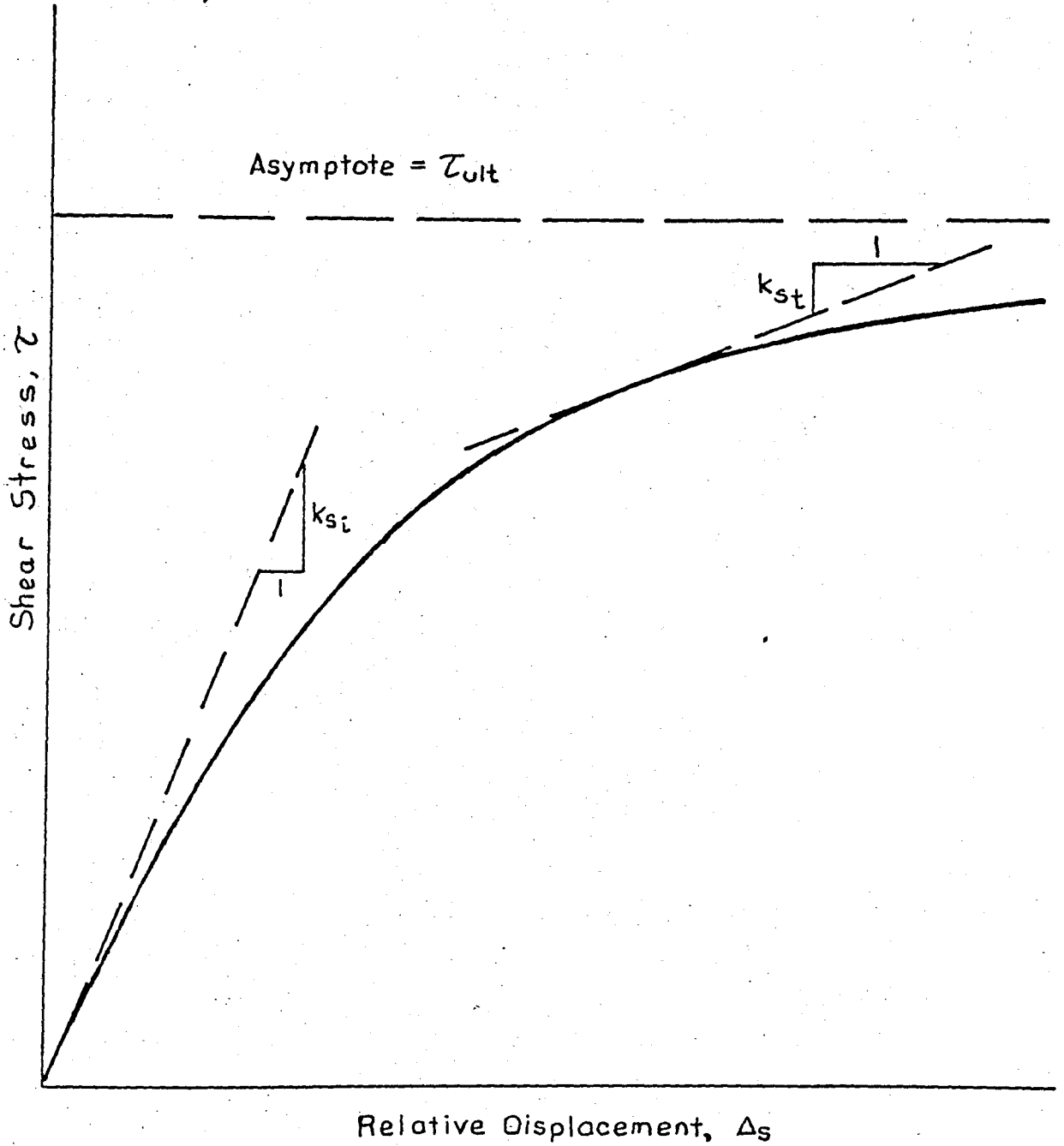


Figure 9. Hyperbolic Representation of the Variation of Shear Stress with Relative Displacement (after Clough, 1969).

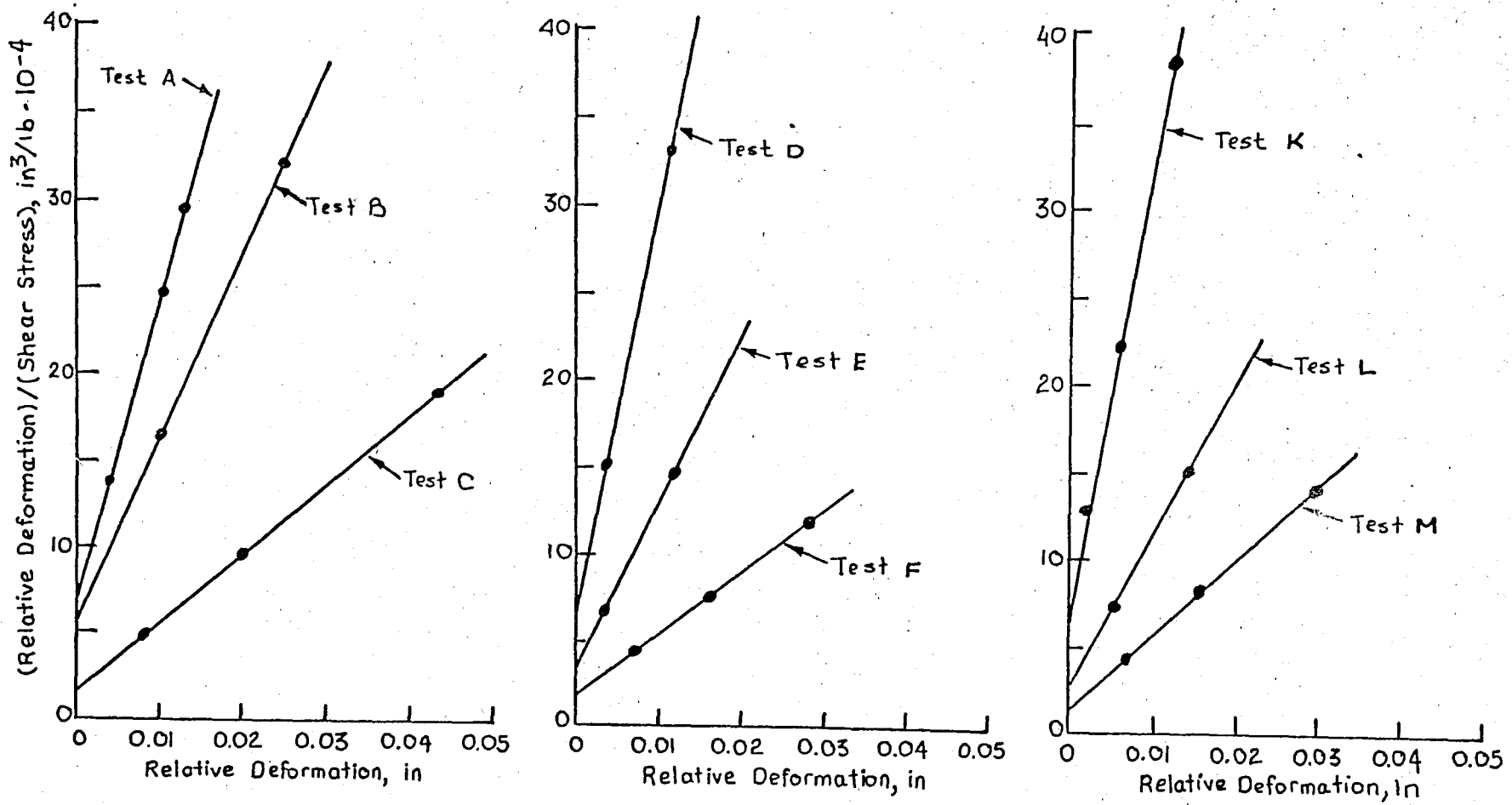


Figure 10. Transformed Linear Hyperbolic Plots For Interface Tests (after Clough, 1969).

Equation (3.16) defines a simplified, practical relationship which describes the nonlinear, stress dependent, stress-displacement behavior of an interface element between soil and concrete. Total stress notation has been used throughout in this derivation, but if the interface is under water, then σ'_n should replace σ_n in equation (3.16).

The interface element formulation of Goodman, et. al., (1968) was incorporated into the incremental finite element program with the hyperbolic shear stress-relative displacement relationship developed by Clough (1969). Because the shear stiffness must be evaluated for each increment at the same time modulus values for the two-dimensional elements were calculated.

3.3 SUMMARY

In this chapter, the load-deformation behavior of interface elements was analyzed. The properties for the interface element were found to be defined by a normal stiffness, k_n and a shear stiffness, k_s .

It has been found that the shear stress and relative displacement on an interface element was nonlinear in form and dependent upon the normal stress on the interface (after Clough, 1969). A general expression was derived to define the stress-displacement behavior of an interface element.

CHAPTER 4

FINITE ELEMENT METHOD

4.1 INTRODUCTION

In order to solve a soil structure interaction problem a method must be capable of simulating:

1. The behavior of a system containing structural elements
2. Interaction between the structure and the soil
3. Complex structure geometry
4. Gravity loading, water pressure loading, temperature loading
5. Anchor and strut loads
6. Non-linear, stress-dependent stress-strain behavior of the soils
7. Arbitrary initial stress conditions in the soils.

If adopted properly, the finite element method can accommodate all these complexities.

The basis for the finite element method has been described by Clough (1960). In the method, a continuum is represented as an assemblage of finite elements assumed to be connected only at the nodal points located along the boundary of the elements. The nodal point displacements $\{\delta\}$ are the basic unknowns of the system and are related to the prescribed nodal forces $\{P\}$ by a general stiffness matrix $[K]$. This relationship is expressed as :

$$[K] \{\delta\} = \{P\} \quad (4.1)$$

The general stiffness matrix $[K]$ is an assemblage of the stiffness of the individual finite elements combined by a process known as a direct stiffness technique. Solving for the unknown displacements requires solution of the set of simultaneous equations described by equation (4.1). This operation necessitates the use of a high speed computer because realistic

systems typically involve several hundred degrees of freedom.

Equilibrium in the finite element method is assured only for the nodal point forces. Local equilibrium conditions along the boundaries of the element may not be satisfied. Generally across element boundaries, only displacement compatibility is assured, and discontinuities in stress and strain will occur.

Element stiffnesses are derived on the basis of an assumed displacement pattern within an element. For two-dimensional plane elements, Clough (1960) derived an element stiffness using a linear displacement function. The assumed displacement patterns control the number of nodes needed for an element because the number of nodes must be consistent with the degree of the assumed displacement pattern, and must be sufficient to insure displacements compatibility between elements.

Most commonly, triangular or rectangular elements are used. Wilson (1963) has shown that the most satisfactory results for general application of the finite element method are obtained by use of quadrilateral elements composed of an assemblage of triangular elements. The use of these elements are described in Appendix A.

Because nodes of adjacent elements are constrained to move together, no relative displacements may develop between elements if they are composed of different materials. Goodman et. al., (1968) developed an interface element which forms a continuous connection along the entire length of the boundary between any two adjacent two-dimensional elements. The amount of relative displacement allowed by the interface element is a function of the stiffnesses assigned in the normal and tangential directions and the joint stresses.

Clough (1960) introduced the application of the finite element method to continuous structures. After his attempt by extending the method, a variety of complex structural, soil and rock mechanics problems have been treated, many of which are described by Zienkiewicz and Cheung (1967).

4.2 INCREMENTAL FINITE ELEMENT TECHNIQUES

The actual construction operations could be simulated in

one or more analytical steps involving changes in loading and geometry by performing an incremental finite element method.

The initial conditions, prior to the beginning of excavation, were defined by an initial state of stress in each element where the vertical effective stresses, σ'_y , were equal to the effective overburden stresses and the horizontal effective stresses, σ'_x , were defined as :

$$\sigma'_x = K_0 \sigma'_y \quad (4.2)$$

where K_0 is the coefficient of lateral earth pressure. The initial displacements and shear stresses on horizontal and vertical planes were assumed to be zero, and the stresses, strains and displacements calculated for each element during every incremental loading step were cumulatively superimposed upon the initial stresses, strains and displacements.

To perform these analyses, all types of operations involved in the actual construction must be simulated analytically. At this stage because loading in finite element analyses can only be represented by application of forces to nodal points, it was necessary to simulate each of the various types of loading by application of the loads to nodal points of the finite element mesh representing the structure (s) and surrounding soil.

4.3 INCREMENTAL EXCAVATION

Dunlop, Duncan and Seed (1968) have shown that excavation may be simulated in the finite element method by applying stresses to the boundary exposed by excavation. The technique which they employed consist of determining stresses at the boundary to be created by excavation, calculating equivalent nodal loads for these stresses and applying equal but opposite nodal loads to the finite element mesh. Because the stresses applied to the excavation boundary are equal in magnitude but opposite in sign to the initial stresses, the excavation boundary is assured to be stress-free following excavation. Elements which are "excavated" are assigned a

minimal stiffness, to avoid any interaction with the remainder of the elements during excavation.

A generally applicable technique for determining boundary stresses can be developed using an interpolation formula to calculate the boundary stresses. The interpolation formula relates the known stresses at the element centers to the unknown stresses at the nodal points on the boundary of the excavation. One of the applicable methods of expressing the interpolation function is a polynomial of the form:

$$\sigma = a_1 + a_2 x + a_3 y + a_4 xy \quad (4.3)$$

where σ is the nodal stress to be interpolated, x and y are the coordinates of the nodal point and a_1, a_2, a_3 and a_4 are interpolation coefficients.

The excavation of a quadrilateral element generally creates four excavation boundaries, and equation (4.3) can be used to determine the stresses at all four nodes of the element. Also, a complete stress distribution may be defined on the boundaries around the quadrilateral element by simply assuming linear variations of stresses between the calculated nodal stresses. Figure 11 shows such a stress distribution for a quadrilateral element. To simulate excavation, this boundary stress distribution is used to determine the equivalent nodal loads which must be applied to the boundary of excavation.

In order to determine the nodal stresses of an element to be excavated, three sets of the interpolation coefficients are calculated (for σ_x, σ_y and σ_{xy}) using the known stresses in the element to be excavated and the stresses in three adjacent elements.

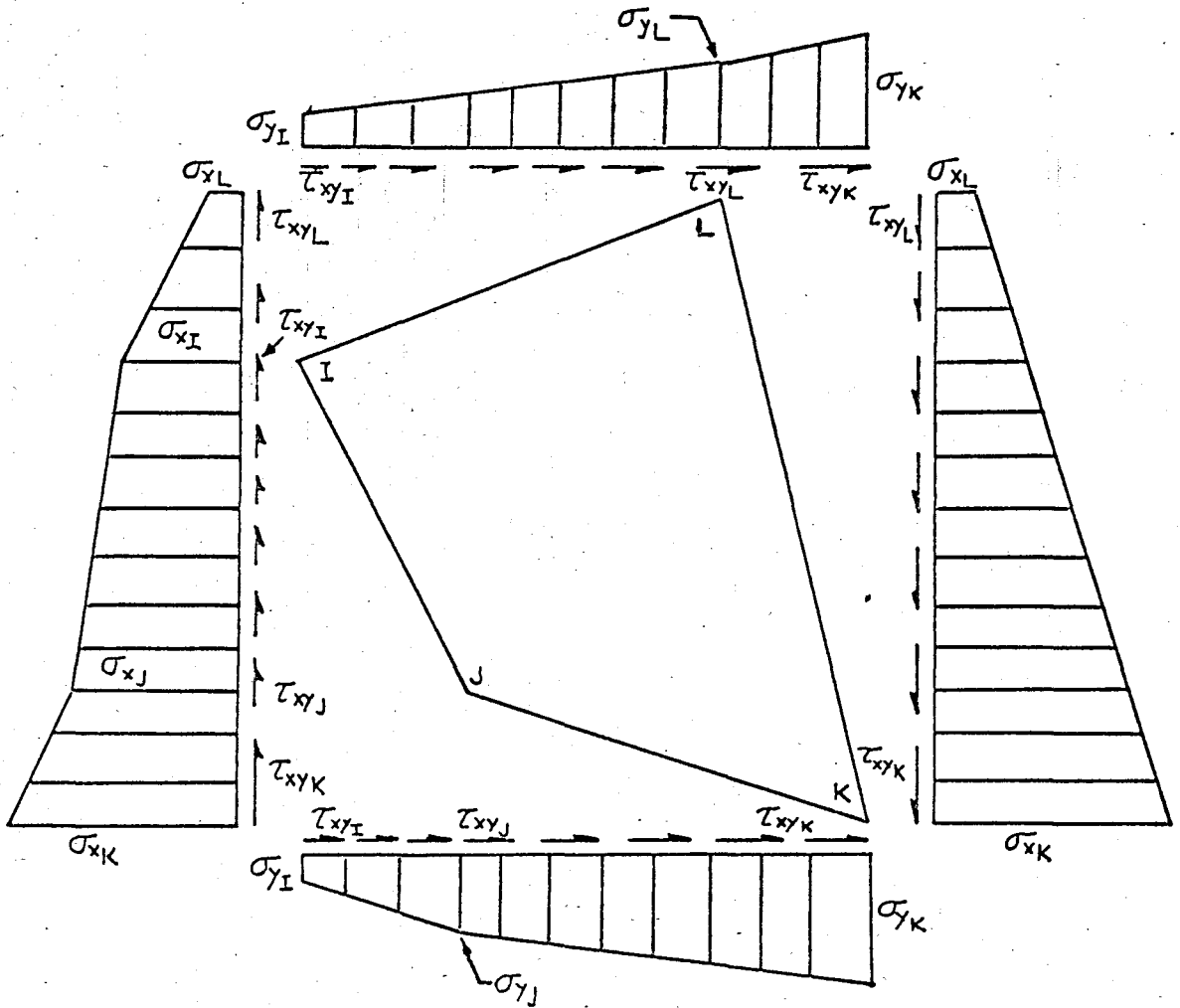
The unknown interpolation coefficients are expressed for a given stress, σ , as follows:

$$\sigma(1) = a_1 + a_2 x_1 + a_3 y_1 + a_4 x_1 y_1 \quad (4.4)$$

$$\sigma(2) = a_1 + a_2 x_2 + a_3 y_2 + a_4 x_2 y_2 \quad (4.5)$$

$$\sigma(3) = a_1 + a_2 x_3 + a_3 y_3 + a_4 x_3 y_3 \quad (4.6)$$

$$\sigma(4) = a_1 + a_2 x_4 + a_3 y_4 + a_4 x_4 y_4 \quad (4.7)$$



$$Y_{IJ} = y_I - y_J$$

$$Y_{JK} = y_J - y_K$$

$$Y_{KL} = y_K - y_L$$

$$Y_{LI} = y_L - y_I$$

$$X_{JI} = x_J - x_I$$

$$X_{KJ} = x_K - x_J$$

$$X_{LK} = x_L - x_K$$

$$X_{IL} = x_I - x_L$$

Note: All Stresses and Gradients Assumed Positive as Shown.

Figure 11. Arbitrary Quadrilateral Element and Boundary Stress Distribution (after Clough, 1969).

where $\sigma(1)$ is the stress in element (1), $\sigma(2)$ is the stress in element (2), etc. It is also possible to express these equations in matrix form as :

$$\{\sigma\}_e = [m] \{a\} \quad (4.8)$$

where $\{\sigma\}_e$ is the vector of known stresses for elements 1, 2, 3 and 4, $[m]$ is the coordinate matrix for elements 1, 2, 3 and 4, and $\{a\}$ is the vector of interpolation coefficients. Equation (4.8) may be expressed as :

$$\{a\} = [m]^{-1} \{\sigma\}_e \quad (4.9)$$

Then the stresses, $\{\sigma\}_n$, at each node of the element to be excavated can be solved by using interpolation coefficients:

$$\{\sigma\}_n = [n] \{a\} \quad (4.10)$$

where $[n]$ is the coordinate matrix for nodes I, J, K and L. The unknown nodal stresses are related to the known element stresses as follows :

$$\{\sigma\}_n = [n] [m]^{-1} \{\sigma\}_e \quad (4.11)$$

Thus σ_x , σ_y and τ_{xy} may be defined at the nodes of an element to be excavated, in terms of known element stresses of that element and three adjacent elements.

Once the nodal stresses have been evaluated, the equivalent nodal forces may be established for the element as shown with respect to the boundary J-K of the element of the quadrilateral shown in Figure 1.1. The equivalent vertical nodal force at node J depends on the magnitude of σ_y and τ_{xy} at nodes I, J and K. Using the principle of virtual work, and assuming linear variations between the calculated nodal stress values, the vertical force at node J may be expressed as :

$$R_y^j = \frac{1}{6} \left[\begin{array}{l} (X_j J) \sigma_{y_j} + 2(X_j J \ X_k J) \sigma_{y_j} + (X_k J) \sigma_{y_k} + (Y_j J) \tau_{xy_j} + \\ 2(Y_j J \ Y_k J) \tau_{xy_j} + (Y_k J) \tau_{xy_k} \end{array} \right] \quad (4.12)$$

By repeating this operation for all vertical and horizontal nodal forces and writing the resultant equations in matrix form, the following equation may be obtained:

$$\{F\}_n = [H] \{\sigma\}_n \quad (4.13)$$

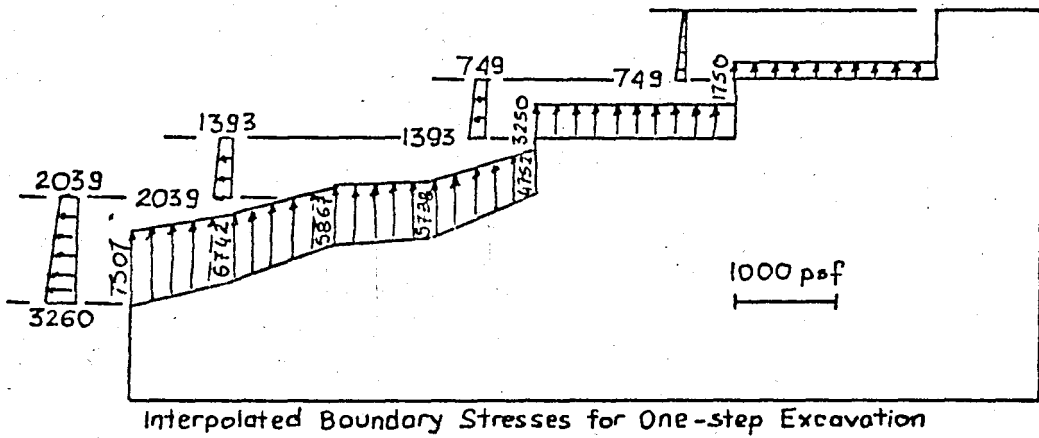
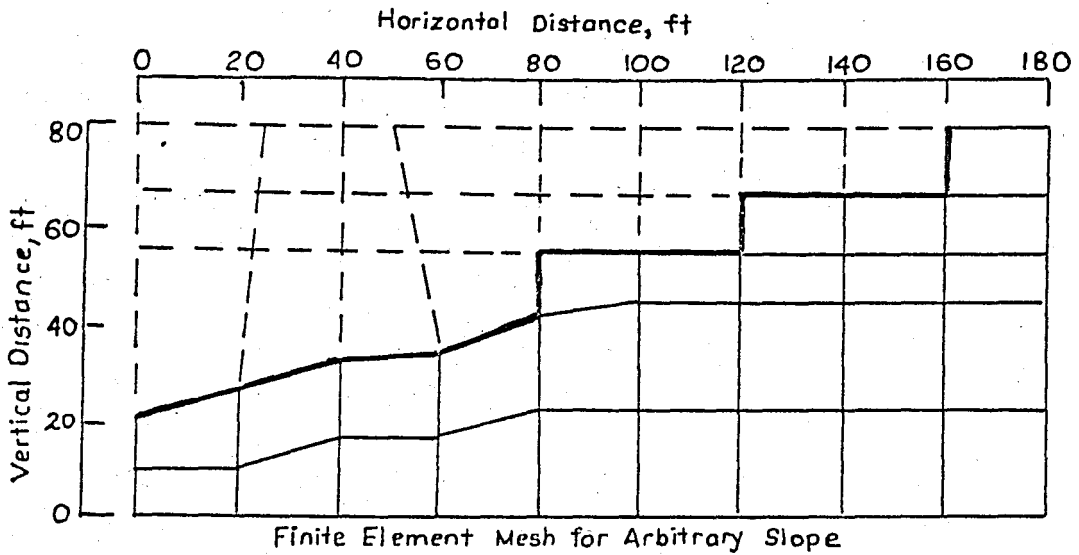
where $\{F\}_n$ is the 8×1 vector containing all element nodal forces, $[H]$ is an 8×12 matrix defining element boundary geometry and $\{\sigma\}_n$ is a 12×1 vector of nodal stresses. The expanded form of this expression is given by equation (4.14), on the following page. Frequently, it is unnecessary to apply all eight of the nodal loads defined by equation (4.13) because equivalent nodal loads need only be applied to those nodes which are common to both an excavated and intact element.

Selections of the elements to be used to obtain the interpolation constants is somewhat arbitrary. One of the elements used should be the element for which equivalent nodal forces are being calculated. The other three elements should be as near as possible to the excavated element, but no three of the four elements selected may have centers that lie on a vertical or horizontal line. If this happens, the matrix $[m]$ becomes singular and no solution is possible.

To obtain a solution for the excavation of a submerged element, effective stress notation should replace the total stress notation through equations (4.3) - (4.13).

An example of this procedure is illustrated by (Lough (1969)) and is given in Figure 12. The excavation boundary is selected to reflect all possible combinations that may occur in a real case (horizontal, vertical and inclined segments are used). Also, unequal size of mesh elements are included into the geometry of the problem.

$$\begin{Bmatrix} R_x^I \\ R_y^I \\ R_x^J \\ R_y^J \\ R_x^K \\ R_y^K \\ R_x^L \\ R_y^L \end{Bmatrix} = \frac{1}{6} \begin{bmatrix} 2(YLI) + 2(YIJ) & YIJ & 0 & YLI & 0 & 0 & 0 & 0 & 2(XJI) + 2(XIL) & XJI & 0 & XIL \\ 0 & 0 & 0 & 0 & 2(XIL) + 2(XJI) & XJI & 0 & XIL & 2(YLI) + 2(YIJ) & YIJ & 0 & YLI \\ YIJ & 2(YIJ) + 2(YJK) & YJK & 0 & 0 & 0 & 0 & 0 & XJI & 2(XJI) + 2(XKJ) & XKJ & 0 \\ 0 & 0 & 0 & 0 & XJI & 2(XJI) + 2(XKJ) & XKJ & 0 & YIJ & 2(YIJ) + 2(YJK) & YJK & 0 \\ 0 & YJK & 2(YJK) + 2(YKL) & YKL & 0 & 0 & 0 & 0 & 0 & XKJ & 2(XKJ) + 2(XLK) & XLK \\ 0 & 0 & 0 & 0 & 0 & XKJ & 2(XKJ) + 2(XLK) & XLK & 0 & YIJ & 2(YIJ) + 2(YKL) & YKL \\ YLI & 0 & YKL & 2(YKL) + 2(YLI) & 0 & 0 & 0 & 0 & XIL & 0 & XLK & 2(XLK) + 2(XIL) \\ 0 & 0 & 0 & 0 & XIL & 0 & XLK & 2(XLK) + 2(XIL) & YLI & 0 & YKL & 2(YKL) + 2(YLI) \end{bmatrix} \begin{Bmatrix} \sigma_{xI} \\ \sigma_{xJ} \\ \sigma_{xK} \\ \sigma_{xL} \\ \sigma_{yI} \\ \sigma_{yJ} \\ \sigma_{yK} \\ \sigma_{yL} \\ \tau_{xyI} \\ \tau_{xyJ} \\ \tau_{xyK} \\ \tau_{xyL} \end{Bmatrix} \quad (4)$$



$E=100,000\text{psf}, \gamma=100\text{pcf}$
 $\nu=0.3, k_0=0.43$

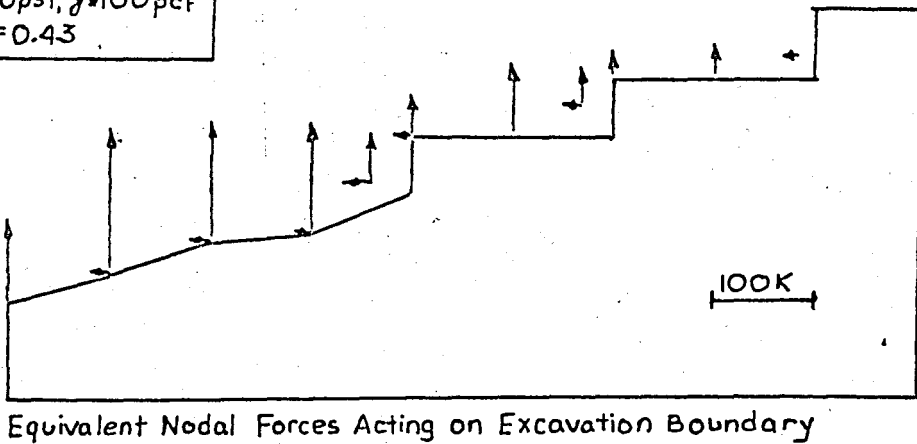


FIGURE 12. Example of Boundary Stress Reversal for Arbitrary Slope. (after Clough, 1969)

The excavation was performed in one step, thus the boundary stresses were equivalent to the assumed initial stresses, $\sigma_y = \gamma h$ and $\sigma_x = 0.43 \gamma h$. The excavation boundary stresses and equivalent nodal loads were determined as shown in Figure 12. Great accuracy was obtained as a result of this analysis.

Because the material in Figure 12 was linear elastic, the stresses calculated by a three-step excavation should give the same result as those given by a single step. A comparison of the results of a three-step and one-step excavation analysis are shown in Figure 13. In most of the elements a good agreement is observed. There exists some large differences in the elements adjacent to the vertical-horizontal excavation boundaries. The reason of these differences is that at vertical-horizontal boundaries the stresses are small and the stress gradients are large. A better solution could be obtained by using smaller elements.

4.4 INCREMENTAL WATER PRESSURE LOADING

It is very important to simulate the effects of changes in water pressure on a soil mass because changes in water pressure produce incremental loading which may cause changes in effective stresses and affect the behavior of the soil. A change in water pressure on one side of an impervious soil produce boundary pressure loading on that side only, however on a pervious material this results in development of seepage through the material. (Clough (1969) has shown that this type of loading is represented as a distributed load, which in finite element analysis may be represented as a load distributed equally to the nodes of each element. Therefore it is important to decide on the appropriate type of loading for each soil. For example, the appropriate type of loading for a clay with low permeability would depend upon the amount of time allowed for seepage to develop through the soil, this means that the rate of loading has to be considered. If the loading rate is rapid and a steady seepage condition does not develop, the clay may be only subjected to a boundary pressure

loading. On the other hand if the loading rate is very slow, the clay may be loaded by a distributed loading.

The variation of water pressures around an element may be accounted for in the loading of a finite element mesh by considering the water pressure changes at each node of an element and assuming a linear variation of the water pressure changes between the nodal points. An arbitrary quadrilateral subjected to linearly varying water pressure changes on each side is shown in Figure 14. This loading shown in Figure 14 is a special case of the boundary stress loading used for excavation, therefore equation (4.14) may be used to evaluate the equivalent nodal forces. Equation (4.14) may be simplified to the following form for water pressure loading :

$$\begin{Bmatrix} R_x \\ R_y \\ R_x \\ R_y \\ R_x \\ R_y \\ R_x \\ R_y \end{Bmatrix} = \frac{1}{6} \begin{bmatrix} 2(YLJ) & 2(YJJ) & & & & & & & YLJ \\ 2(XJL) & 2(XJJ) & & & & & & & XJL \\ & YJJ & 2(YJJ) & 2(YJK) & & & & & 0 \\ & XJJ & 2(XJJ) & 2(XKJ) & & & & & 0 \\ 0 & & YJK & 2(YJK) & 2(YKL) & & & & YKL \\ 0 & & XKJ & 2(XKJ) & 2(XLK) & & & & XLK \\ YLJ & & 0 & & YKL & 2(YKL) & 2(YLJ) & & \\ XLJ & & 0 & & XLK & 2(XLJ) & 2(XLK) & & \end{bmatrix} \begin{Bmatrix} \Delta u_J \\ \Delta u_K \\ \Delta u_L \\ \Delta u_L \end{Bmatrix} \quad (4.15)$$

If the loading on an element is to be distributed as a body load the horizontal and vertical forces are summed and divided by four. By performing these operations on equation (4.15), equation (4.16) is obtained :

$$\begin{Bmatrix} R_x \\ R_y \end{Bmatrix} = \frac{1}{8} \begin{bmatrix} (YLJ+YJJ) & (YJJ+YJK) & (YJK+YKL) & (YKL+YLJ) \\ (XJL+XJJ) & (XJJ+XKJ) & (XKJ+XLK) & (XLK+XJL) \end{bmatrix} \begin{Bmatrix} \Delta u_J \\ \Delta u_K \\ \Delta u_L \\ \Delta u_L \end{Bmatrix} \quad (4.16)$$

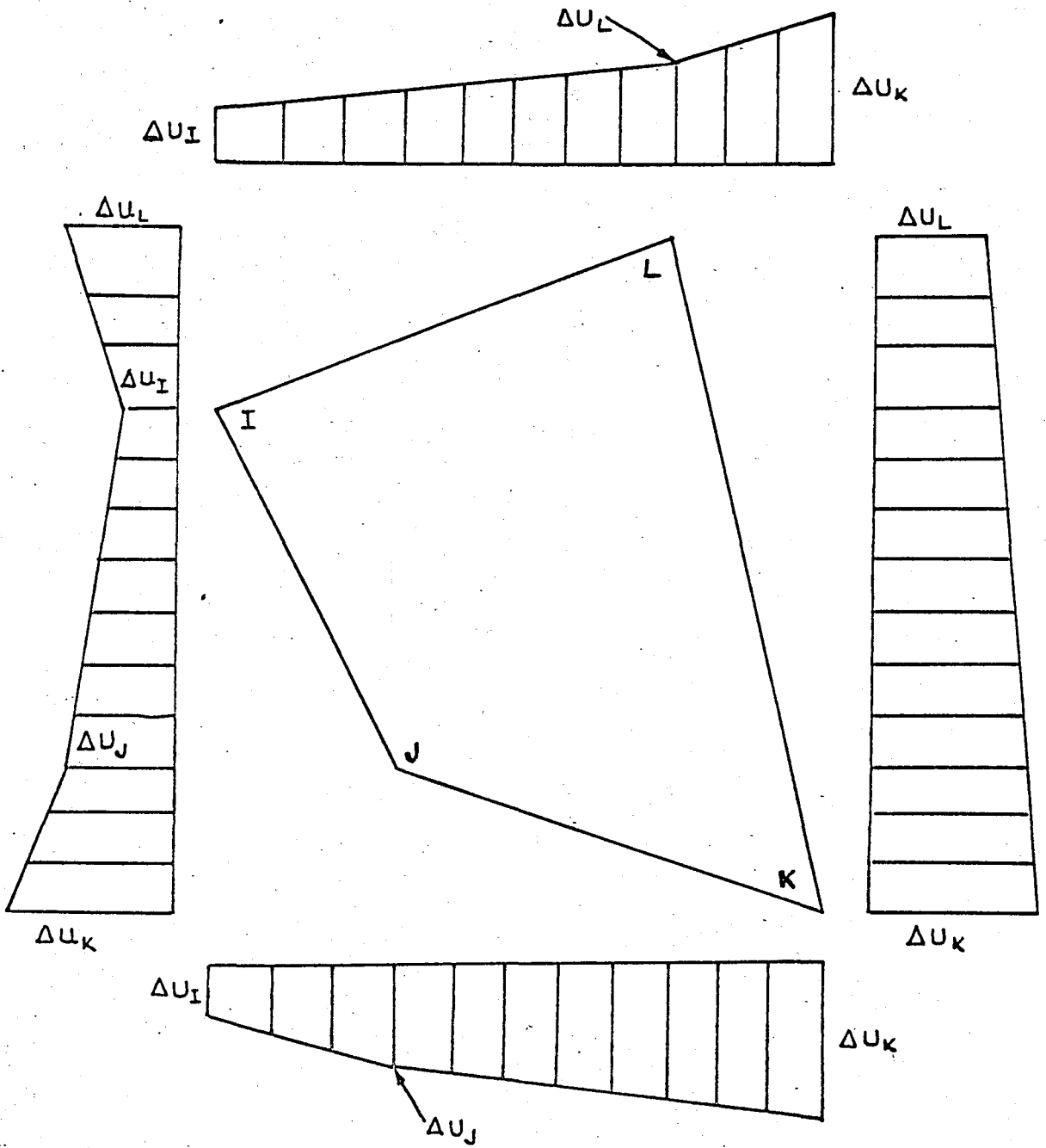


Figure 14. Arbitrary Quadrilateral Element and Boundary Water Pressure Distribution (after Clough, 1969).

in which $\begin{Bmatrix} R_x \\ R_y \end{Bmatrix}$ are the loads distributed to each nodal point on the quadrilateral.

Figure 15 shows an example of distributed type of loading due to a lowering of ground water table on four elements. As can be seen in this figure, while the water pressure changes on elements 2 and 3 are different, the net element loading is the same; namely, four vertical forces equivalent to $(\gamma_w \times \text{Element Area})/4$. For element 4, although there is a large change in water pressure on all sides of the element there is no net loading because the element was subjected to no differential water pressure changes.

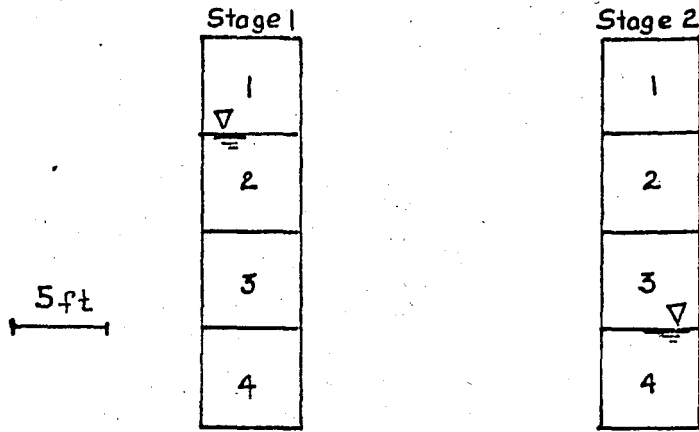
4.5 NUMBER OF INCREMENTS REQUIRED TO SIMULATE EXCAVATION

In practice, earthwork involves accomplishment of many steps during a real job. For example, excavation is frequently accomplished by successive removal of a number of layers of soil, which might be fifteen to thirty cm. thick. Thus a 115 meters depth of excavation involves 50 to 100 separate load increments. The use of 50 to 100 increments for finite element simulation of excavation is not desirable from a standpoint of the time required for computer analysis. In an economical point of view, this simulation of these construction operations would be accomplished using a much smaller number of layers, it means the use of a smaller number of steps in the analyses.

Closed Form Solutions. If homogeneous soil conditions and no water level changes are involved in some simple problems, it can be defined some closed form solutions to represent the deflections of incremental excavation. The modulus, E was assumed to vary with confining pressure according to the relationship:

$$E = K_m P_a \left(\frac{\sigma_3}{P_a} \right)^n \quad (2.6)$$

as mentioned before. Clough has determined the deflections for many cases and has plotted some curves. The results of these analyses for excavation is shown in Figure 16: that is the variation in errors with number of layers.



ELEMENT	1	2	3	4
ΔU on Element, Feet of Water				
Equivalent Nodal Loads, Lbs				
Distributed Loading on Element, Lbs				

Figure 15. Example of Water Pressure Loading on Pervious Soil Element (after Clough, 1969).

It can be seen from Figure 16 that the amount of error is a function of :

- a-the number of layers used in a solution
- b-the stresses used to calculate the modulus value
- c-the value of exponent n .

Clough has developed two alternative sets of curves. One set is based on a modulus value calculated prior to the execution of the increment called the "past stresses". The second one is based on a modulus value calculated from the average of the stresses from the past and present increments, called the "average stresses". It can be seen in Figure 16 that the curves based upon the average stresses converge more rapidly to the small layer solution for fewer increments than those based upon the past stresses.

If the average stresses are used in a finite element analysis each increment must be analyzed twice. The first analysis is performed and the new stresses are obtained, then by using the average of these two values (the past and obtained stresses), an average stress may be calculated. Subsequently, a second analysis of the same increment is performed using improved values of modulus based on the newly calculated average stresses. By doing this, twice as much computational time is expended as is used for a straight-forward incremental analysis. However, Figure 16 shows that the "average stress" solution generally requires fewer than half the increments required by the "past stress" solution for the same degree of accuracy. To choose which approach could be applicable depends upon the degree of accuracy required.

The exponent n also controls the number of layers to simulate the excavation process. The curves in Figure 16 show that the amount of error varies with the exponent value n . For higher exponent values, a greater number of increments are required to obtain the same degree of accuracy. Clough has shown that the reason of this changes is related to the modulus value which becomes more sensitive to the value of the minor principle stress which, in turn, is dependent upon the

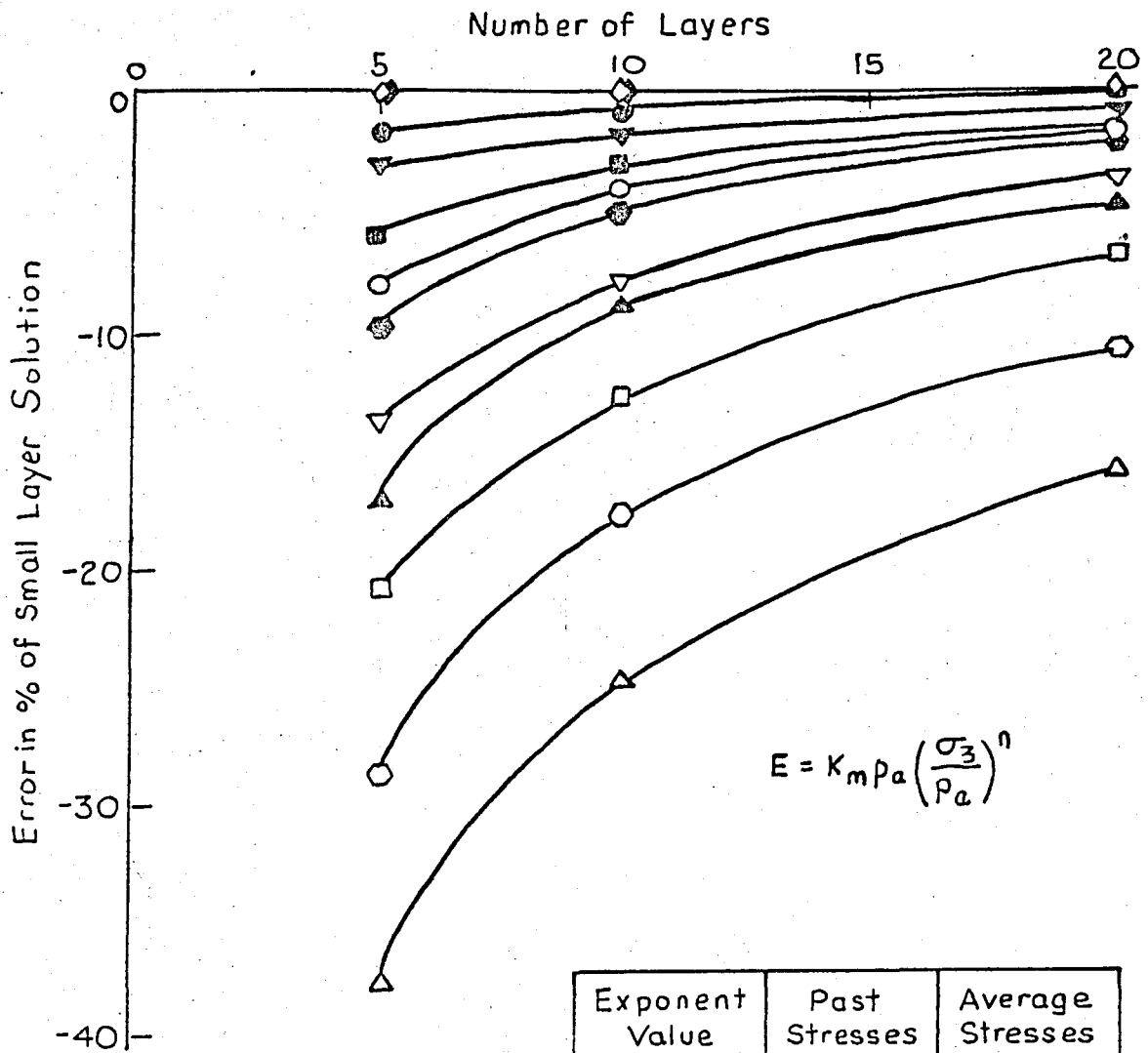


Figure 16. Values of Errors in Simulation of Small Layer Excavation For $n: 0.3, 0.5, 0.7, 0.9$ and 1.1 (after Clough, 1969).

size of the layers used in the problem. However for an elastic material with a modulus value that does not vary with confining pressure, the value of exponent, n , is zero, and the curves in Figure 16 show the solution for any number of increments corresponds to the small layer solution.

The usage of curves in Figure 16 may be illustrated by an example. In order to determine the number of layers required for an excavation in which deflections within 10% of the values calculated using layers of infinitesimal thickness are considered satisfactory, the engineer must decide on the exponent value, n and enter to the chart to get the required number of layers. For an exponent value of 0.7, five and fourteen layer solutions are required for the average and post stresses respectively, and in an economical point of view the five-layer solutions must be chosen.

During this section, the number of increments required to simulate excavation has been analyzed and some curves were developed. Clough has shown that the modulus value could be assumed to be a function of confining pressure, and making use of it some closed form solutions could be obtained.

4.6 ANCHOR INSTALLATION

In order to maintain the static equilibrium of the system or to prevent large soil movements which could be occurred during an excavation, the excavated area must be somehow restrained. Anchor installation is a most common way to do it in practice. The simulation of anchor installation can be easily done in the incremental analysis by using a number of rigid one-dimensional elements which connects the face of the wall to the anchorage. In the computer analysis, the cross sectional area and flexural stiffness of the actual anchor element must be specified in order to compute the stresses in the bar element during the whole analysis. The first and last nodal points of the one-dimensional bar element must also be specified.

If the other rod is prestressed, this must be also given as an input in the program, but this does not apply the force which

must be applied to the face of the wall. The prestress load if applied serve to obtain, the stress-load behavior of the bar element during excavation. The latter one, which must be given as a concentrated load at specific nodal points in the concentrated force option contributes directly to the behavior of the soil system and acts as a restraining factor.

In the incremental analysis, simulation of anchor installation could be performed very closely to the actual case by choosing the appropriate number of anchor rods, the prestressed loads on them and the most convenient geometrical representation of the case, including the length of anchor rods and their slopes. At this point, it is useful to point out that the initial finite element mesh of the problem should take into account the installation of one-dimensional elements.

4.7 SUMMARY

In this chapter, the basis for the finite element method was described. Incremental finite element techniques developed by Clough (1960) were explained and the basic parts of the finite element method such as incremental excavation, incremental water pressure loading, number of increments required to simulate excavation and anchor installation were described and some closed form solutions were proposed (after Clough, 1969).

CHAPTER 5

CLASSICAL DESIGN METHODS OF FLEXIBLE EARTH RETAINING STRUCTURES

5.1 INTRODUCTION

The foundations for most structures are established below the surface of the ground. Therefore, they can not be constructed until the soil or rock above the base level of the foundations has been excavated.

There is no need to support the surrounding material in shallow excavations if there is adequate spaces to establish slopes at which the material can stand. The steepness of the slopes is a function of the type of the soil, the climatic and weather conditions, the depth of the cut and time.

In a clayey soil, the maximum slope at which the material can stand is a function of the depth of the cut and the shearing resistance of the soil. If the clay is stiff, some cracks could develop near the ground surface. If these cracks become filled with water, the hydrostatic pressure reduces the factor of safety and may cause slope failures. For these reasons, bracing is often used to support the sides of excavations in clay, even though the clay would stand to the necessary height without lateral support. Sheet pile retaining walls are also an alternative method to support the sides. Tied-back and anchored walls are also considered in this chapter.

5.2 BEHAVIOR OF FLEXIBLE EARTH RETAINING STRUCTURES

Most of the retaining walls are capable of rotating about their bases far enough to satisfy the strain requirements for the active state of stress in the failure wedge. The active earth pressure and its linear distribution with depth is the total earth pressure which acts against the wall.

But the walls of anchored bulkheads (Figure 17a), braced cuts (Figure 17b) and tie-back cuts (Figure 17c) consist of members with small flexural rigidity and they are supported at various elevations by anchor or struts.

The characteristic deformed shapes of the walls are shown in Figure 17 by dashed lines. Usually, the top deformations are less than those corresponding to the active Rankine State, whereas those near the bottoms are greater. Consequently the magnitude of the earth pressure against the walls differs somewhat from the active earth pressure, and a linear distribution with depth is not valid.

The actual earth pressure against the flexible wall and its supporting members depend on the soil properties and also on the sequence of construction. Therefore, the pressures used for design can not be determined by theory but, since they are influenced by the construction operations, must be modified by experience and the results of observations and measurements on full-sized structures.

5.3 DESIGN OF SHEET PILE RETAINING WALLS

The design of sheet pile retaining walls requires several successive operations :

a-Evaluation of the forces and lateral pressures that act on the wall

b-Determination of depth of piling penetration

c-Computation of maximum bending moment

d-Computation of the stresses and selection of the piling section

e-Design of the anchorage system.

Before these operations, controlling dimensions must be determined. These include the height of the wall, the dredge line etc...

Cantilever Walls

For moderate heights, sheet piling is driven to a sufficient depth into the ground to become fixed as a vertical cantilever. This type of walls usually undergo large lateral deflections.

Since the lateral support for a cantilevered wall comes from passive pressure exerted on the embedded portion, depths of penetration can be too high: this results in excessive stresses and yielding. A maximum of 5 meters height is recommended for a cantilevered wall.

Figure 18 shows the distribution of earth pressure against a cantilevered wall. When the lateral active pressure, P is applied to the top of the wall, the piling rotates about b , mobilizing passive pressure above and below the pivot point. The term $(p_p - p_a)$ is the net passive pressure, p_p , minus the active pressure, p_a .

At point b , the net pressure is equal to zero. The diagram $oabc$ represents the resulting earth pressure. For the design purpose, the curve abc is replaced by a straight line dc . The location of point d is chosen to assure static equilibrium of the system.

Cantilever Sheet Piling in Cohesive Soils

Since both the strength of clay and the lateral earth pressure change with time, the design of sheet piling in these soils is complicated. The depth of penetration and the piling size must satisfy both existing and future pressure conditions. Immediately after the sheet piling is installed, earth pressure may be calculated in terms of undrained strength parameters. The method is called " $\phi=0$ " analysis in which a cohesion value, c , equal to one-half the unconfined compressive strength, q_u , is taken.

Figure 19 (after Teng) shows the initial pressure conditions for sheet piling embedded in cohesive soil for its entire depth. Since $K_a = K_p = 1$ when $\phi=0$, the passive earth pressure on the left side of the piling is given by:

$$p_p = \gamma_e(Z-H) + q_u \quad (5.1)$$

and the active pressure on the right side:

$$p_a = \gamma_e Z - q_u \quad (5.2)$$

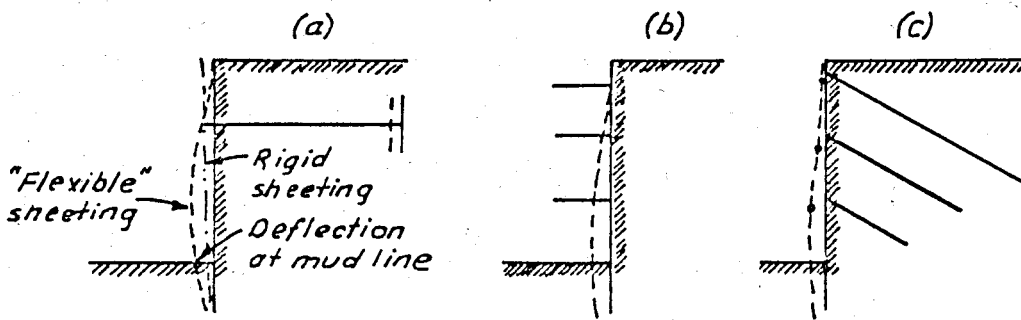


Figure 17. Typical Patterns of Deformation of Vertical Walls of a-Anchored Bulkhead, b-Braced cut and c-Tie-Back cut (after Peck, 1974).

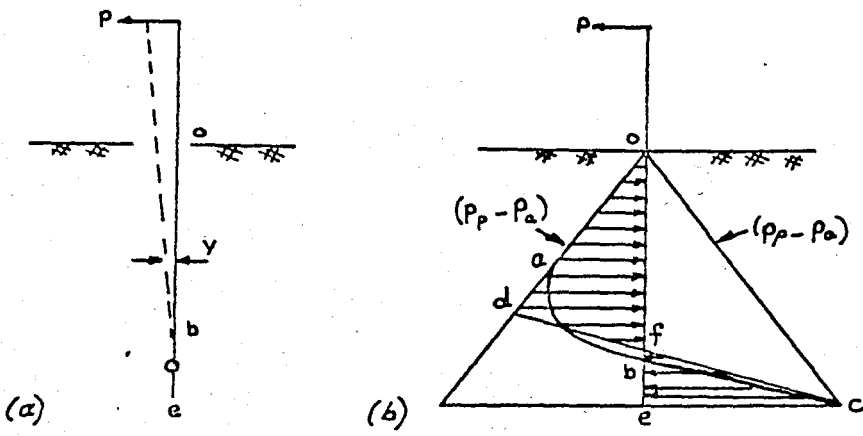


Figure 18. Earth Pressure on Cantilever Sheet Piling (after Teng, 1975).

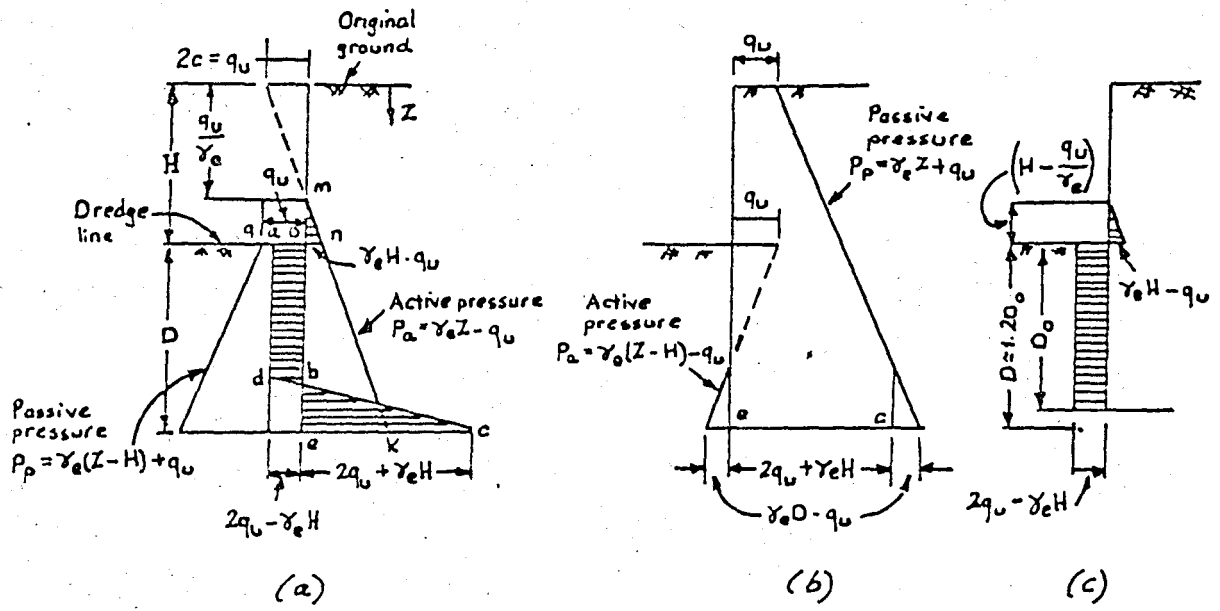


Figure 19. Initial Earth Pressure for Design of Cantilever Sheet Piling Entirely on Cohesive Soil (after Teng, 1975).

where: Z = depth below the original ground surface

$q_u = 2c$ = unconfined compressive strength

γ_e = effective unit soil weight

The negative earth pressure or tension zone is ignored because the soil may develop tension cracks in the upper portion. Since $K_a K_p$, the net resistance on the left side of the wall is constant below the dredge line and is given by :

$$p_p - p_a = 2q_u - \gamma_e H \quad (5.3)$$

Note that, theoretically, the wall will fail if $\gamma_e H$ is greater than $2q_u$. The height, $H_c = 2q_u / \gamma_e$ is called the critical height.

For the lower portion, where the piling moves to the right the net resistance is given by:

$$p_p - p_a = 2q_u + \gamma_e H \quad (5.4)$$

which is illustrated in Figure 19b. The net pressure distribution is shown in Figure 19a: the point d and the penetration depth, D , are chosen so as to satisfy the static equilibrium conditions.

The design could be made using the pressure diagram shown in Figure 19c: i.e., by assuming the passive pressure on the right side of the piling is replaced by the concentrated reaction, C . The depth, D_o , should be increased by 20 to 40 percent to obtain the total design depth of penetration using this method.

5.4 BRACED CUTS

When the depth of excavation exceeds 5 or 6 meters, the use of vertical timber sheeting becomes uneconomical, and other methods of sheeting and bracing are commonly employed. According to one procedure steel sheet piles are driven around the boundary, then the soil is removed from the enclosure wales and struts are inserted.

Figure 20 shows the commonly used sheet piles. In Figure 21 two typical cross section of a braced excavation is shown. The wales are commonly of steel, and the struts may be of steel or wood.

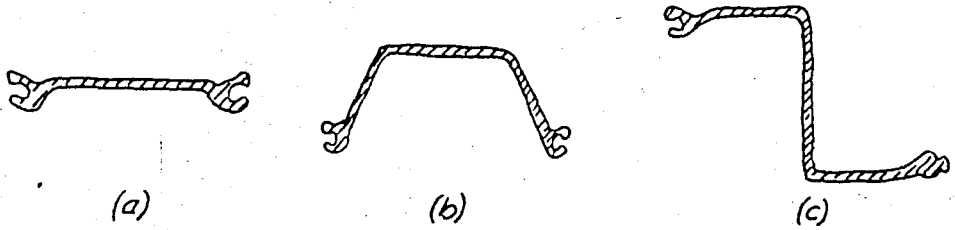


Figure 20. Types of Steel Sheet Piles Commonly Used for Bracing Sides of Deep Excavations. a-Flat Web, b-Arch Web, c-Z Piling. (after Peck, 1974)

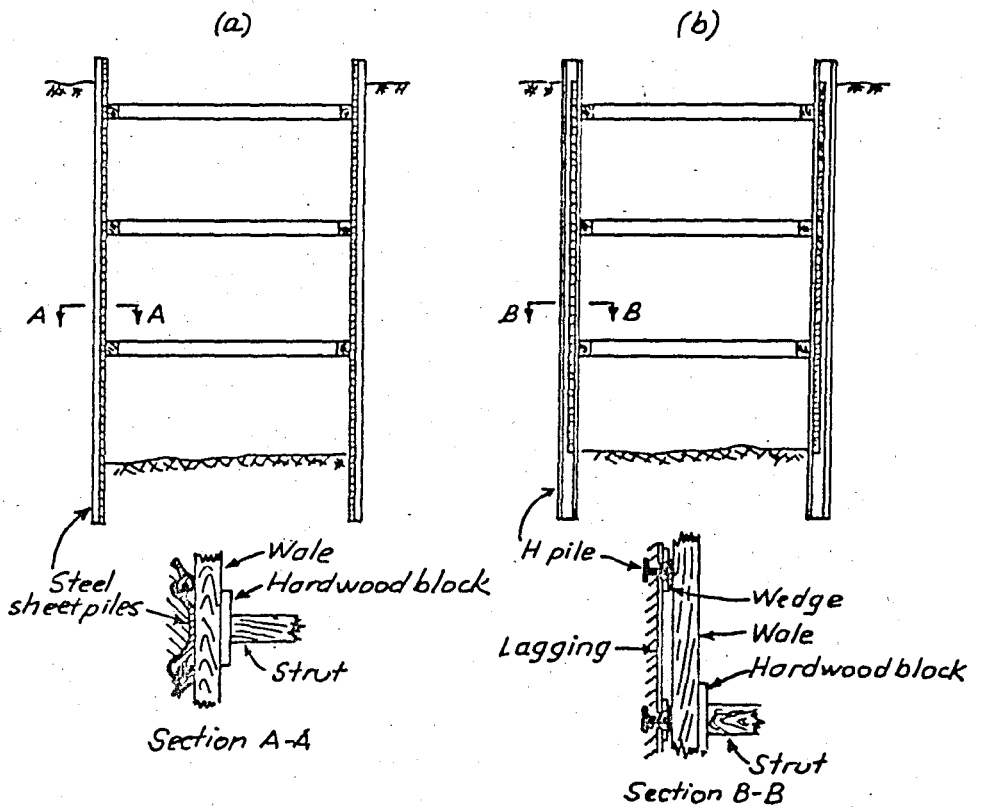


Figure 21. Cross Sections Through Typical Bracing in Deep Excavations. a-Sides Retained by Steel Sheet Piles. b-Sides Retained by H-Piles and Lagging (after Peck, 1974).

It is important to provide vertical support for bracing. This may be done by keeping posts beneath the system of bracing to transfer its weight to the underlying soil or by suspending the bracing from beams extending across the top of the cut.

If the width of a deep excavation is too great to permit the economical use of struts across the entire excavation, inclined bracing may be used (Figure 22).

Modes of Failure in Clay

During an excavation, the water content of the clay could not find enough time to change, hence undrained or $\phi=0$ conditions prevail. As the depth of the cut increases, the soil outside the walls behaves like a surcharge and causes the soil beneath the excavation to rise. If the cut becomes too deep with respect to the strength of the clay, the heave of the bottom may be uncontrollable, settlements of the surrounding ground surface may become excessive and the bracing system may collapse.

In clays failures by bending of wales or of sheet piles are unusual.

Base Failure of Cuts in Clay

The strength of the clay has an important influence on the behavior of the bracing system and the surrounding soil. The bearing capacity equation best describes the ability of the soil to withstand the surcharge γH of the clay outside the excavation :

$$q_d = c_b N_c \quad (5.5)$$

where, c_b is the undrained shearing resistance below base level, N_c is a constant between 5 and 6 as shown in Figure 23. By rearranging equation (5.5), it is possible to obtain an expression for N_c as $\gamma H / c_b$. Experience has shown that if $\gamma H / c_b$ is less than about 6, movements of the bracing system and heave of the clay below base level are small. If this value reaches about 8 the movements of even a well-designed bracing become intolerably large.

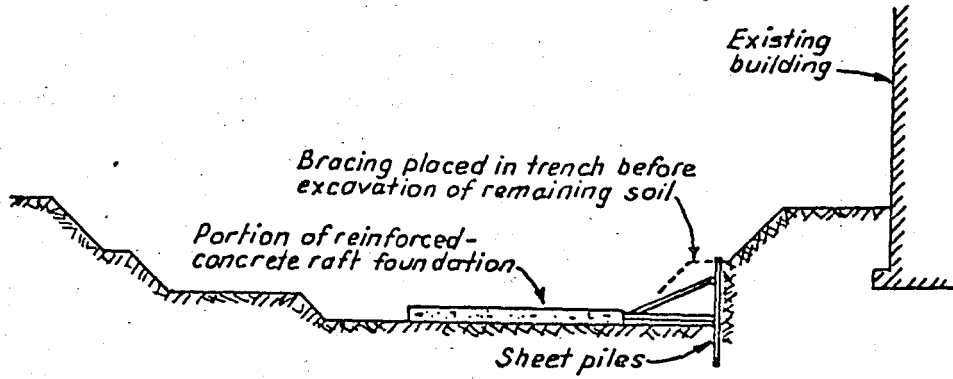


Figure 22. Typical Bracing in Deep Wide Excavations (after Peck, 1974).

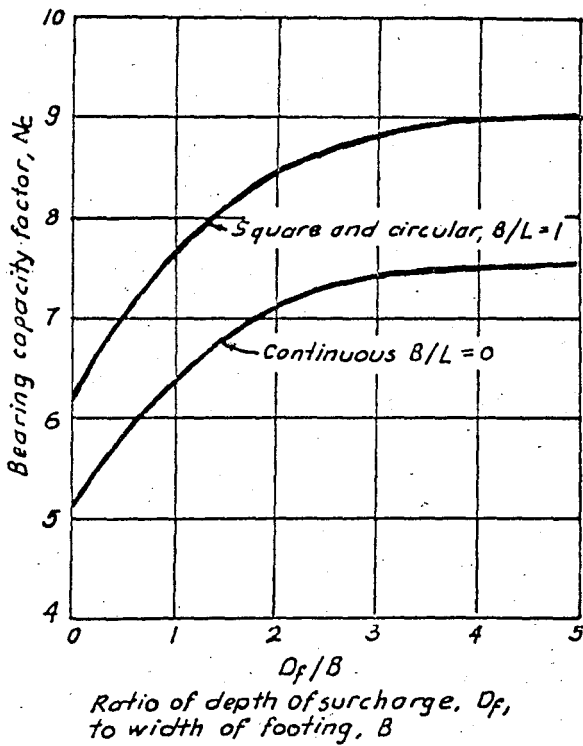


Figure 23. Bearing Capacity Factors for Foundations on Clay Under $\phi=0$ Conditions (after Skempton, 1951).

Loads on Struts in Clay

If the base stability of an open cut in clay is adequate for all depths of excavation, the strut loads can be determined from apparent pressure envelopes shown in Figure 24. The apparent pressure envelope depends on the value of $\gamma H / c$, where c is the average undrained shear strength of the clay along-side the cut. If the ratio of $\gamma H / c$ is less than or equal to 4, the corresponding apparent pressure envelope is as shown in Figure 25c. If this ratio exceeds about 4, the apparent pressure envelope may be taken as in the diagram shown in Figure 25d, provided that the width of the envelope is greater than that in Figure 25c. Otherwise, the value from Figure 25c governs, regardless of the value of $\gamma H / c$.

The diagram in Figure 25d may be used for values of $\gamma H / c$ as great as 10 or 12. On the other hand, if $\gamma H / c$ exceeds about 7 and base failure is imminent, the strut loads may be much larger than indicated by the diagram. Hence, the stability of the base should always be investigated before an estimate is made of the strut loads.

Other Considerations

The settlement of the piles can be reduced if they can be driven far enough into a bearing stratum to develop tip resistance at least equal to the dragdown forces caused by its own weight, the weight of bracing, surcharge loads, etc... For these reasons the embedment of piles may be increased beyond that required even this embedment depth would appear to be unnecessarily great.

To reduce the general movements of the bracing system, the struts should be prestressed as soon as they are installed. About 40 and 70 percent of the maximum strut loads are usually applied as a prestress load. The vertical distance between struts controls the inward lateral movements of the walls and consequently the settlement of the adjacent ground surfaces. Hence, if the movements are likely to be excessive, the distance between struts should be restricted and excavation should be permitted to extend no deeper than necessary to permit installation of each of the struts.

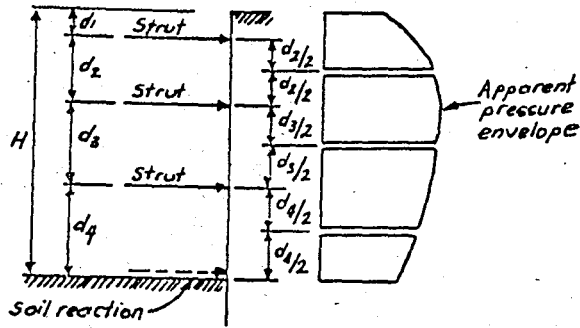


Figure 24. Diagram Illustrating Method of Calculating Strut Loads from Apparent Pressure Diagram (after Peck, 1974).

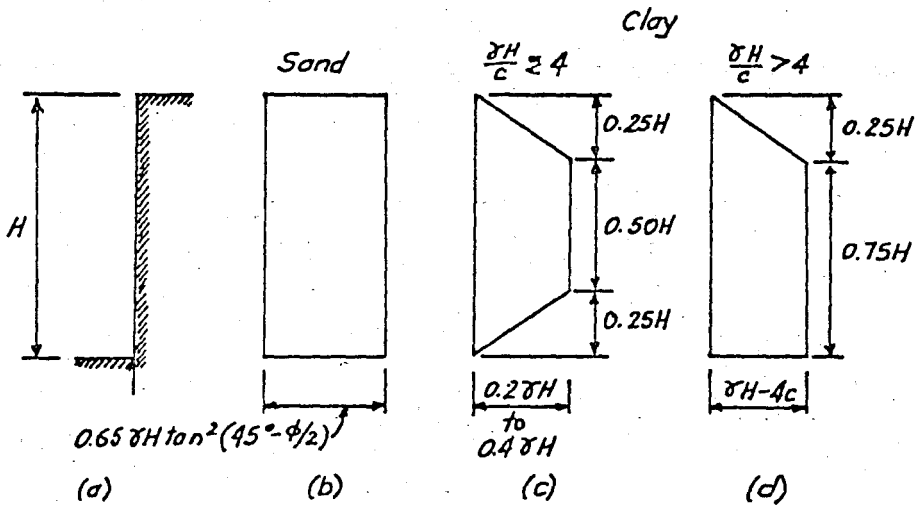


Figure 25. Apparent Pressure Diagrams for Calculating Loads in Struts of Braced Cuts. a-Sketch of Wall of Cut, b-Diagram for Cuts in Sand, c-Diagram for Clays if $\gamma H/c$ is less than 4, d-Diagram for Clays if $\gamma H/c$ is greater than 4, provided that $\gamma H/c_p$ does not exceed about 4. (after Terzaghi and Peck, 1974).

In plastic clays, the vertical distance between the struts should not exceed $2c/\gamma$, where c is the average undrained shear strength of the clay for a depth of about $B/2$ below the level of the following strut, and B is the width of the cut, in order to obtain a minimum vertical movement.

Inclined Bracing

In wide excavations, cross-lot bracing may be impractical and inclined braces or rakers are often used. Preferably, the load in the rakers is transferred to a completed portion of the foundation (Figure 22). Otherwise, an inclined footing or "kicker block", supported by the soil usually provides the reaction.

The ultimate bearing capacity of an inclined kicker block (Figure 26a) can be estimated for saturated clays. The bearing capacity factor depends on the ratio D_f/B and the inclination α . Values of N_{cq} may be obtained from Figure 26b and the ultimate bearing capacity determined from,

$$q_d = c N_{cq} \quad (5.6)$$

The force diagram in Figure 26c indicates that under the influence of the raker load, the sheeting tends to move upward with respect to the soil beneath excavation level, so adequate embedment must be provided to resist the uplift. The apparent pressure diagrams in Figure 25 may be used to estimate the horizontal components of the raker loads.

5.5 TIED-BACK CUTS

As an alternative to cross-lot bracing or inclined struts "tiebacks" are often used. Figure 27 shows a typical tie-back system. To build a tie-back, holes are drilled into the soil, an enlargement is formed at the end of the hole, tensile reinforcement is placed and concreted into the hole. Each tieback is usually prestressed before the excavation progressed.

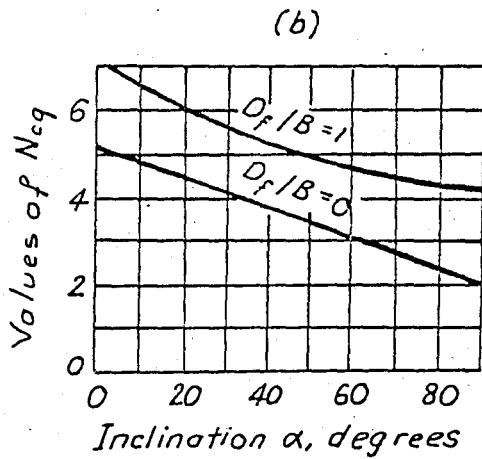
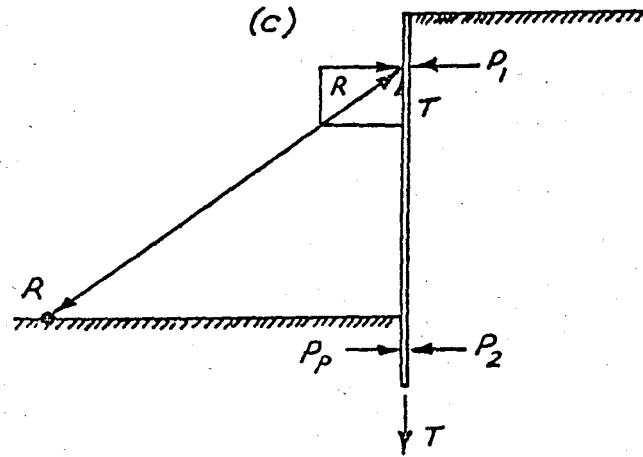
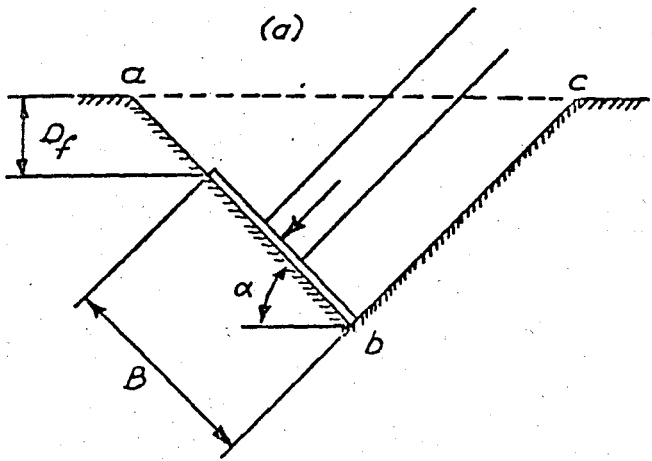


Figure 26. a-Geometry of Kicker Block for Inclined Strut, b-Bearing-Capacity Factors for Kicker Block in Saturated Clay, c-Simplified Diagram of Forces Acting on Sheeting in Raker System: P_1 and P_2 , components of active earth pressure: P_p , passive pressure: T , tension in the pile to be resisted by uplift resistance of embedded portion: R , raker load (after Meyerhof, 1953).

Modes Of Failure

Almost all failures of tieback bracing systems have been the result of inadequate anchorage. This happens when the anchors have been located too close to the wall or the individual anchors have pulled out, etc...

As the excavation progresses and the walls move in, the soil outside the cut settles and exerts a downward force on the system. If the tiebacks are inclined as in Figure 17 c, the force on them adds to the downward load on the walls. Hence, when the depth of excavation reaches to its maximum depth, the capacity of the wall could be exceeded. The resulting downward movement of the piles may destroy the effectiveness of the lowermost anchors. The load in the lower anchors is then transferred to some of the upper anchors. If the upper anchors are thus overloaded, a failure may be initiated. Hence, adequate tip resistance or embedment of the vertical piles is the most important controlling factor for the stability of a tieback system.

Anchorage

The lateral movements associated with the construction of a tieback anchorage shown in Figure 17c resemble those for a braced cut shown in Figure 17b. Since the variation of the lateral earth pressure envelopes is not well defined and the changes in stresses are time dependent for a clayey soil, the limited observational data available is the only way to make an estimate of the tieback loads. It indicates that the horizontal components of the anchors may be determined by assuming that their horizontal components are given by the apparent pressure diagrams for braced cuts (see Figure 25) .

The choice between the use of horizontal or inclined tiebacks depends on several factors. If the shear strength of the soil is varying with the increasing depth, or if there exists some non-homogeneity in the soil-strata in the form of particularly resistant layers at a reasonable depth below weaker materials, inclined anchorages deriving their support from the strong material may be preferable. On the other hand, as mentioned before,

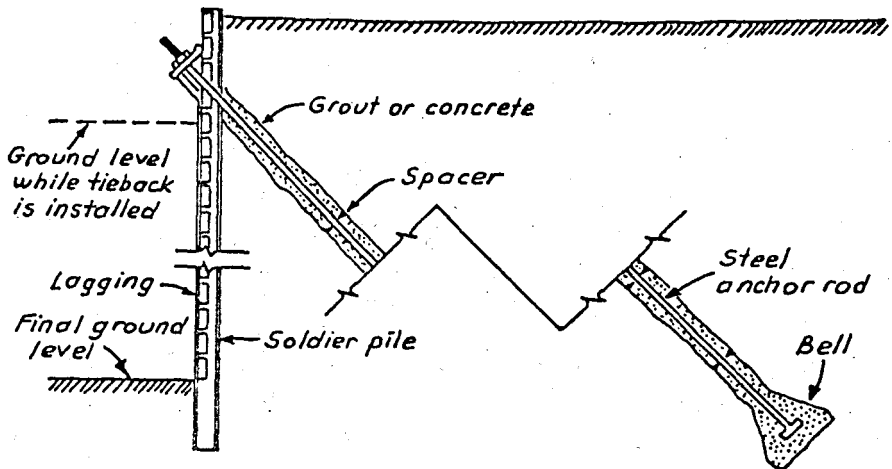


Figure 27. One of the Several Tieback Systems for Supporting Vertical Sides of Open Cut. Several Sets of Anchors may be used at different elevations (after Peck, 1974).

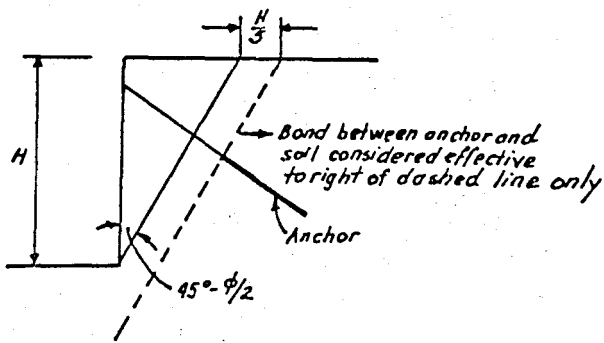


Figure 28. Limits beyond which the Anchorages of Tiebacks must be located to avoid general failure (after Peck, 1974).

if the sheet piles or soldier piles do not enough resistant to restrict their downward movement, the lower anchors in some of inclined tiebacks may become ineffective.

Anchors which consist of steel rods or tendons inserted in small-diameter holes and grouted to the supporting material can easily be installed at any inclination. Moreover, larger diameter anchors with enlargement or bells at their ends to provide the pull-out resistance, must be so located that the bells can be formed in cohesive materials to have a greater resistance.

In every case, the tiebacks must develop their anchorage within the stable soil behind the failure wedge that contributes to the active earth pressure on the wall. Figure 28 shows the possible dimensions of the wedge. Within this wedge as indicated by the dashed line, no contribution for the anchor resistance should be assumed. In practice, it is preferable within this zone indicated by the dashed line to backfill the anchor holes with some material that will not develop a bond between the anchorage material and the surrounding soil. Beyond the dashed line, anchors must be grouted far enough to develop the required resistance by bond or belled anchors must develop the necessary bearing capacity.

If properly grouted, anchor rods or tendons must develop an ultimate bond resistance which is nearly equal to the shearing resistance of the surrounding soils.

In most cases, it is practical to apply prestress force to anchors. The equipment for prestressing can be used for performing pull-out tests to determine the ultimate capacity of a number of anchors to assure safety of the design. A factor of safety of about 2-3 must be taken into account based on the results of pull-out tests, to assign a design load to the anchors.

One of the principal advantages of a tieback bracing system is the ability at low cost to test each anchor at least to its expected working load. By this way the repair or replacement of defective anchors could be made and a possible failure by

inadequacy of individual anchors could be eliminated.

Performance of Tie-Back Support Systems

Table 2 shows a technical description of seven tied-back supporting system (after (Lough, 1975)). In all these cases the observed behavior of the structures has been reported.

It is observed that the soils retained by tied-back walls varied from sensitive clays to sands. But it must be noted that none of the walls were constructed in particularly difficult soils.

The methods of calculating anchor prestress loads are shown in Table 3. The important observation is that a considerable variety exists in these techniques. The main reason of this is that the state-of-the-art in this area is not well-defined.

Reported maximum lateral and vertical movements of the tied-back walls are shown in Table 4. Also shown are these movements expressed as a percentage of the wall height. Figure 29 shows the percent vertical movements plotted on the settlement chart devised by Peck for braced excavations. All of the reported settlements are found within the zone 1 on the chart, called the minimum settlement zone. After these figures, it has been concluded that the variations in the wall flexibility or prestress loads on the anchors did not have a significant influence on the movements of tied-back walls.

Another interesting common behavioral facet reported for all tied-back wall systems was the variation of the tie loads as the excavation progressed. In each case the loads in the tie rods decreased slightly from their prestress value as the excavation was cut.

It could be said that design procedures presently used for prestress loads for tie-back walls are quite variable. However, movements behind these walls regardless of the prestress loads have been small. Finally, obtaining secure anchorage in soft clays had been found to be difficult, and additional investigation could be useful to maintain the stability of the tie-backs during whole excavation.

Table 2. Description of Tied-Back Walls with Observed Behavior (after Clough, 1976).

Reference	Max. Wall Height (H) - Ft	Type Wall	EI/ft. Kip. ft.	Type Anchorage	Soils
Kapp	60	Slurry Trench	90000	Grouted into rock	Dense Sand-Fill - Organic Silt
Mansur & Alizadeh	45	Soldier Pile 14 wf 61 8 ft. o.c.	17000	Fully Grouted tie-rod	Silty Clay-Shale
Rizzo, et al.	37	Soldier pile		H-piles	Sand-Silt
Shannon & Strazer	78	Soldier pile 8 wf 35 3 ft. o.c.	8700	Grouted Bar in Soil	Dense Sands- o.c. Clays
Clough, et. al.	65	Soldier pile 8 wf 35 3 ft. o.c.	8700	Grouted Bar in soil	O.C. Clays
Liu & Dugan	55	Soldier pile 2 15 [33]		Grouted Bar in Soil	Sand-Clay-Fill
Larson et al.	50	Soldier pile 14 bp 89 6 ft. o.c.	32000	Grouted Bar in soil	Dense Sand

Table 3. Reported Methods of Calculating Prestress Loads (after Clough, 1976).

Reference	Method
Kapp	Percentage of Allowable Tie-Rod Load (20-60%)
Mansur & Alizadeh	At-Rest Pressures
Rizzo, et al.	Active to At-Rest
Shannon & Strazer	50% Anchor Yield Load
Clough, Weber and Lamont	Terzaghi-Peck Rules (0.47H)
Liu & Dugan	15 x Height Wall (in psf)
Hanna & Matallana	Pressures Halfway Between Active and At-Rest
Oosterbaan & Gifford	Active pressures
Larsen, et al.	Pressures Between Active and At-Rest

Table 4. Tied-Back Wall Movements (after Clough, 1976).

<i>Reference</i>	<i>Maximum Settlement Behind Wall Δ - ft.</i>	<i>Δ/H %</i>	<i>Max. Wall Lateral Movement δ - Ft.</i>	<i>δ/H %</i>
<i>Mansur & Alizadeh</i>	0.09	0.20	0.05	0.11
<i>Rizzo, et al.</i>			0.15	0.40
<i>Shannon & Strazer</i>	0.25	0.30	0.25	0.32
<i>Clough, et al.</i>	0.06	0.10	0.10	0.15
<i>Liu & Ougaz</i>	0.05	0.09	0.05	0.09
<i>Larson, et al.</i>	0.08	0.16	0.08	0.16

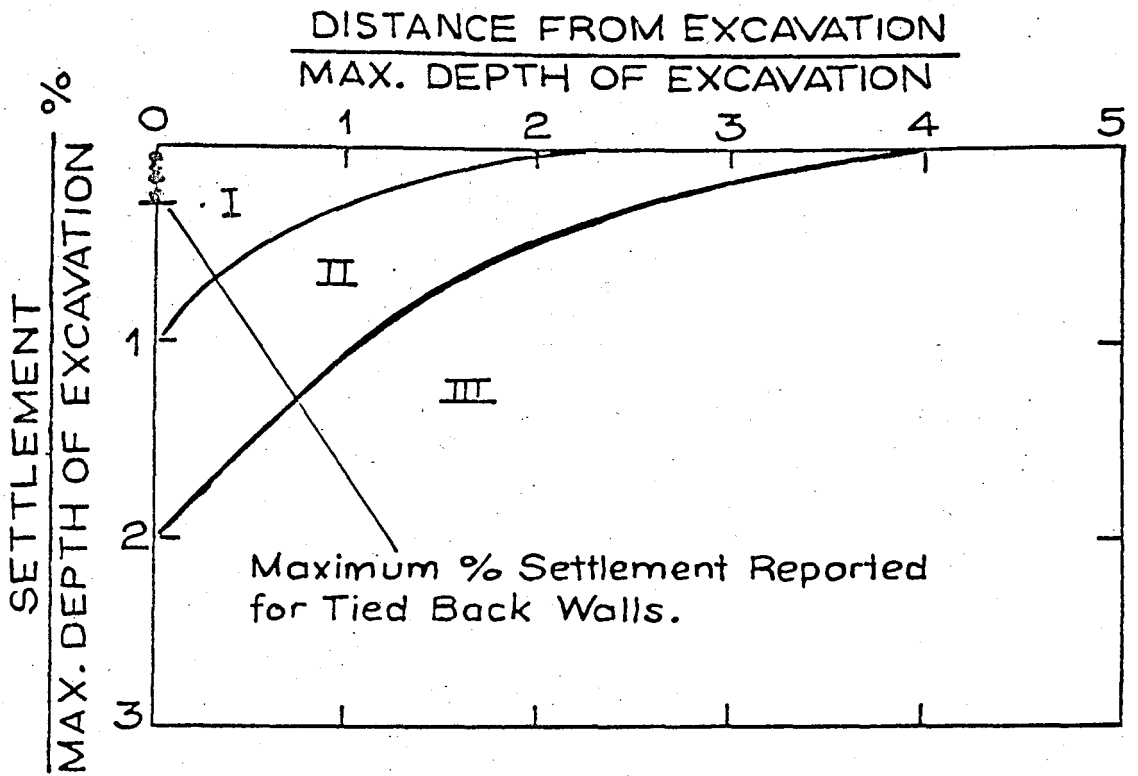


Figure 29. Reported Tied-Back Wall Settlements (after Clough, 1976).

5.6 ANCHORED BULKHEADS

Anchored sheet-pile bulkheads are frequently used in port and foundation engineering. These bulkheads can be classified in the following way :

1-Materials Used

2-Type of Anchorage

3-Construction Sequence

1-Materials Used : Timber Sheet Piles are used for temporary sheeting or for cantilevered shore protection walls of 2-3 m height.

Reinforced Concrete Sheet Piles of great variety of cross sections are used. Straight Web Piling Bar is the most commonly used. Prestressing of concrete sheet pile reinforcement may be an advantage, especially in seawater, since cracking of the concrete in the tension zone is thereby largely eliminated and the danger of corrosion of the reinforcement is decreased.

Steel Sheet Piles are the most commonly used, because they: are the most economical; have a great variety of cross section; are stiff enough to be driven without buckling; are available in many different combinations to increase wall sectional modulus.

2-Type of Anchorage : Most of the troubles reported are caused by wrong design or poorly constructed anchorages. Figure 30 shows the typical types of anchors.

Single Deadman Anchor (Figure 30a) consist of a tierod and deadman.

Double (or More) Tie Rod Anchorages (Figure 30b-d). The reason to use more than one is to provide acceptable stresses in the sheet-pile wall. The disadvantage of this anchorage is the independent yield of both tie rods. This yielding depends mainly on elastic deformation of the rods and on the density of soil in front of the anchor. The anchorages shown in Figure 30c-d are preferable in nonuniform soil conditions. The tie rods must be placed as shown in Figure 31a with a negative

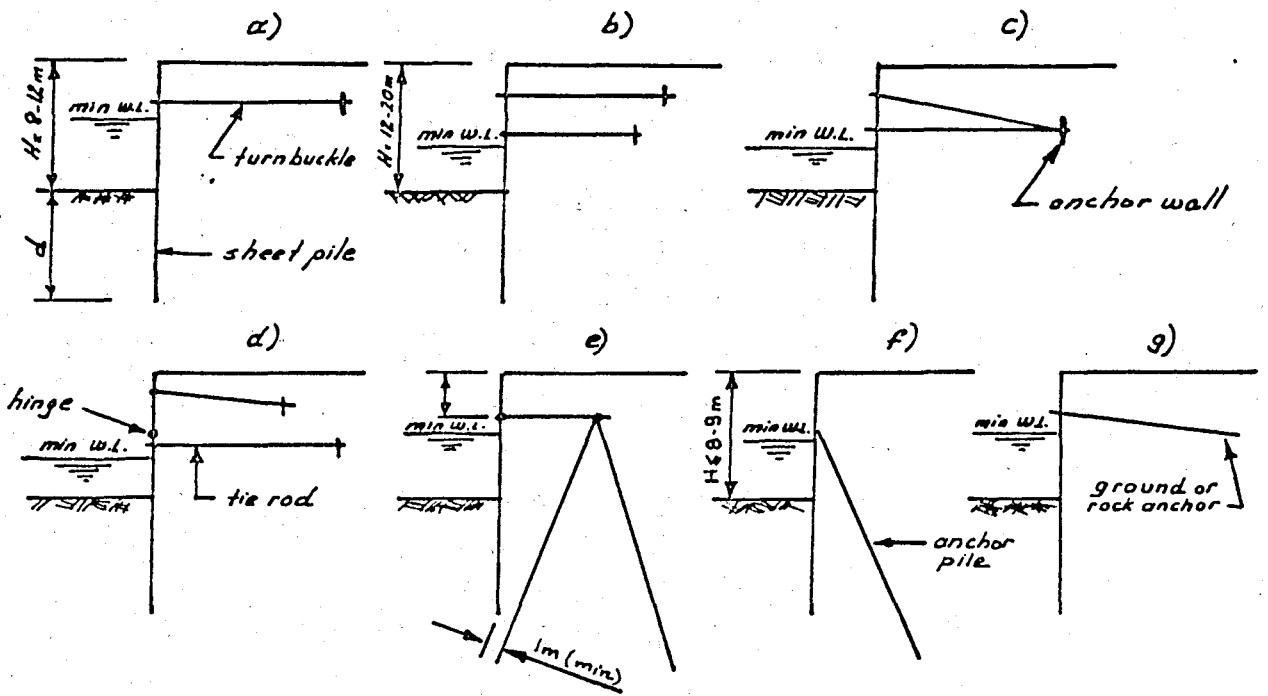


Figure 30. Anchored Bulkhead-Structural Schemes (after Tsinker, 1983).

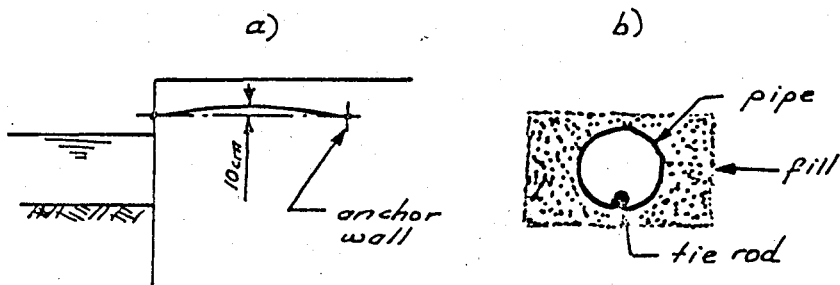


Figure 31. Placement of the Tie Rod (after Tsinker, 1983).

sag of about 10 cm to resist to the weight of overlying fill. Also, they may be placed in pipes, somewhat larger than the expected settlement of the fill, as shown in Figure 31b.

A-Frame Type of Pile Anchorage (Figure 30e)

Tschebotarioff recommends this type of anchorage in soft compressible soil which can not be removed by dredging. Two tension piles are usually provided for each compression pile.

Anchor Piles (Figure 30f). The advantage of this type of anchorage is simplicity of construction.

Tsinker and Budin have shown that anchor piles could have a significant effect on sheet pile wall design. It has been found that rigidly joined a bulkhead/anchor pile system works as a rigid frame, and this results in reduction of bending moment acting in the bulkhead. This reduction depends on the ratio $n = (IE)_f / (IE)_p$ where $(IE)_p$ is the rigidity of anchor piles per meter of the bulkhead and $(IE)_f$ is the rigidity of sheet pile wall per meter. For $n \leq 10$ the reduction of bending moment is insignificant but the vertical component of anchor force to the sheet piles has to be considered in design of the bulkhead.

Soil and/or Rock Anchor (Figure 30g) consist of a stressing tendon (rod or cable) which connects a fixed anchor to a bulkhead. Anchors are usually inclined downwards, transmitting the vertical component of anchor force into the sheet pile. When the tie rod is fixed within the rock, the yield of the system will be equal to the elastic elongation of the tendon only and, therefore will be negligible: this is called a "rigid anchor".

3-Construction Sequences. The two basic type of construction sequences are :

1-Backfilled Construction, where the construction sequence is shown in Figure 32a is: dredging; sheet pile driving; anchor construction; and backfilling.

2-Dredging Construction (Figure 32b) ; sheet-pile driving; construction of anchor system; backfilling (if required) ; and dredging.

In Figure 32, the deflection of the bulkhead in both cases of the wall construction is shown. Where,

1=a natural slope

2=dredged line

3=anchorage

4=backfill

5=sheet-pile deflection (stage 1 of construction)

6=sheet-pile deflection (stage 2 of construction)

Soil Pressure

Since the sheet-pile bulkheads are considered as "flexible" the problems involved with them are more complicated than those of regular retaining walls.

The soil pressure is the main force acting against the sheet-pile wall. The magnitude of this pressure depends upon the physical properties of the soil and the character of the interaction of the soil / structure system.

Lasebnik has established a relationship between the degree of sheet pile flexibility, expressed as,

$$\rho = H^4 / EI \quad (5.7)$$

and the reduction of actual bending moment as compared to conventional methods employing active pressure as a basic load distribution against the wall. Here, "H" = the height of the wall (in centimeters), and "EI" = the rigidity factor of the bulkhead (in kg-cm² per one meter of the wall). Figure 33 shows the relationship between the sheet piles' deflection, bending moments, and soil pressure (after Lasebnik). In the figure, curves 1 and 4 represent deflection and bending moment for the bulkhead $\rho = 0.55$; curves 2, 5 and 8 represent deflection, bending moment, and soil pressure for the bulkhead $\rho = 2.12$; curves 3, 6 and 9 represent deflection, bending moment and soil pressure for the bulkhead $\rho = 8.2$; and 7 represents bending moment determined by using a conventional method ($\delta_a = 0$ and $\delta_p = \frac{2}{3}\phi$). R_4, R_5, R_6, R_7 are reaction forces corresponding to bending moments represented by curves 4-7.

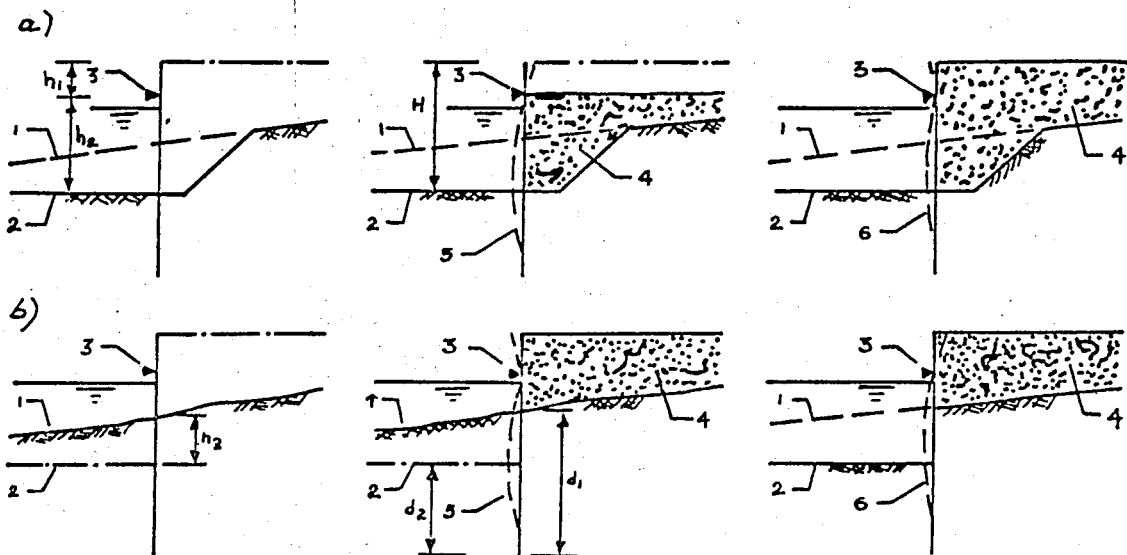


Figure 32. Construction Sequences: a-Backfilled Bulkhead, b-Dredged Bulkhead, Heredity Effect. (after Budin, 1979).

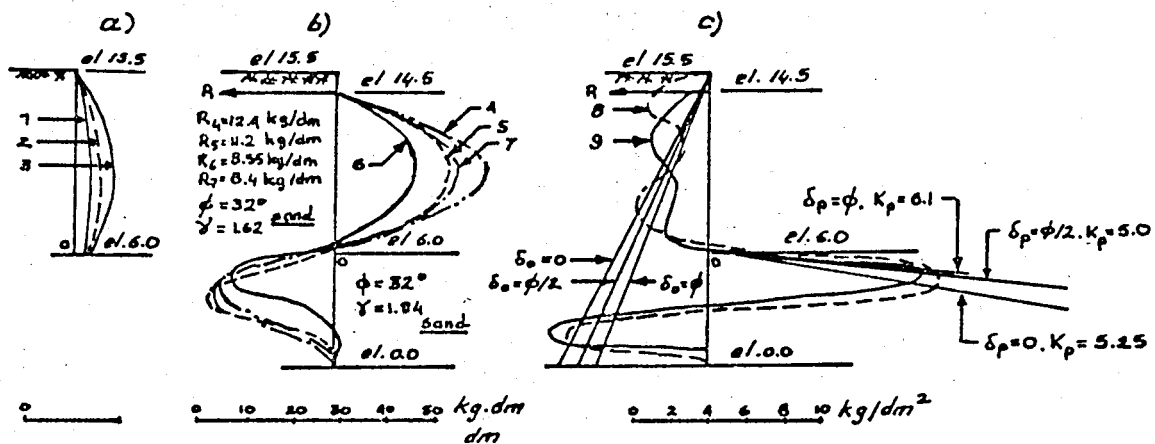


Figure 33. a-Large-Scale Model Bulkhead Deflection, b-Bending Moment, c-Lateral Pressures. (after Lasebnik, 1961).

- Some of Lasebnik's principal conclusions are as follows:
1. Bulkhead flexibility has a dramatic effect on bending moment and reaction force. Reduction of bending moments is especially drastic in the range of $\rho = 0.2-6$. Further increase of bulkhead flexibility has no significant effect on reduction of bending moments. Anchor force for rigid walls with non-yielding anchorage could be 30-40% larger than that determined by using Coulomb's soil pressure theory.
 2. The total active pressure against a flexible wall is 25-30% smaller than that acting against a rigid wall.
 3. In all cases investigated, under different locations of anchor tie rod the active pressure against the bulkhead above its anchorage never reached the value of passive pressure.
 4. It was found that bending moments and anchor forces depend on the yield of the anchor system. Yield of the anchor decreased the anchor force and the bending moment at bulkhead midspan and increased the bending moment at the point of sheet piles fixity into the soil.
 5. With values of $\rho \gg 5.6$, the anchor yield may not have a significant effect on the shape of the active pressure diagram. The total area of an active pressure on a flexible bulkhead with yield anchors is very close to that determined by Coulomb's theory under various values of δ . Here δ = angle of friction between soil and sheet pile.

Design of Anchored Bulkheads

There are two basic types of anchored bulkhead design procedures which are in common use today:

- a- Free Earth Support Method
- b- Fixed Earth Support Method

Free Earth Support Method is based on an assumption that the soil into which the sheet pile is driven is incapable of producing an effective restraint from passive pressure to the extent necessary to induce negative bending moment. The second method is based on the assumption that the sheet pile is driven deep enough so that the soil beneath the dredge line provides the deflected shape of the pile which reverses

its curvature at the point of contraflexure and becomes vertical. Thus, the bulkhead acts as a built-in beam subjected to positive and negative bending moments.

In the case of retaining structures, soil pressure is the principal load acting against them. Since most of the time the soil is not homogeneous, the determination of soil pressure is somewhat difficult. The nonhomogeneity of soils also affects the mechanism of soil-structure interaction. As mentioned before, the state-of-the-art in this area is not well established, and most of the designers still rely on past practice.

Usually, bending moment and reaction force acting in an anchored bulkhead can be determined by;

$$M_D = M_{\max} \cdot K_M \quad (5.8)$$

$$R_D = R_a \cdot K_R \quad (5.9)$$

where M_D and R_D are design bending moment and design reaction force; M_{\max} and R_a are the values of bending moment and reaction force obtained on a basis of Coulomb's theory of earth pressure acting against the bulkhead; and K_M and K_R are factors to obtain more or less realistic values of design bending moment and reaction force.

It was found that the values of K_M and K_R depend on the rigidity of bulkhead, ratio $n = h_1 / h_2$ (see Figure 32), yield of anchor system, density of foundation soil, and conditions created by backfilling behind a flexible anchored sheet-pile bulkhead.

The values recommended by Budin (1979) for K_M and K_R are given in Table 5. They are based on data observed from results of numerous large-scale and field observations of anchored sheet-pile bulkheads.

The values of K_M and K_R given in Table 5 assume that the actual distribution of active pressure acting against the wall is somewhat different than that determined by the Coulomb theory. They assume possible load concentration at the level of anchors and possible unequal yield of adjacent anchorage.

Table 5. Imprical Values of K_M and K_R (after Budin,1979).

$h_3/H - h_1$ (1)	$n \leq 0.25$		$n > 0.25$	
	K_M (2)	K_R (3)	K_M (4)	K_R (5)
1	0.6	1.65	0.56	1.7
1/2	0.65	1.6	0.6	1.65
1/3	0.7	1.5	0.65	1.55
0	0.74	1.4	0.7	1.45

Table 6. Factors of Safety. (after Tsinker,1983).

Part of bulkhead (1)	Load Condition	
	Normal (2)	Extreme (3)
Sheet pile	1.1-1.3	1.05-1.1
Anchor system	1.5-2.0	1.2-1.5

As it can be seen in Table 5, the rigidity of the sheet pile and possible yield of anchorage were not taken into account directly. Lasebnik, on the basis of his and other studies, has suggested 24 typical schemes for analysis of anchored bulkheads. These schemes are shown in Figure 34. He recommends usage of Sokolovski's equation for determination of the coefficient of passive pressure K_p ;

$$K_p = \frac{1 + \sin \phi \cos \xi}{1 - \sin \phi} e^{\xi \tan \phi} \quad (5.10)$$

where ; ϕ = angle of internal friction

$$\xi = \delta_p + \arcsin \delta_p / \sin \phi$$

in which δ_p = angle of friction between soil in passive zone and the bulkhead.

The following design procedure is suggested by Lasebnik :

1. Density of foundation soil is established. The soil could be considered as "dense" with $D \geq 0.7$, and "loose" with $D < 0.7$. Here "D" is the relative soil density.

2. Preliminary calculation using the free earth support or fixed earth support method is performed. At this stage, values of $\delta_a = 0$ and $\delta_p = 3/4 \phi$ are used. Bending moment obtained as a result of preliminary calculations are used for preliminary selection of sheet pile size.

3. The preliminary designed bulkhead is then identified with one of the 24 schemes as presented in Figure 34. The identification is done according to preliminary values of "d" and "p" and assumed values of "D" and " Δ ". The values of Δ depends heavily on anchor yield. Anchors such as rock bolts or piled structures have to be considered as relatively unyielding. Others, like different kinds of anchor walls or ground anchors could be assumed as yielding. The value of " Δ " also depends on the density of a soil placed in front of the anchor.

4. The final calculation is than undertaken using the values of δ_a and δ_p as recommended by Figure 34. The shape of the passive pressure diagram will be as recommended by Figure 34, but the total area of the passive pressure diagram has to be equal to

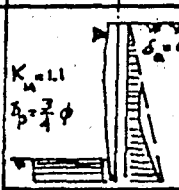
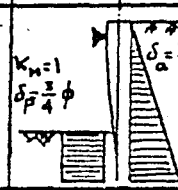
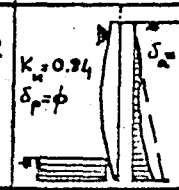
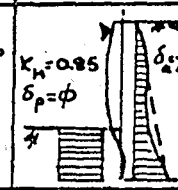
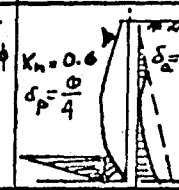
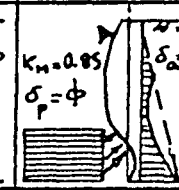
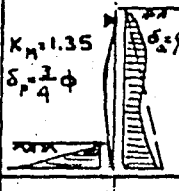
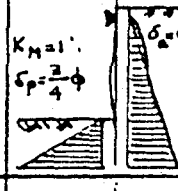
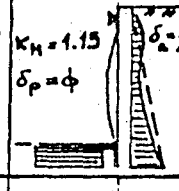
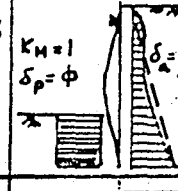
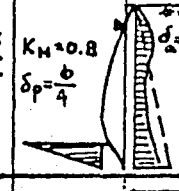
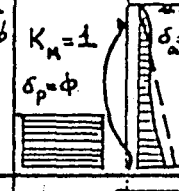
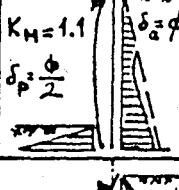
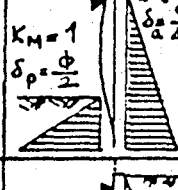
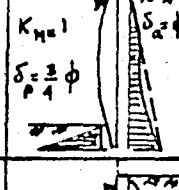
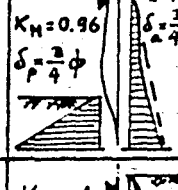
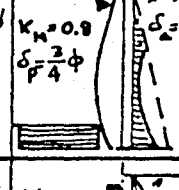
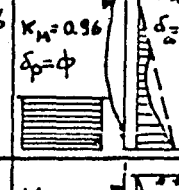
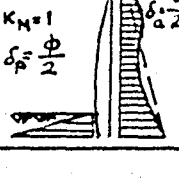
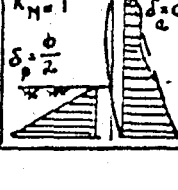
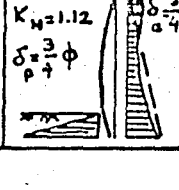
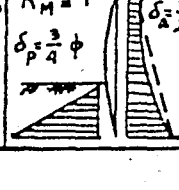
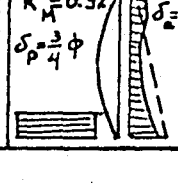
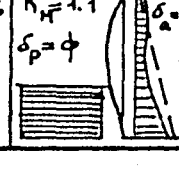
		BULK HEAD					
		RIGID $0.55 \leq \rho = \frac{H^4}{EJ} \leq 1$		MEDIUM RIGIDITY $2 < \rho = \frac{H^4}{EJ} < 4$		FLEXIBLE $\rho = \frac{H^4}{EJ} \geq 0.55$	
		F.E.S.	F _x .E.S.	F.E.S.	F _x .E.S.	F.E.S.	F _x .E.S.
		DENSE SOIL $D \geq 0.7$		DENSE SOIL $D \geq 0.7$		DENSE SOIL $D \geq 0.7$	
DENSE SOIL $D \geq 0.7$	YIELDING ANCHOR						
	NOT YIELDING ANCHOR						
LOOSE SOIL $D < 0.7$	YIELDING ANCHOR						
	NOT YIELDING ANCHOR						

Figure 34. Design Schemes. (after Lasebnik, 1961).

that obtained by using the conventional method of calculation with K_p determined by equation (5.10). The design values of bending moment will be obtained using the recommended value of K_m . For bulkheads with $\rho > 4$, if the bulkhead is designed according to fixed earth support schemes, the obtained value of "d" could be reduced by 20-25% (depending on soil foundation density). A value of K_R is recommended to be equal to 1.4 for unyielding anchors of "backfilled" bulkheads, and 1.5 for unyielding anchors of "dredged" bulkheads. For yielding anchors a value of $K_R = 1$ must be used."

Since the anchor system is the most sensitive part of a bulkhead, great attention must be given to its design and construction. Table 6 shows the recommended values of factor of safety for design of anchored bulkheads. This value would depend on the importance and desired durability of the structure.

5.7 SUMMARY

Some classical methods were reviewed and the behavior of flexible earth retaining structures was explained.

Design of sheet pile retaining walls and a practical design method for cantilever sheet piling in cohesive soils were presented. Braced cuts were examined, and modes of failures and loads on struts were determined. Tied-back cuts and their modes of failure, as well as their anchorage systems were shown and performance of tied-back systems was given depending on the previous reported cases.

The types and construction sequences of the anchored bulkheads were described and a design procedure proposed by Lasebnik was given.

CHAPTER 6

CASE HISTORY STUDIES

6.1 INTRODUCTION

Traditionally, the design of temporary retaining wall structures has been based on semi-empirical methods usually set in terms of the equations of the classical Coulomb or Rankine earth pressure theories. This approach has proven to be satisfactory for structural design of retaining structure components. However, evaluation of the probable displacement behavior of retaining structure has been based on interpolation of only observational data. Since the observational data changes from site to site, the extrapolation of these results to each specific problem is very difficult.

For the above mentioned reasons the finite element method as an analytical technique that seemingly can provide a more reliable means for evaluating displacements and furnishing a stronger base from which to extrapolate performance is the best tool to deal with these problems. The principal advantages of the finite element method are that the soil and the structure can be considered interactively and that both design loads and expected displacements can be studied. Thus, the finite element method makes possible to compare various system designs for minimizing displacements within an analytical rather than an empirical framework. Also, the nonhomogenities in soil parameters can be considered with greater facility than with classical methods and actual construction sequences can be accounted for. In recent years, many applications of this technique as applied to tied-back and braced walls have been reported.

6.2 DESIGN AND OBSERVATION OF A TIED-BACK WALL, CASE No: 11

The bank of California Center, have being constructed in Seattle, Washington, consists of a 42-story office tower and a

low-rise bank building. A parking structure extending as deep as six level below grade, exists under the whole structure. During its construction, an excavation of 240' x 250' in plan and upto 64' in depth has been performed. The foundation soil is highly overconsolidated clay. A soldier pile and prestressed tie-back system with as many as six rows of tie-backs was employed to support the excavations.

In this section, the observed behavior of the tied-back wall is presented based upon the studies made by Clough, Weber and Lamont, 1972. In addition, the results of two series of finite element analyses of the wall are described. The first series were conducted by Clough before the wall was built as a part of the original desing study. The second series were also conducted by Clough after the wall was built in an effort to simulate as closely as possible the actual construction sequences.

Both cases are reanalyzed and two series of finite element analyses were performed. During these analyses, the soil and initial conditions as well as the construction sequences and the finite element meshes are taken as the originals described by Clough. The results of these analyses were given with those of Clough on the same figures in order to see the resulting similarities or differences.

This sections including, site investigation, soil characteristics are based on the investigations made by Clough.

Site Investigation

The site, shown in plan in Figure 35, covered a city block area in Seattle.

Figure 35 shows the eight borings with their places. The soil profile which is shown in Figure 36 consists of a 15 to 20 ft layer of dense gravelly clay underlain by a deposit of stiff, fissured Seattle clay about 60 ft. thick. No static water table was found at the site.

Soil Characteristics

Laboratory tests on undisturbed samples were conducted to classify the soils and to determine their shear strength and stress-strain behavior. The most intensive testing was

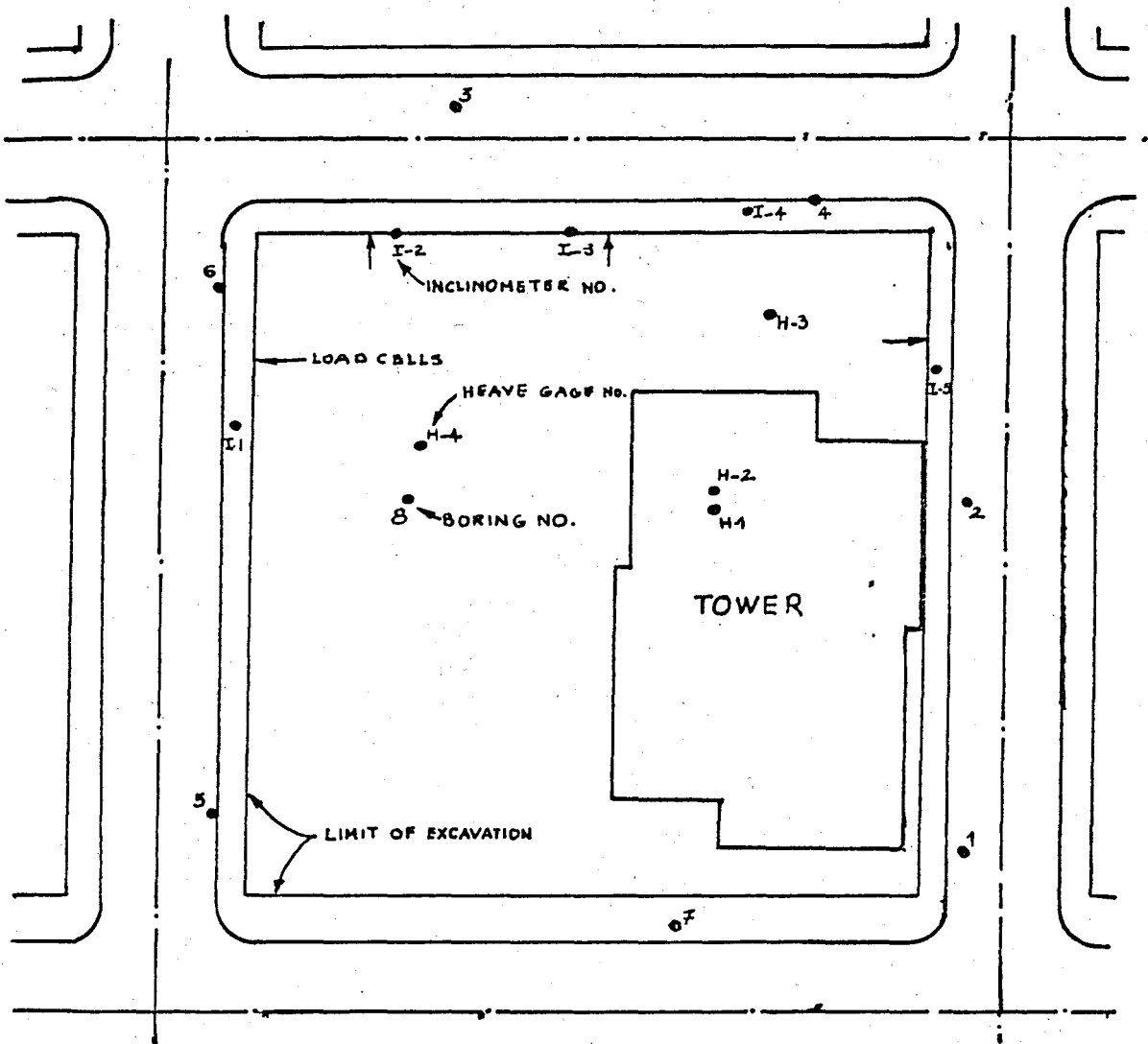


Figure 35. Site Plan, Tied-Back Wall, Case No. 1

performed on the clay because the excavation was confined to this material.

Unconsolidated-undrained triaxial tests, consolidation tests, K_0 tests, and direct shear tests were conducted to determine the stress-strain and strength characteristics of Seattle clay. Description of Seattle Clay—Seattle clay is a stiff-fissured, varved, lacustrine clay which has been overconsolidated by glacial ice. The bedding dip varies from nearly level to $10-15^\circ$ below the horizontal. The structure is broken by numerous shear zones with slicken sides on the contacts.

Consolidation tests show a preconsolidation pressure of 15 to 20 tsf, and the overconsolidation ratio (OCR) varies between 4 and 8. Stress-Strain and Strength Characteristics of Seattle clay were as follows. Undrained behavior was considered to best fit for the design, because the construction time was expected to be short relative to the consolidation rates observed for the clay. A total of 47 undrained tests were performed. A typical stress-strain curve from such a test is shown in Figure 37. As can be seen, each test specimen was confined at the overburden stress and sheared to failure. To provide data to define the unload-reload response, in a number of tests, the sample was unloaded and then reloaded before failure was reached.

The undrained shear strength for the clay is taken to be equal to 2.1 tsf. This value is obtained by simply taking the average of the data available for the strengths varying from 0.55 tsf to 3.75 tsf.

The stress-strain curves were evaluated by the techniques described by Duncan and Chang (1970) in order to obtain initial tangent modulus values and unload-reload modulus values. By these techniques, the stress-strain curve on primary loading is assumed to be a hyperbola and the unload-reload hysteresis loop is approximated by a straight line.

The variations of the initial tangent modulus and unload-reload modulus values with confining pressure are plotted on log-log scale to derive their functional relationship. If these variations are approximated by straight lines, the following

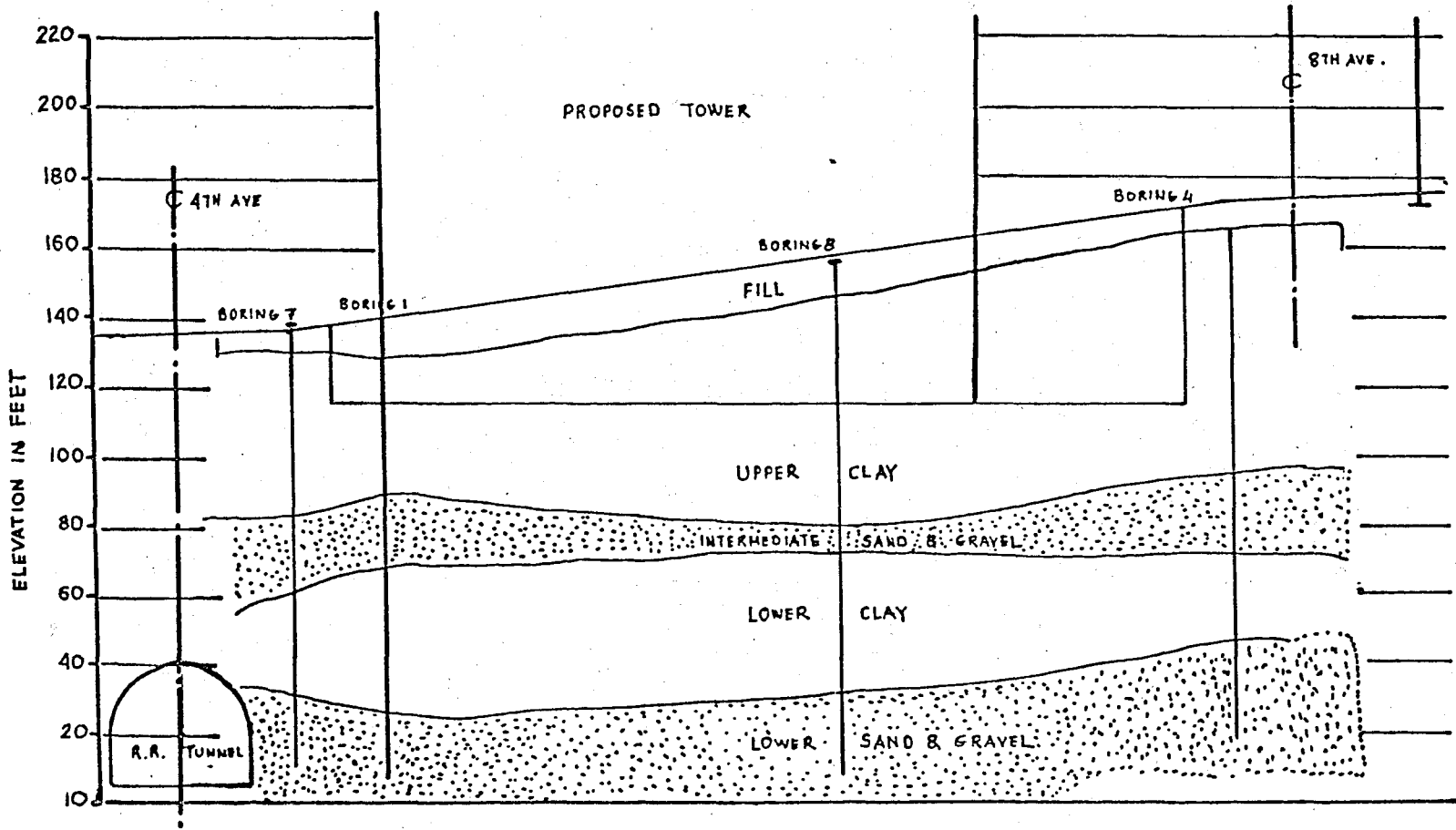


Figure 36. Soil Profile, Tied-Back Wall, Case No. 1

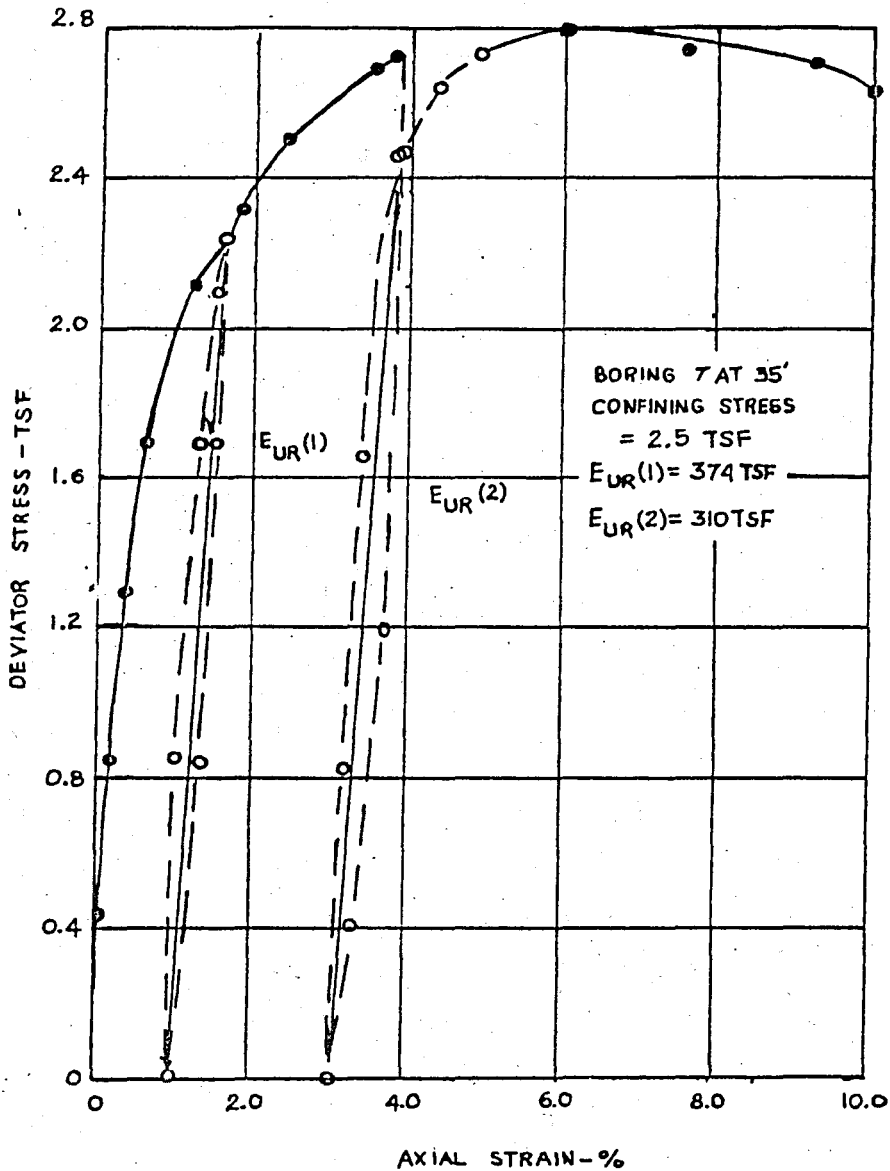


Figure 37. Triaxial Compression Test Data, Unconsolidated-Undrained, Tied-Back Wall, Case No. 1 (after Clough, Weber and Lamont, 1972).

equations describe the lines ;

$$\epsilon_i = 200 p_a \left(\frac{\sigma_3}{p_a} \right)^{0.55} \quad (6.1)$$

$$\epsilon_{ur} = 350 p_a \left(\frac{\sigma_3}{p_a} \right)^{0.55} \quad (6.2)$$

Three drained shear tests were conducted on clay in order to check the wall design for drained conditions. The strength at maximum deviator stress was defined by an angle of internal friction of 24° with 0.35 tsf cohesion. The residual shearing strength was defined by an angle of shearing resistance of 20° .

Initial Stresses in Seattle Clay-The coefficient of earth pressure at rest, K_0 , for Seattle clays with essentially identical characteristics to those at the site has been shown by Sherif and Koch (1971) to be between 1.4 and 1.6. Estimates of the K_0 values using the data of Brooker and Ireland (1965) suggest similar values between 1.3 and 1.7. Therefore, an average value of 1.3 was assumed in the analyses of the wall system.

Design Analyses

Usually, the design of tied-back wall systems is based upon empirical earth pressure diagrams such as those suggested by Terzaghi and Peck (1967). But, since the available data for the movements of a tied-back wall in an overconsolidated clay is very limited and the experience is meager, it was decided to attempt to analyse the wall by means of finite element techniques.

The finite element analyses were designed to simulate the observed soil behavior, the initial stresses, and the construction process. The soil behavior was simulated by a non linear elastic approach described by Clough and Duncan (1969). This method allows the variation of shear modulus with the shearing and confining stresses. At the same time the bulk modulus was kept at a very high value to simulate the incompressibility of the saturated clay.

The finite element mesh for the design studies, shown in Figure 38, was drawn to account for the presence of the wall and to allow for future representation of the various excavation levels and tie-back anchors. A rigid base at the bottom of the mesh was assumed to exist at the level of first clay-sand contact and the wall was assumed fixed at the bottom of the mesh. The soil above the rigid base was assumed to consist only of Seattle clay. The upper dense clay was neglected as a conservative design convenience. The same mesh was used during the re-analyses of the problem.

The tie-back loads were estimated using the Terzaghi-Peck (1967) recommendations.

In the analyses, the excavation and tie-back installation sequence were simulated by an incremental loading technique. As a first step, the soil was "excavated" to the first tie-back level; then the installation and prestressing of the tie-back at that level was simulated. In this process, the soil elements in the anchor zone were replaced by elements having the properties of concrete. Equal and opposite nodal point loads were then applied to the end of the anchor and at the face of the wall to simulate the effects of the prestressing loads. Then, the connection between the anchor and the wall was made by converting to concrete the soil elements on a line between the anchor and the tie rod wall connection. This assumed that the tie rod to be grouted over its full length. This procedure was then repeated until the final level of excavation was reached.

The discontinuous soldier pile wall was simulated in the analyses as a continuous wall having a flexural rigidity which was equal to the actual wall.

The number of elements used for the reanalyses of the problem are not equal to those used in the analyses of Clough.

Results of Finite Element Design Studies

Predictions for deflections and stresses of the wall and the soil were obtained for each stage of excavation. Figure 39 shows a typical example of boundary displacements for the soldier pile system before and after tensioning the last row of

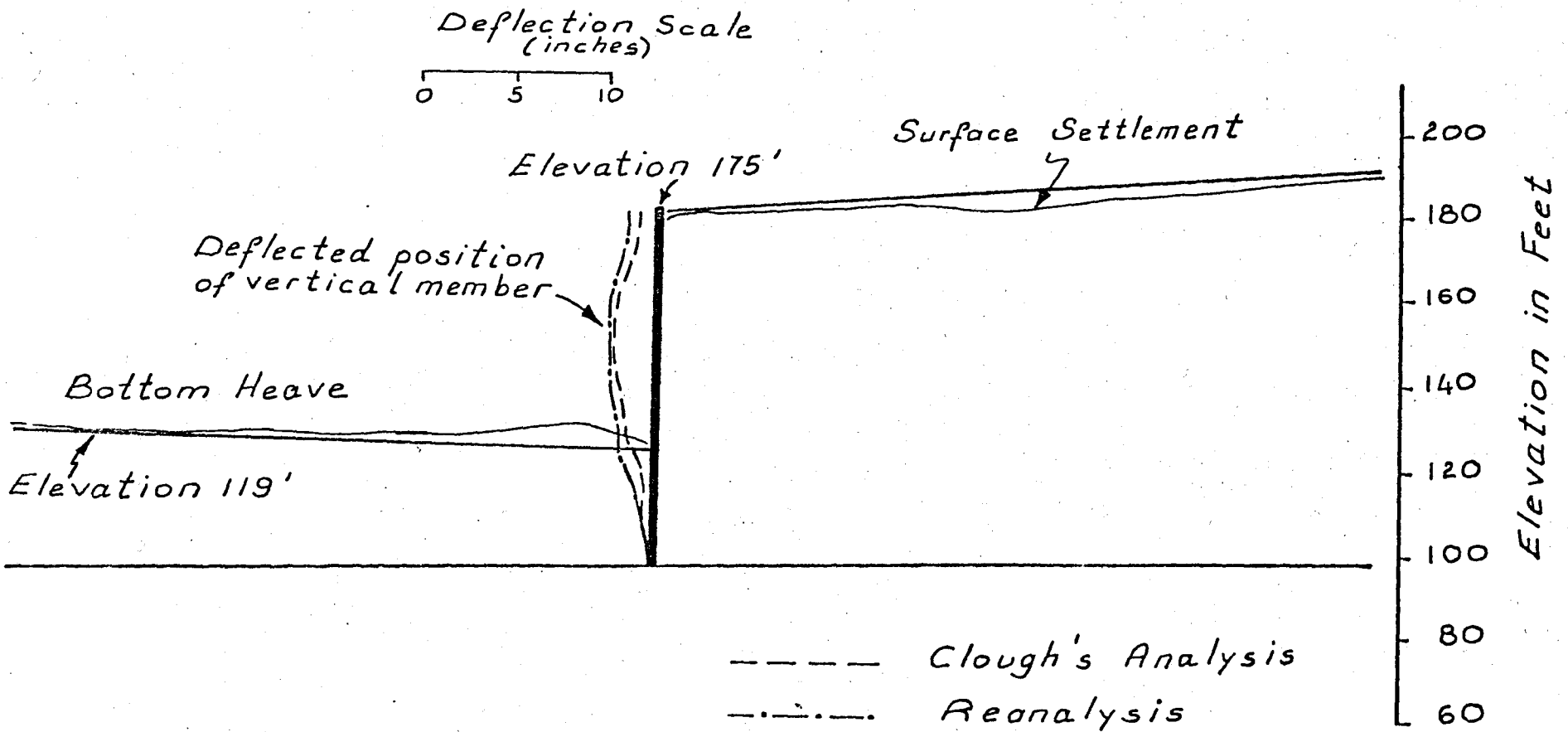


Figure 39. Computed Boundary Displacements.

tie-back anchors. In the figure both of the solutions of Clough's analyses and reanalyses are given. The displacement patterns appear consistent with observed behavior from similar excavations, also a good agreement is noted between the two finite elements analyses. The maximum lateral movement predicted was 2 inches (5 cm). The top of the wall was moved downward 1 inch as a consequence of the vertical component of the tie-back forces.

The predicted distribution of net lateral earth pressure before and after tensioning the last row of anchors for both analyses is shown in Figure 40. Note that the agreement between the solutions of Clough and solutions of reanalyses is very good. The small differences of these predicted stresses come from the unequal number of mesh elements.

No failure zones are predicted in both of the analyses. Only a few elements near the top of the wall failed in tension.

In the design studies Clough has shown that if the anchors were located 20 ft. behind a line inclined at 60° to the horizontal and extending from 5 ft. below the toe of the cut, the pressures on the wall would not be affected by the pressure bulb from the anchor itself. Also, it must be noted that the wall deformations would be smaller if the bearing end of the soldier pile was located in the sand rather than the clay.

Observed Wall Behavior

The observed behavior of the wall was generally in agreement with that predicted. However, Clough had reported that certain conditions assumed in the design analyses were not matched in the final design and construction. These are: the tendon bundles were not grouted beyond the anchor portion so that the assumption of concrete tie rods was not correct and the number of anchor rows used in construction was 6 instead of 4. Therefore, a second set of analyses must be performed to simulate the actual conditions of the excavation.

Figure 41 shows the observed behavior of the wall. In general the design analyses appear to have closely predicted the form of the wall movements. The bottom heave and wall bulge were somewhat less than estimated. Street settlement was greater than both

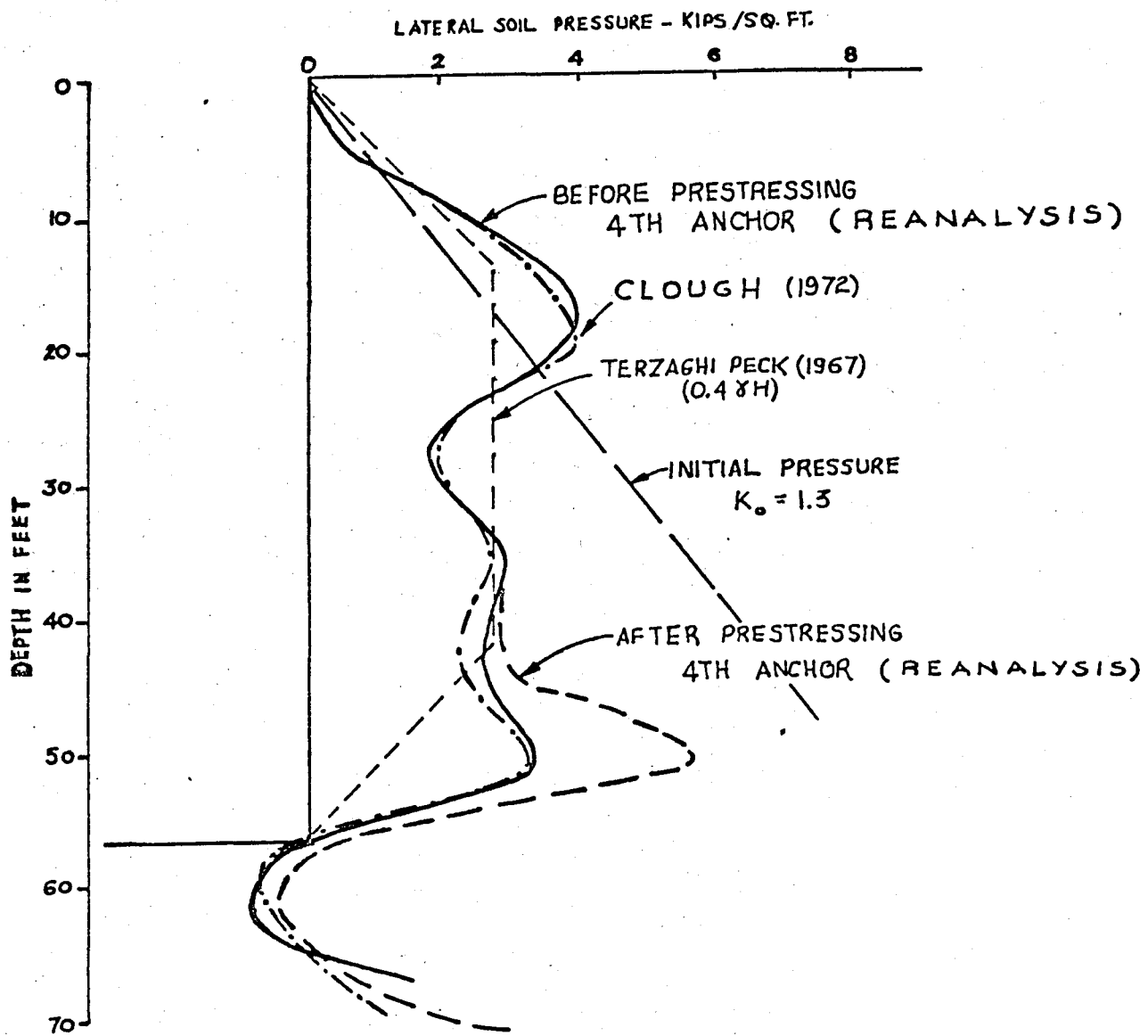


Figure 40. Distribution of Lateral Soil Stress.

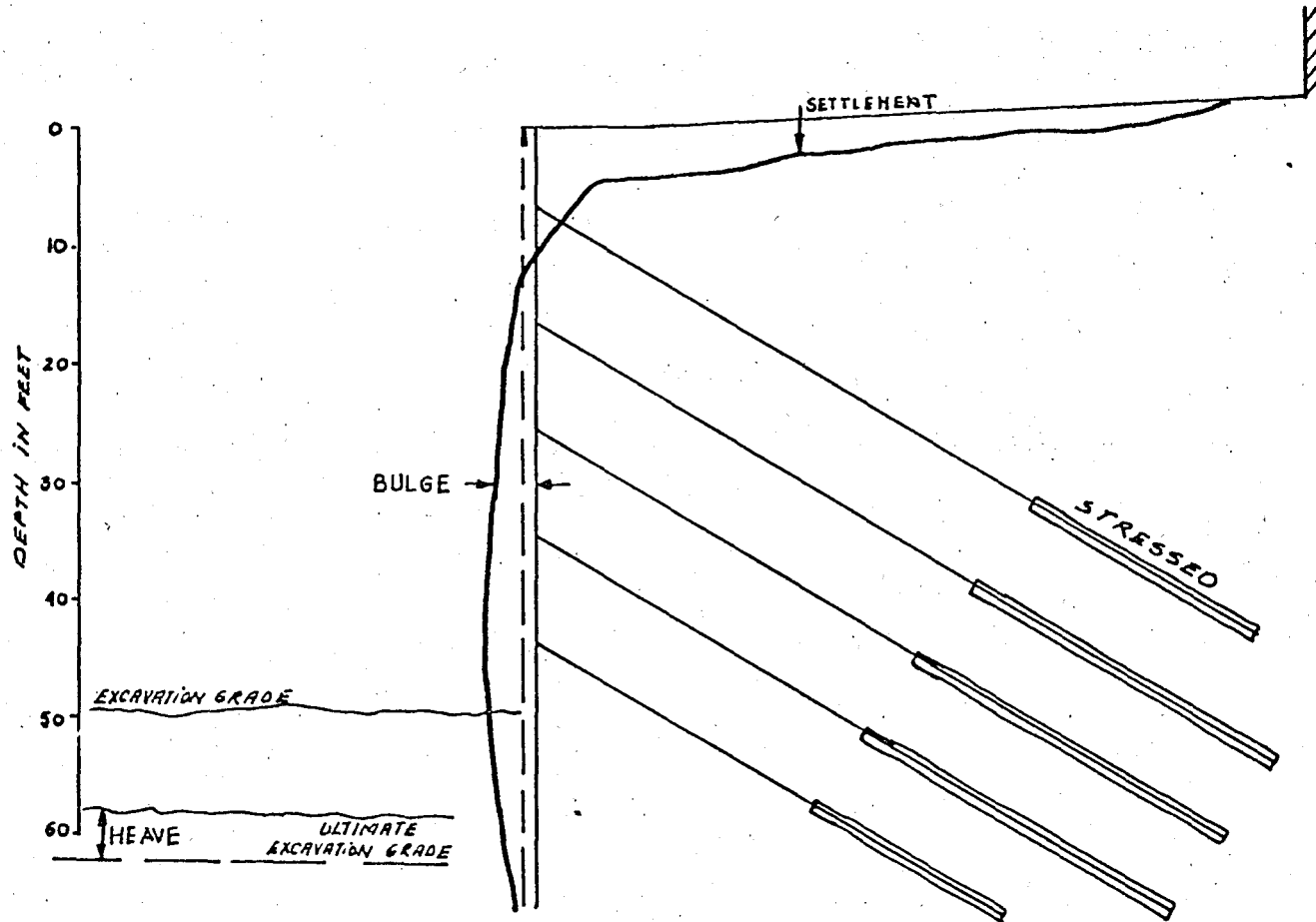


Figure 41. Observed Boundary Deflections, Tied-Back Wall, Case No. 1
(after Clough, Weber and Lamont, 1972).

analyses near the excavation. At the top of the wall an inward movement of about 2 inches occurred, but the design analyses results show an outward movement of the wall.

The variation of measured anchor loads is shown in Figure 42. The initial prestressing loads were retained in all load cells during the whole excavation. It was reported by Clough that this behavior was consistent with that predicted by the finite element analyses.

The tie-back loads are often been a confusing part of the analyses. Some investigations (Mansur et.al., 1970) have compared prestressed tie-back loads with the design soil pressure as proof of the accuracy of the soil pressure theory. However, Clough (1972) has shown that no such conclusion can be drawn. If a prestress load is applied by a shoring system which is inherently stable (i.e., the prestress load is greater than the minimum practical load to maintain stability), the measured tie-back load only reflects the prestressing load and is not a measure of the minimum lateral pressure which might have developed in the soil. Clough has reported that the conclusions to be drawn from a comparison of measured and design loads are:

- 1-The anchors must be placed far enough behind the wall to effectively sustain the load, and
- 2-The lateral earth pressure could not be any greater than that measured.

The reported tie-back anchors "loosening" on some other projects as the excavation proceeded, must arise from improper installation or anchor failure.

Post-Construction Finite Element Studies

In this second set of analyses, all the material parameters were kept equal to the design analyses. For this analysis, a new mesh was drawn as shown in Figure 43. The same mesh is used in the reanalyses of the problem, in order to compare the results with those obtained by Clough. The results of both post-construction analyses are shown in the same figure for the stresses and displacements. In this new mesh six rows of anchors were used. The sequence of excavation and anchor prestressing are shown

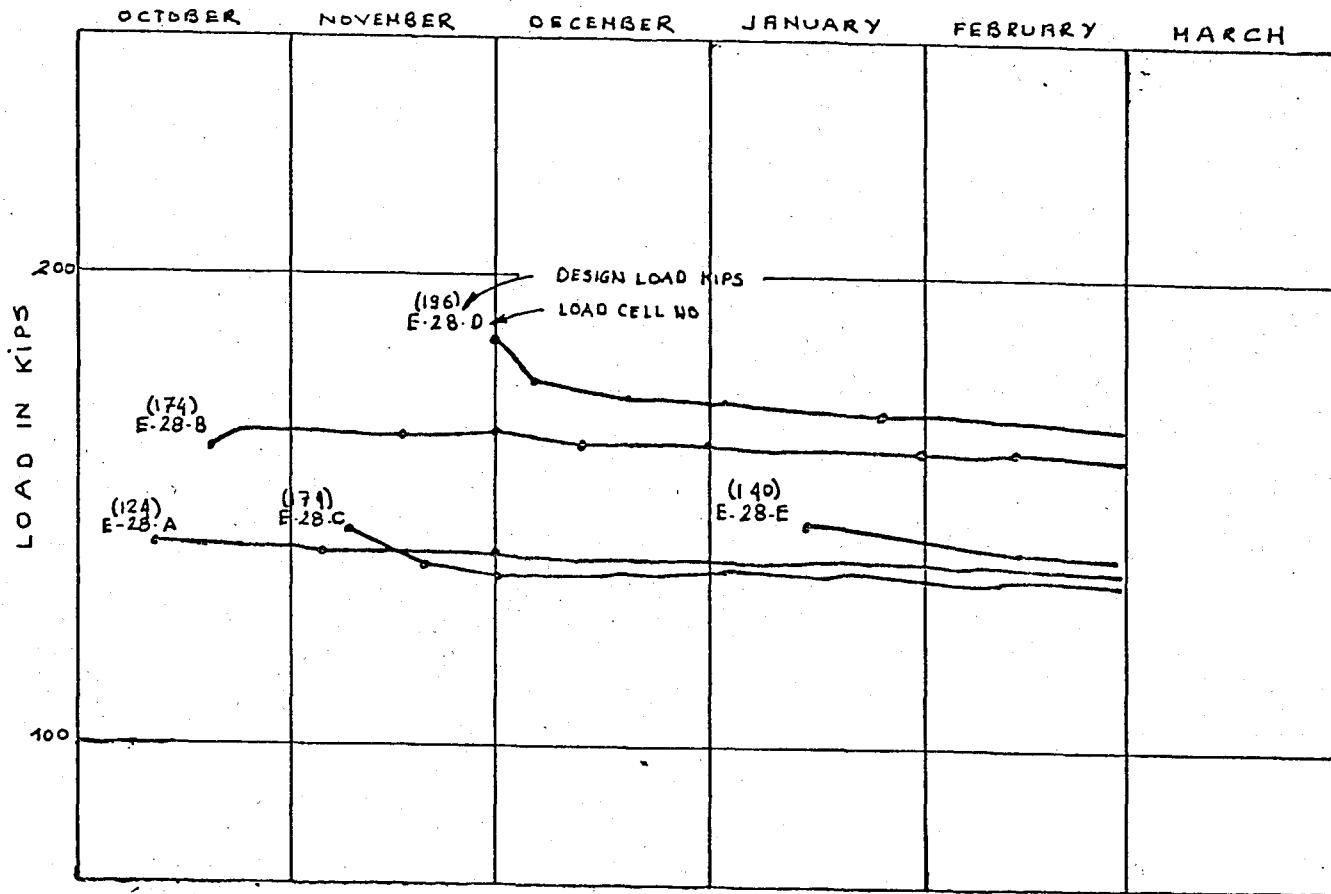


Figure 42. Tieback Load Data, Tied-Back Wall, Case No. 1 (after Clough, Weber and Lamont, 1972).

-06-

ANALYSIS SEQUENCE-EXCAVATION AND ANCHOR PRESTRESSING

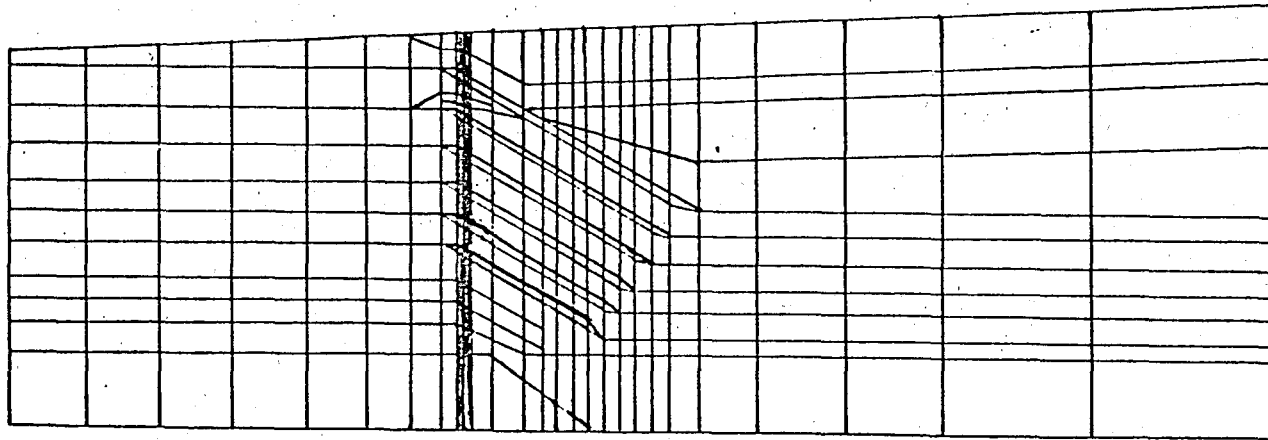
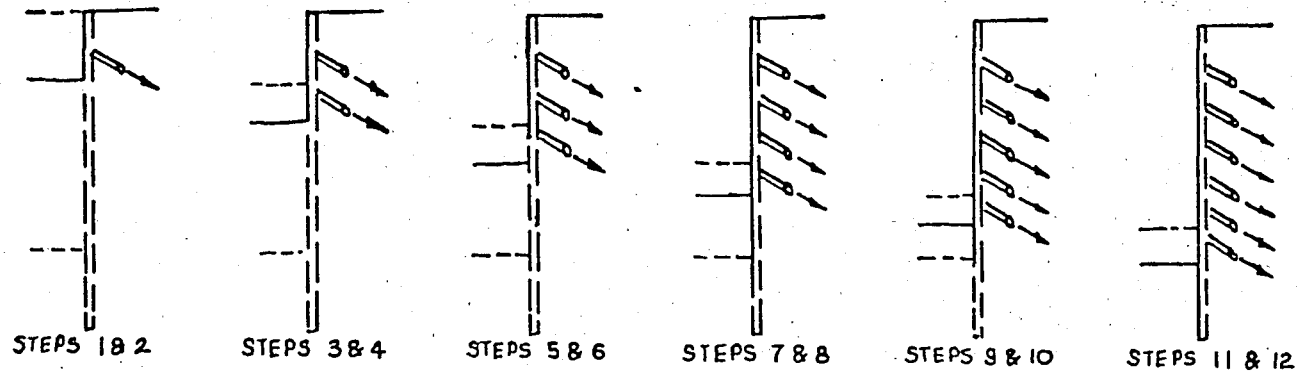


Figure 43. Finite Element Mesh-Post Construction Analysis.

in Figure 43. The lower sand layer is also taken into the mesh in order to best simulate the actual soil behavior.

An improved simulation of the anchor was also added. A one-dimensional bar element was used to connect the concrete anchor to the face of the wall. These elements are capable of sustaining only axial loading, and their area was proportioned according to the cross section of tendon bundles.

The observed wall movements as well as the results of the two finite element analyses are shown in Figure 44. In both analyses, the predicted deformed wall shape is very close to that observed. The small differences between the two predicted results arose from the simulation of anchor rods and structural material properties. The wall deformations are overestimated as shown in Figure 44.

The predicted distributions of net lateral earth pressure before tensioning the fifth row of anchors are shown in Figure 45. The initial lateral stresses for $K_0 = 1.3$ and the Terzaghi-Peck design pressures are also shown in this figure. The two resulting sets of finite element stresses are, in general, much lower than the original stresses, except at the top of the wall where they are higher. It can be seen that the predicted finite element pressures are in good agreement with the Terzaghi-Peck design pressures.

Discussion of Finite Element Analyses

A comparison of the finite element stress results with actual field load data raises some interesting points.

First, the agreement of results obtained from both analyses (Clough's analyses and reanalyses) is perfect. A small change in the shape of the finite element mesh does not affect the results, but this must be done by taking into account the critical stress zones.

Second, a definitive increase of lateral soil stress is noted at the tie-back levels. The soil stress is at its peak value at the tie-back location and drops between them.

Finally, anchor prestressing was excessive. A reduction of about 70% could be made on the last two rows of anchors. In fact,

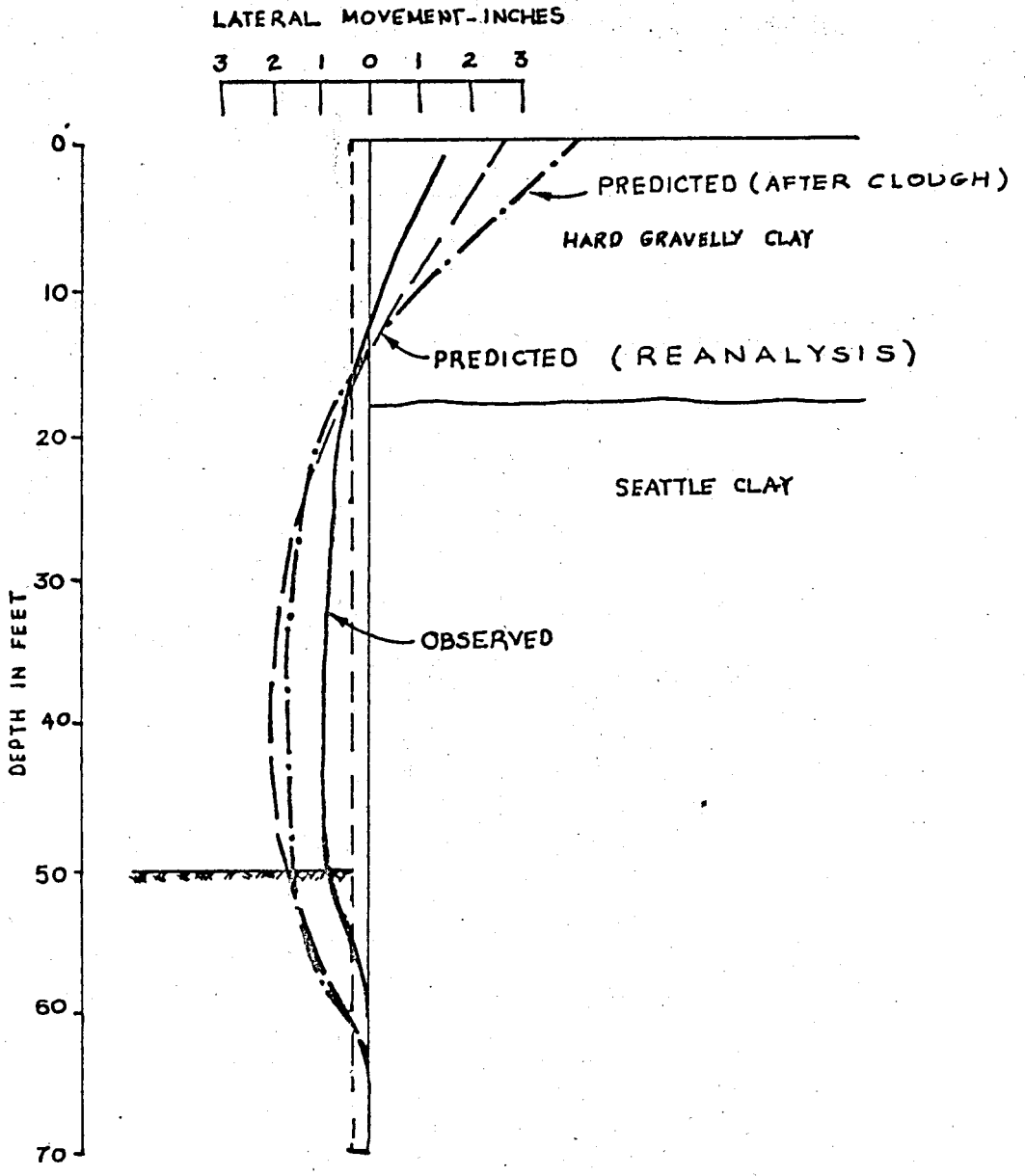


Figure 44. Predicted and Observed Lateral Wall Movements.

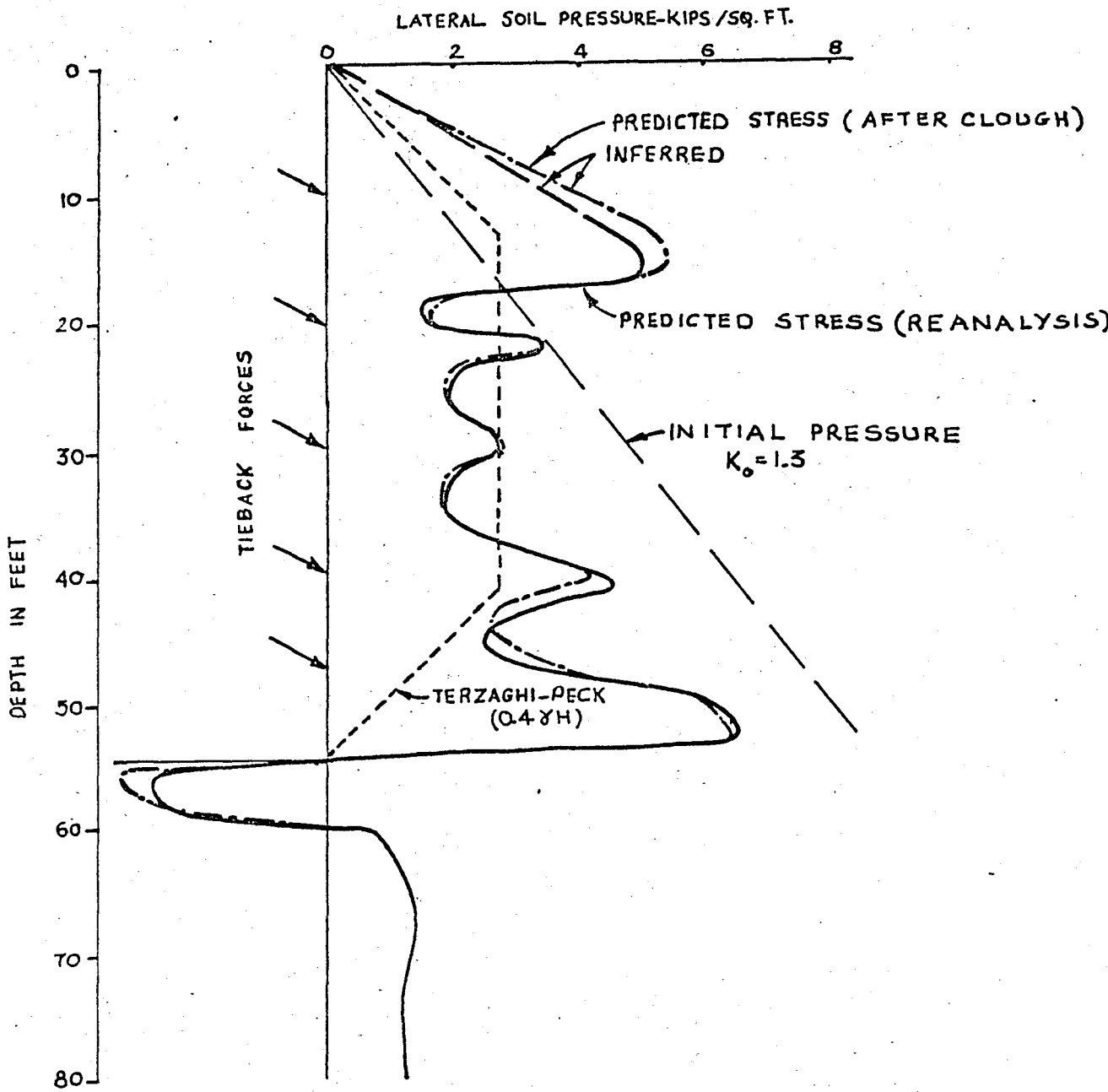


Figure 45. Distribution of Lateral Soil Stress.

it has been reported that in the actual excavation, the wall footings were installed without prestressing the last row of anchors. As a conclusion, it must be noted that a very little load had to be applied to the bottom of the excavation to maintain the stability of the wall.

This can be explained by only reviewing the finite element stresses as shown in Figure 45. In both analyses, the stresses on the wall below the fifth row of anchors were near to the initial at-rest condition, with $K_0 = 1.3$. This indicates that the mobilization of the soil strength is very small in this zone. The conclusion is that, the lateral restraint need not be applied until lateral movements produce soil stresses tending toward the active condition.

Conclusions

The tied-back wall system analyzed in this investigation was constructed in a highly overconsolidated clay. The reanalyses of the problem show that the design studies and post-construction analyses performed by Clough were a good approach to predict the behavior of the system. It has been noted that the observed behavior of the system was better than expected.

The prestressing of the anchors served to reinforce the pre-existing shear zones in the clay and prevent development of large lateral deformations. In the reanalyses, there was no possibility to measure the anchor loads, therefore the prestressing loads which could be obtained from the finite element analyses were not taken into account. Only, the nodal point loads developed as a consequence of the anchor prestressing were added to the incremental analyses.

The finite element method makes the comparison of various types of wall systems, anchor locations and wall depths possible thus a safe and economical design could be made.

These analyses could be useful also as a means of control during construction. Load reductions in the lower tie-backs and the elimination of some tie-backs altogether produced construction economies which more than offset the cost of the analyses. The post-construction analysis has also shown that even closer predictions

could be obtained by paying more attention to the details and the construction sequences.

The reanalyses show that the observed behavior of the wall system and the predicted behavior are in good agreement. However, there exists differences between the observed and predicted behavior. These differences can not be easily explained. In either analyses, the controlling soil parameters and the amount of anchor prestressing needed for tied-back walls in overconsolidated clays must be carefully examined. It has been suggested that further research is necessary on these subjects.

6.3 TEMPORARY EXCAVATION IN VARVED CLAY-CASE NO.2 and 3

The behavior of tied-back and braced retaining structures has been evaluated frequently in recent years, by using the finite element method. The purpose of this study was to examine two projects involving excavation into varved clay, to give the results of the observed and predicted results of the past analyses and to reanalyze these projects to see the versatility of the method on this problems. The results are given in the same figures to have a possibility to compare them with those obtained by Clough, Murphy and Woolworth (1975).

Project Descriptions

CASE NO.2-HARTFORD Basement construction for a 10-story office building in Hartford-Conn. required excavations up to 30 ft. (9m) deep through fill and varved clay into glacial till. In the excavation, it is decided to restrain the side slopes by a conventional "Berlin-Type", steel H-beam, timber lagging wall supported by prestressed tendon anchors grouted into underlying glacial till. Figure 46 shows the plan and section views of the excavation.

Terzaghi-Peck type earth pressure distribution is used to design the system. The undrained shear strength of the varved clay is taken as 400 psf (20 kN/m^2) and a unit weight of 120 pcf (1900 kg/m^3) is assigned to it. The actual range of undrained strengths measured in the laboratory was 400 psf-1200 psf.

For purposes of retaining structure studies, the glacial till was considered similar to the till at Bowline Point as described herein.

CASE NO. 3-BOWLINE POINT Construction of a cooling-water intake structure associated with the overall construction of a power plant at Bowline Point in Haverstraw N.Y., necessitated cutting a 50 ft (15 m) deep excavation through fill, organic silt, and varved clay into glacial till. A slope failure occurred during the open cutting. At this time the bottom of the excavation had been reached to elevations in the range of from -10 to -20. Following this failure, a number of stabilization alternatives were considered such as flattening slopes, cellular cofferdams, slurry trench walls and braced sheeting. The latter was selected as being most viable in terms of available space, practicality, and estimated cost. As a first step, the original cut was backfilled to elevation -20. Sheet piles then were driven and the excavation was carried to elevation -45 by bracing and sheeting with the strut and water system as shown in Figure 47. All of these materials were weak either naturally or as a consequence of remolding. For design purposes, an undrained shear strength of only 40 psf (2 kN/m^2) was assigned to these materials. On the east side of the site from elevation -14 to -30 the clay had been disturbed by the slope failure. For this reason, an undrained strength of 130 psf (6.5 kN/m^2) was used in design for this zone. Triaxial test results showed that undrained strength values of the undisturbed samples of varved clay, range from 400-1200 psf ($20-60 \text{ kN/m}^2$). For the initial design studies the lowest value, 400 psf was assumed in developing earth pressure loadings.

The glacial till was assumed to have an angle of internal friction of 35° and a buoyant unit weight of 60 pcf (960 kg/m^3). Drained conditions in the till were assumed. For the clay, undrained behavior was considered, because the corresponding lateral stresses were more critical than those for the drained case.

Specific Soil Properties At Project Sites

These data are obtained from the investigations and laboratory tests reported by Clough, Murphy and Woolworth. The most important soil parameters for the retaining structure design are undrained and drained shear strength and deformation moduli. The laboratory test results indicated that the varved clays at each site are slightly overconsolidated, with overconsolidation ratios in

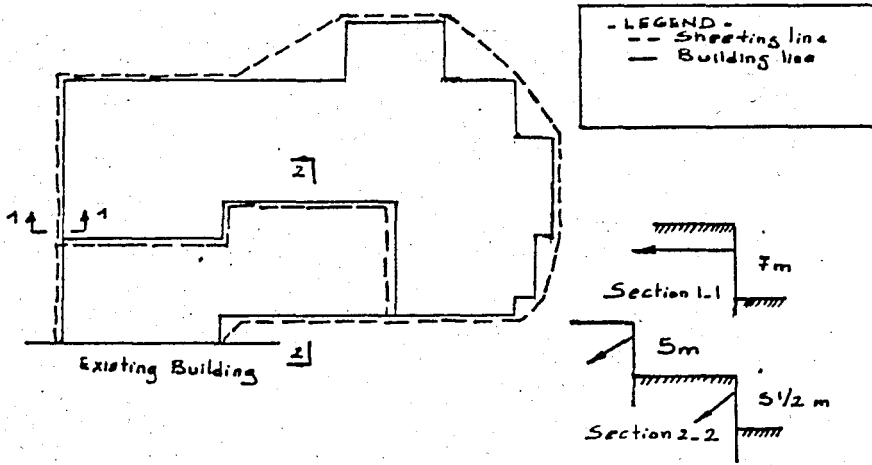


Figure 46. Tied-Back Excavation-Hartford, Conn., Case No. 2

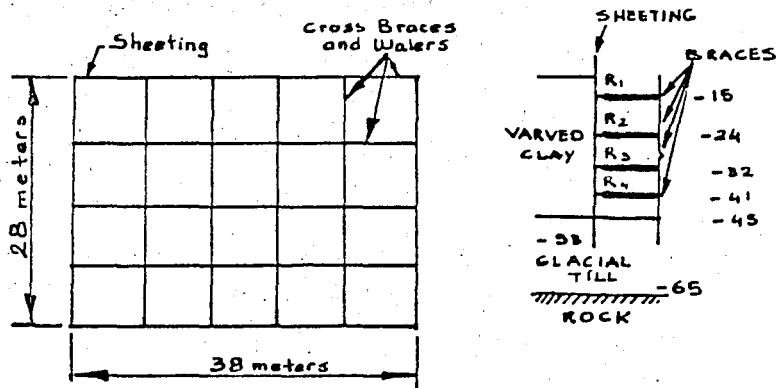


Figure 47. Sheeting and Bracing-Bowline Point, Case No. 3

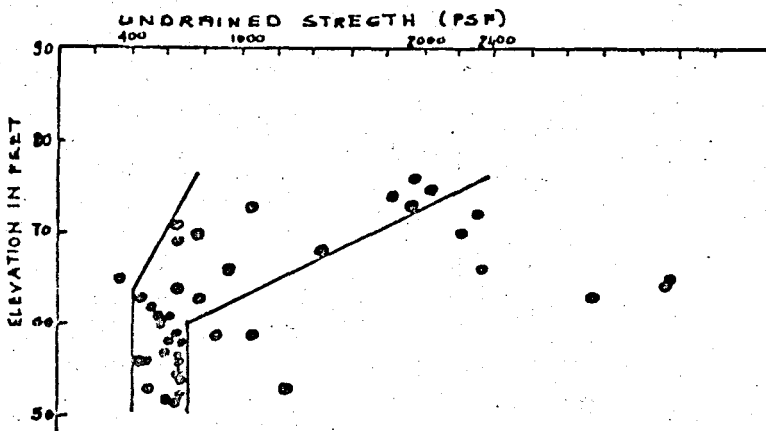


Figure 48. Undrained Strength Versus Depth-Hartford, Based on Field Vane Data

in the range of 1 to 3. They have undrained strengths in the range of 400-1200 psf, with $s_u / \bar{\sigma}_v$ ratios of about 0.10-0.25 and sensitivities of from 3-5. Initial tangent moduli E_i used in this study were based on $600s_u$. A typical field vane testing results are shown in Figure 48, for the Hartford excavation.

Finite Element Modeling-Hartford-Case No.2

The same approach of Clough, Murphy and Woolworth is used in this analyses. The movements in front and behind the wall are to be predicted by finite element analyses which were performed with the program Soil-Struct, a general purpose program developed by Clough and Tsui for analysis of soil-structure interaction.

Inclined spring supports located at the level of the actual tie-backs are used to simulate the wall and the anchorage system. The main reason of doing this is not to constrain unrealistically the wall movements by assuming that the wall and the tie-backs to be continuous planar elements. But, if the ties were assumed to be present as planar elements, the wall and the anchorage would be connected rigidly to each other to prevent the movement around the ties. The axial stiffness of the ties is assumed to be that of the actual tie divided by the horizontal tie spacing. The flexural stiffness of the planar wall is assumed equal to that of one of the soldier pile of the actual wall divided by the soldier pile spacing.

Figure 49 shows the finite element mesh for the two-tier excavation. The left boundary of this mesh is located at the center line of the excavation while the right boundary is located at a sufficient distance. This boundary was located by trial in order to not influence the behavior of the wall.

One dimensional interface elements are used on either side of the wall to allow for realistic relative movement between the wall and the soil. Adhesion strengths were assigned to the interface elements equal to one-half the soil shear strengths. In the analyses, a nonlinear elastic model of Duncan and Chang is used to simulate the soil behavior. The model assumes that as shear stresses increase the soil behavior is nonlinear, but that upon a decrease in shear stresses in a soil element the soil behavior is elastic. For saturated clays, the required inputs for this

model are the initial tangent modulus, the unload-reload modulus and the undrained strength of the soil.

Construction sequences of the walls were simulated as closely as possible to the actual construction of the wall: as alternate sequences of excavation and installation and prestressing of the anchors. For each increment two iterations were performed to allow for convergence of the nonlinear material properties to the values that best correspond to the stress levels existing in each increment. This is very important in the prestressed wall problem where loading and unloading occur in alternate cycles as a result of the alternating excavation and prestressing operations.

Soil Material Parameters and Initial Conditions-The till being about 10 ft (3m) below the bottom of the excavation in the analyzed sections, was taken as a rigid base. For practical purposes, the varved clay was assumed to have uniform properties with depth. Further, the soil was assumed to be isotropic and have the same shear strength in extension and compression. An undrained shear strength value of 400 psf (20 kN/m²) was used. The initial tangent and unload-reload modulus values for the nonlinear soil model were assumed to be 600 s_u . This value is about two to four times greater than those measured in the laboratory. In selection of this multiplier reliance was placed on recent experience in prediction of field performance in soft clays.

Initial stresses were computed in terms of an "at rest" condition with the lateral stresses, σ_x , determined as a function of the vertical stress, σ_y , as:

$$\sigma_x = K_o \sigma_y \quad (6.3)$$

where K_o is the coefficient of lateral earth pressure. This coefficient would be expected to vary with overconsolidation ratio in the varved clay. A simple value of one was used throughout the deposit.

Results-Hartford. Case No. 2

Figure 50 shows the results of the finite element analyses for the two tier excavation. A maximum of 10cm of lateral wall movements are predicted. Also shown is the results of the analyses performed by Clough, Murphy and Woolworth, for $s_u = 400$ and $s_u = 800$ psf.

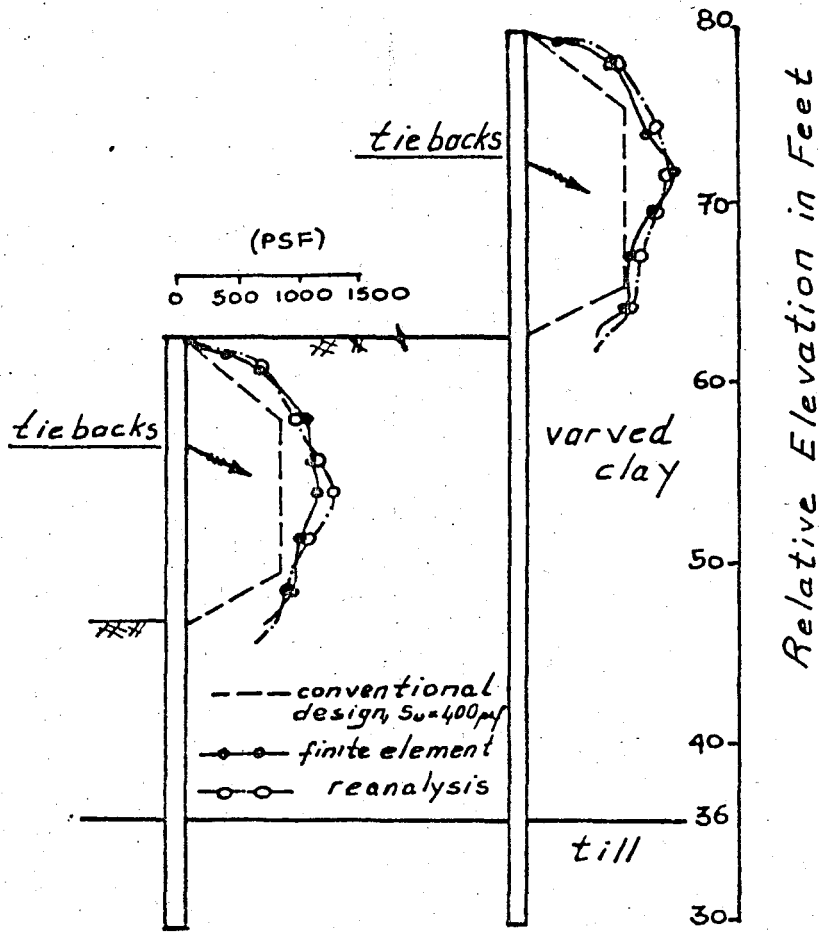


Figure 51. Earth Pressure Design Analysis-Hartford, Case No. 2

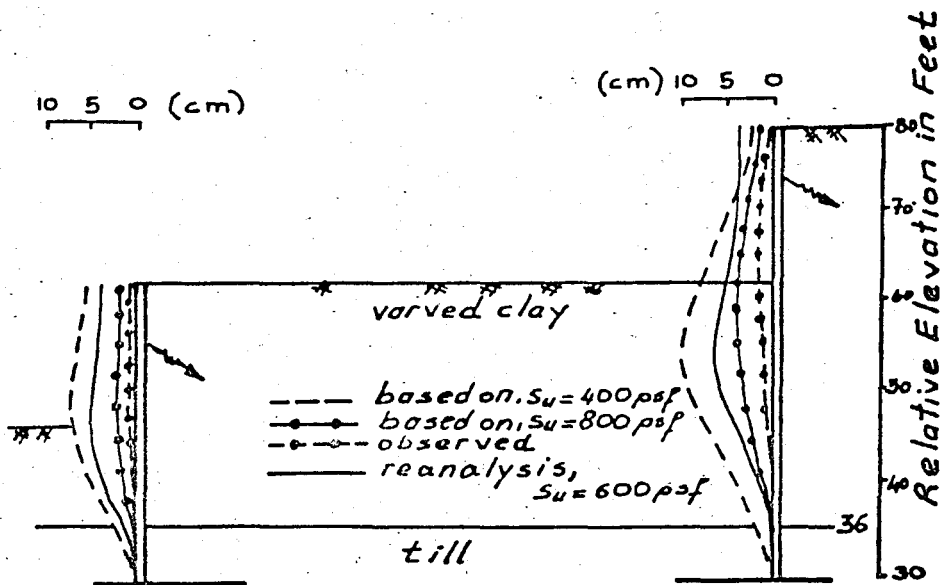


Figure 50. Predicted and Observed Displacements For Two-Tier Excavation Hartford-Case No. 2

It has been noted that the best approximation of wall behavior was obtained by using a higher value for undrained shear strength, thus it means that a greater modulus value was used. The computed earth pressures are shown in Figure 51. It can be seen that these results are very close to the conventional Terzaghi-Peck pressures.

Finite Element Modeling-Bowline Point.(Case No.3)

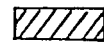
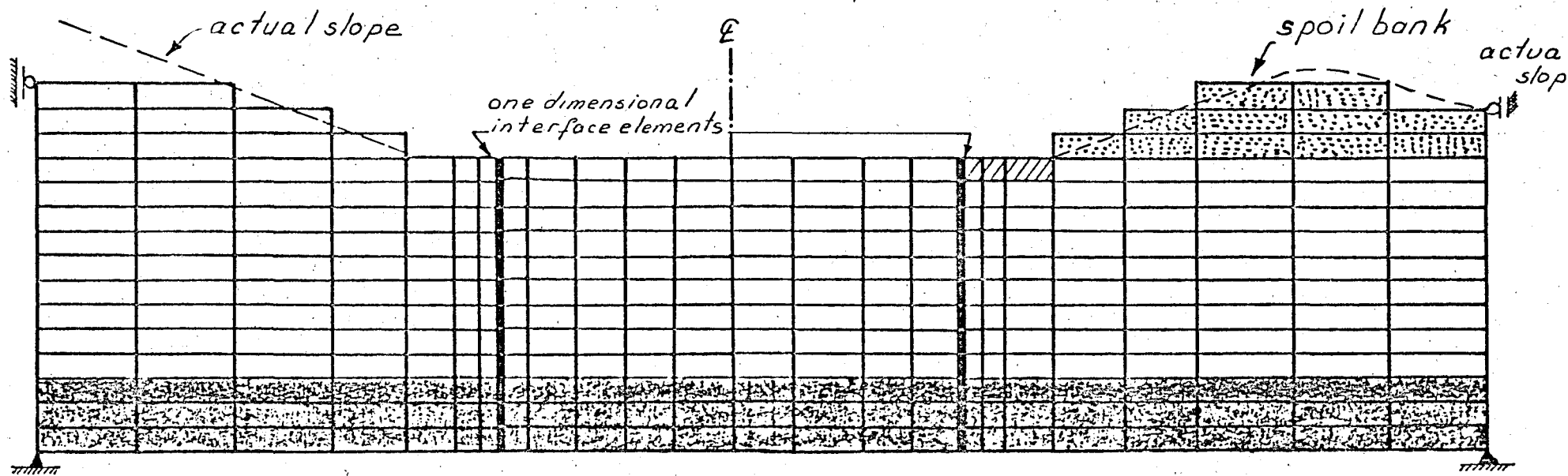
The finite element procedures employed for the analyses of the Bowline excavation were essentially identical to those used for the Hartford analyses. The difference is that in this case, the wall was a sheet pile wall and it was braced rather than tied-back. Continuous walers supported the wall between the struts, thus the planar wall model was assumed to be applicable. The spring supports were used to simulate the behavior of the struts. Their stiffness were taken equal to that of the struts divided by strut spacing.

The 404-element finite element mesh was used in the analyses. Figure 52 shows this mesh, including its boundary conditions and soil types. The mesh allowed for simulation of the original topography of the site as well as the placement of spoil around the site. The analyses reported by Clough, Murphy and Woolwoth are based on a 423-element finite element mesh and performed after the construction was complete. They covered both east-west and north-south axis. In this reanalysis only the north-south axis was considered.

The construction sequences simulated consisted of a series of excavations and brace installations. The braces were simulated in the analyses by means of one-dimensional bar elements connecting the two opposing walls. Vertical constraints were added to the bars to prevent buckling of the bar elements. Figure 53 shows the construction sequence for the north-south axis.

Soil Material Parameters-Bowline Point. The mesh of the analyses consist of mainly two soils: glacial till and varved clay. The glacial till could not be assumed rigid since the excavation was carried into it. $\phi=35^\circ$, and submerged unit weight of 60 pcf (960kg/m^3) were assigned to the till. Using a nonlinear elastic simulation of Duncan-Chang, the till was treated. Initial tangent modulus of 400s_w, poisson ratio values of 0.4 and 0.49 (before and after failure respectively) were used.

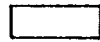
For the spoil fill and shallow failure zone, a shear strength



remolded fill, $S_u = 40$ psf



remolded varved clay, $S_u = 130$ psf



undisturbed varved clay, $S_u = 800$ psf



glacial till

Figure 52. Finite Element Mesh-Bowline Point, Case No. 3

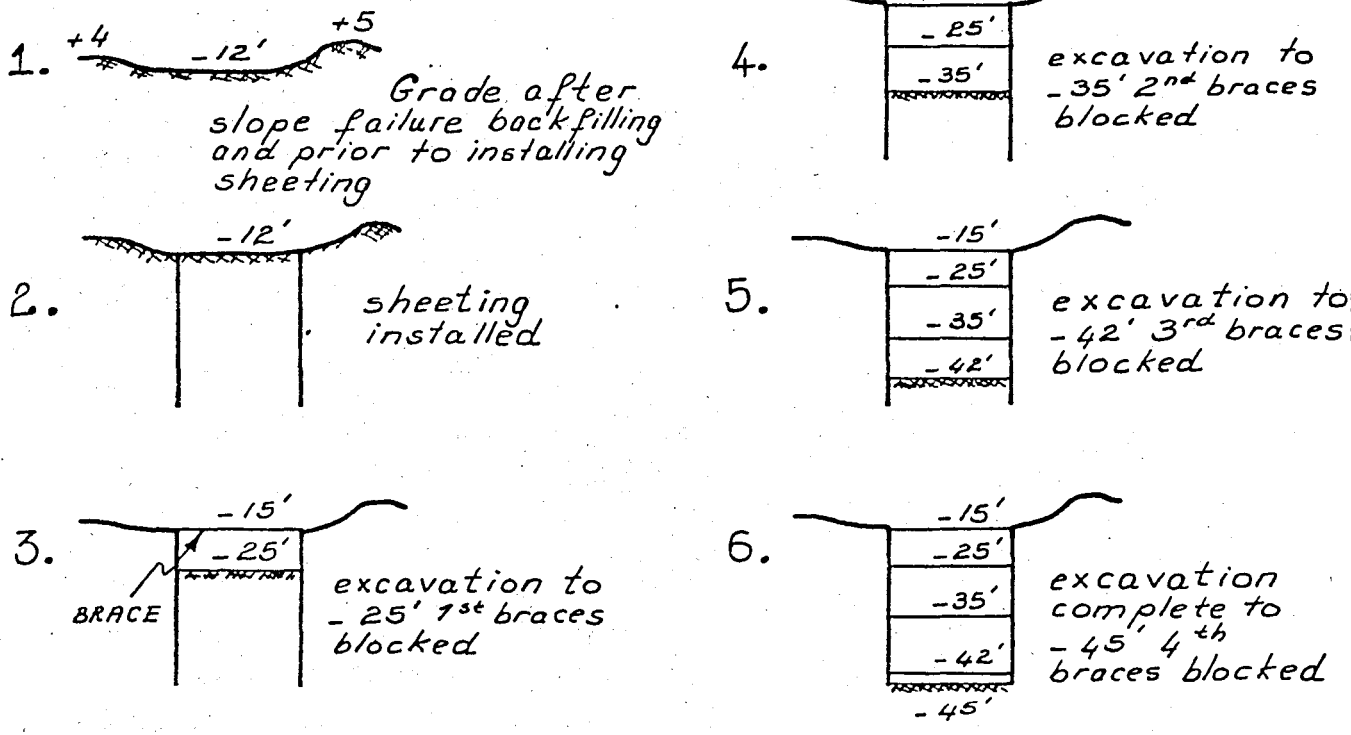


Figure 53. Geometry and Sequence-Bowline Point, Case No. 3

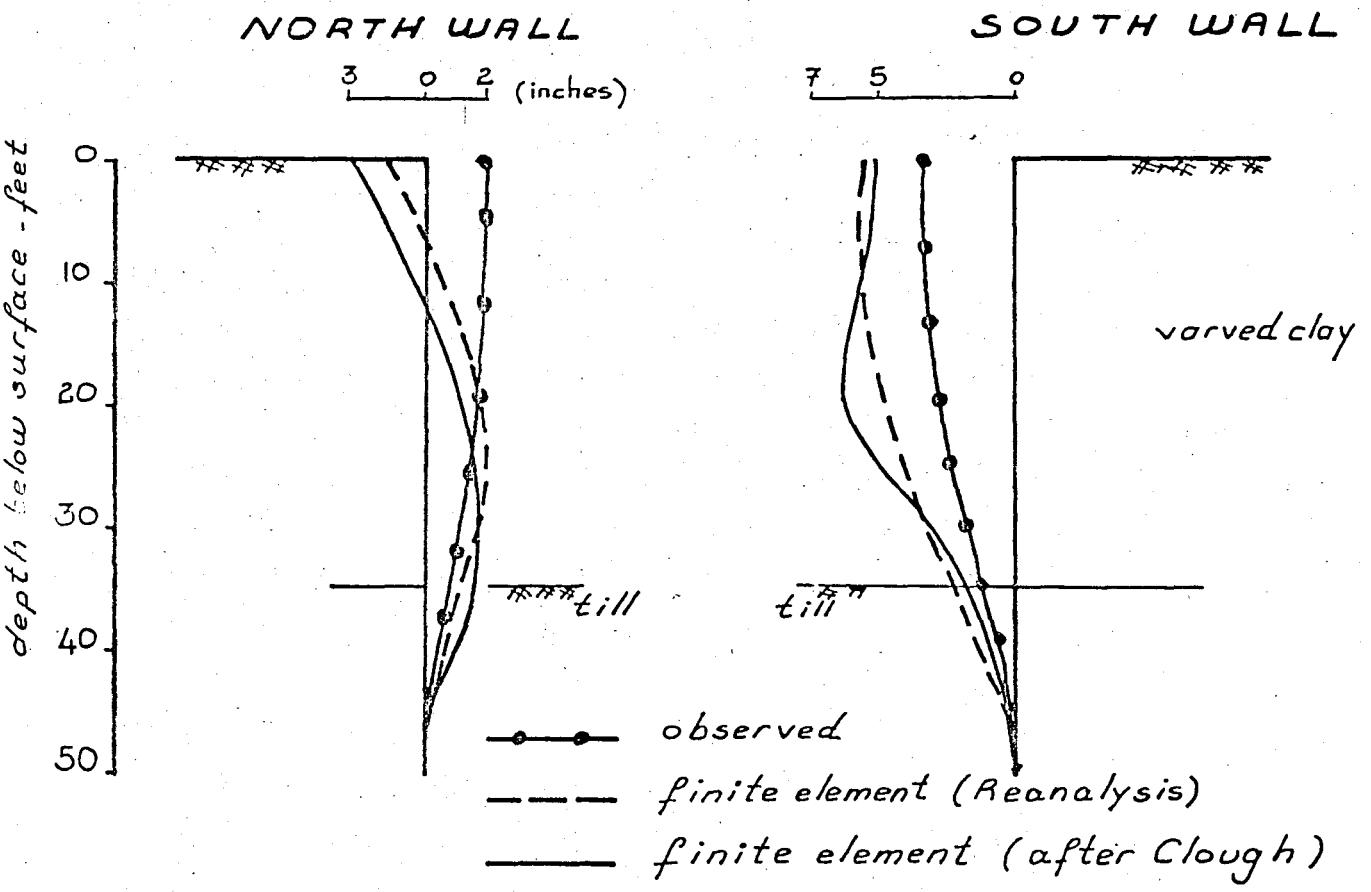


Figure 54. Computed and Observed Displacements-Bowline Point, Case No. 3

of 130 psf (6.5 kN/m^2) was assigned. For the undisturbed varved clay, the parameters used are: s_u 800 psf (40 kN/m^2); K_o 1.0 and E_i 600 s_u . For the small zone of highly disturbed organic fill and clay which was located behind the south wall, a shear strength of 40 psf (2 kN/m^2) was assigned.

Results-Bowline Point. (Case No. 3)

The observed and predicted wall displacements of the two finite element analyses performed are shown in Figure 54. The large lateral movement of the south wall has been observed; the reason of this movement could be related to the presence of a large spoil bank of weak material behind the wall.

The results of both analyses are not found to be satisfactory for the south and north walls. Based upon the results of the reanalyses and those of Clough, Murphy and Woolworth, it has been found that the toe of the south wall had moved and that the south wall was pushing the north wall back into the soil. The reason for this behavior is the failure of the till in front of the wall toe as shown in Figure 55. Unfortunately, it is not possible to simulate this behavior, because the large relative movements required between the wall toe and the underlying soils could not be accommodated in the finite element mesh.

Table 7 shows the observed and predicted strut loads (after Clough). Only, the first three strut levels are shown in this table. Clough had reported that reasonable agreement was obtained between the values of lower struts, but at the first level, the observed values were much higher apparently due to wracking effect observed in the upper wall movement patterns. The existing small differences between the two finite analyses could be related to the differences in simulation of shoring systems and the unequal number of mesh elements.

6.4 SUMMARY

In this chapter, three case history studies were cited and reanalyzed using the same soil parameters and construction sequences of the previous analyses by using a finite element program named "SOIL-STRUCT THE ELDER" developed by Clough, to see the possibility to use this program in similar cases.

Table 7. Strut Loads at end of construction, in kips (kilonewtons), Case No. 3 (after Clough, Murphy and Woolworth, 1975)

Level	Elevation	Observed average loads	Predicted average Loads	
			Clough's Analysis	Reanalysis
1	-15	180 (800)	83 (370)	100 (445)
2	-24	310 (1,380)	312 (1,390)	300 (1,335)
3	-32	265 (1,180)	218 (970)	250 (1112)

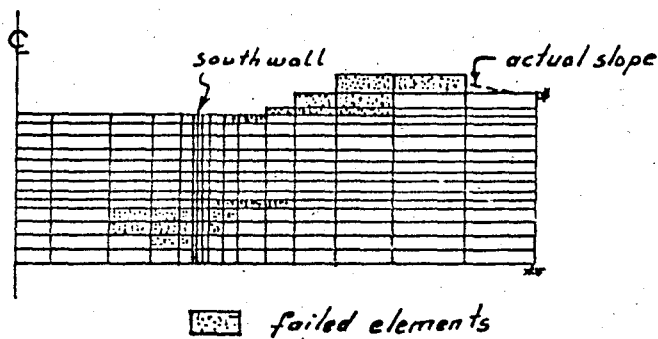


Figure 55. Predicted Failure Zones-South Wall for Bowline Point Case No. 3 (after Clough, Murphy and Woolworth, 1975).

It has been found that a close prediction of the past behavior of the cases was obtained. It must be also noted that the predictions of both Clough's analyses and reanalyses were completely the same: except some little differences were found due to a different simulation method of shoring systems used in the reanalyses.

CHAPTER 7

FACTORS AFFECTING TEMPORARY EXCAVATIONS IN CLAY

7.1 INTRODUCTION

In order to benefit from the advantages of the finite element method in excavations problems, the experienced designer must take care of some important factors which could control greatly the predicted results. The consistent usage and reliable solutions of the finite element method could be obtained by this way.

These factors are the simulation of excavation, the soil modeling, soil parameters and construction variables.

7.2 EFFECT OF METHOD OF EXCAVATION SIMULATION

Most methods used to simulate excavation are designed so that the actual construction sequences can be modeled as closely as possible. An incremental loading procedure is used for this simulation. Each actual excavation step, is simulated by an equivalent distributed force system which is applied to the excavation boundary to reduce stresses on this boundary to zero. This is performed by transforming the distributed boundary loading to equivalent nodal forces and then applying the opposite of these forces to appropriate nodal points. Almost all excavation simulation techniques use this general approach, but they differ in the means for determining the force system to be applied to the excavation boundary.

The method proposed by Clough and Duncan is the most general for lower order elements in which only the center stresses of the elements are known and the boundary forces must be calculated based on this known stresses. This procedure is illustrated in Figure 56. The area to be excavated is shown by dashed lines. Clough and Duncan recommend that stresses on a segment abc, be determined by fitting a nonlinear interpolation polynomial to the stresses at the centers of the four elements adjacent to the abc segment. These elements are shown in Figure 56 as 1-2-3-4.

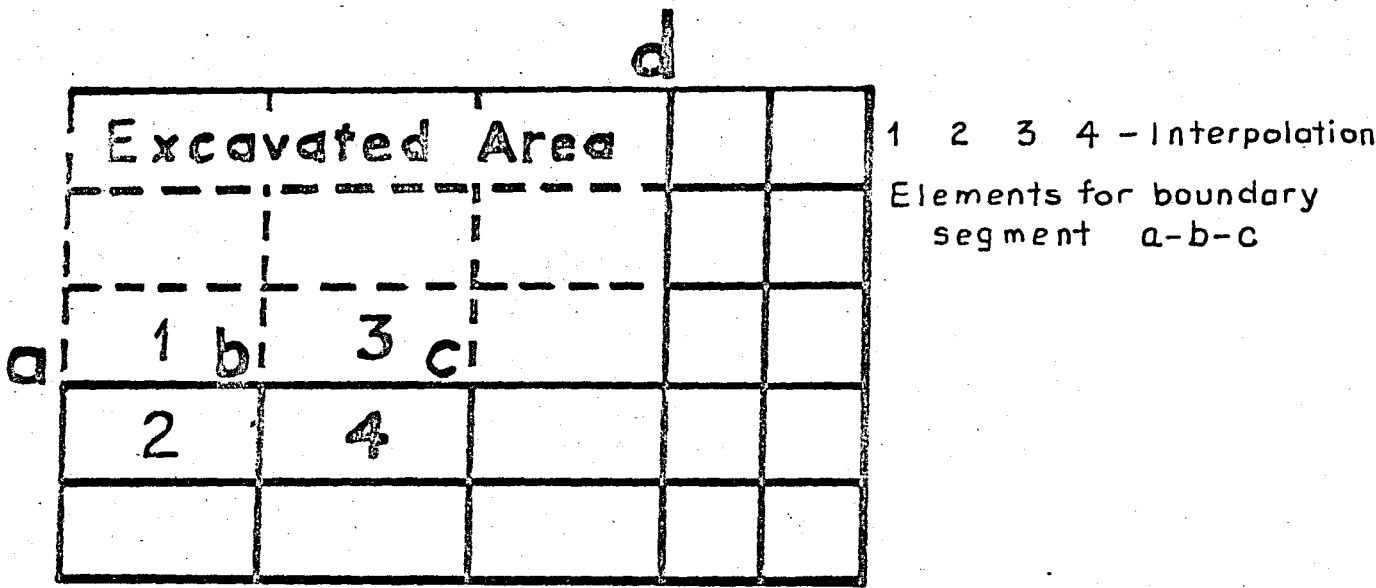


Figure 56. Determining Boundary Stresses For Excavation By Interpolation (after Clough, 1972).

Then, the polynomial is used to calculate stresses on the excavation boundary and equivalent nodal forces are determined and applied to the boundary in the reversed sense.

This method has been shown to be satisfactory for a wide variety of excavations, but the four interpolation elements must be chosen appropriately when corners or discontinuities in materials are encountered.

If a higher order element is used (linear strain or above) stresses at each node of an element could be calculated. This allows direct determination of stresses on an excavation boundary. However, it is theoretically known that these stresses are not reliable and that the most accurate stresses are those determined at interior Gaussian integration points. Thus the desirable procedure is to calculate boundary forces from the interior points. Mana (1975) has proposed a method of this type. The equivalent excavation boundary forces are found, for an eight node isoparametric element, as:

$$\{F\} = \sum_{m=1}^M \int_V [B]^T \{\sigma\} dV \quad (7.1)$$

where: M = number of elements which have a common boundary with unexcavated elements.

$[B]$ = displacement-strain matrix

$\{\sigma\}$ = stress vector

$\{F\}$ = vector of nodal forces

The integral is evaluated numerically using values of $\{\sigma\}$ and $[B]$ at the Gaussian integration points.

Figure 57 shows a problem in which a comparison of both methods was made. These are the results of the finite element analyses using the scheme proposed by Clough and Duncan for lower order elements and that proposed by Mana for higher order elements. The problem was an excavation into a linear elastic mass in first one and then three steps. Since the media is elastic, the predicted behavior from either one or three step analyses should be the same. Clough and Duncan in their analysis have used a four node isoparametric element.

The predicted shapes of deflected vertical boundary for both

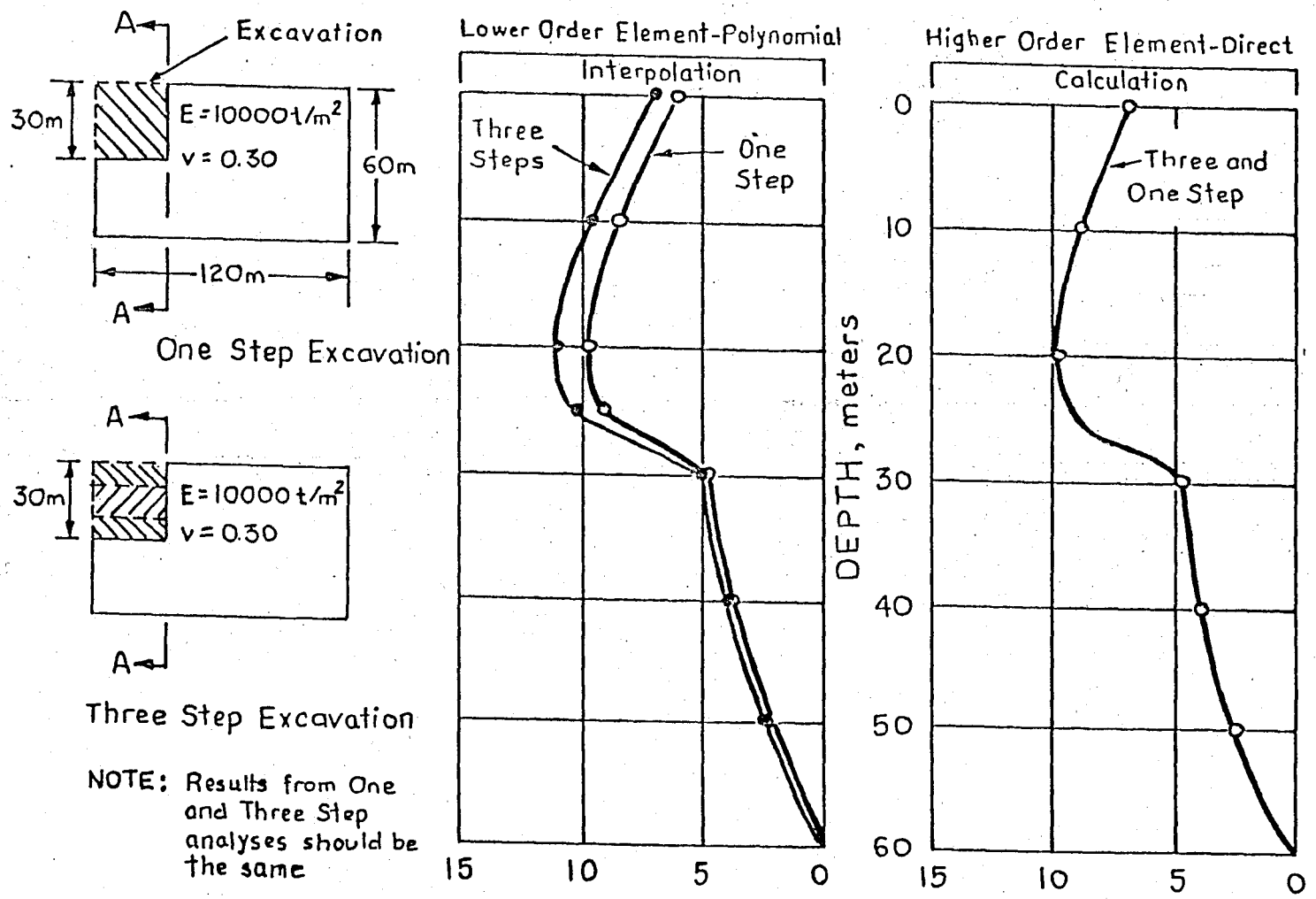


Figure 57. Predicted Movements Using Different Excavation Simulation Procedures (after Clough, 1975).

three and one step analysis using different procedures are given in Figure 57. There exists small differences in the deflections obtained by using a four node isoparametric element, but the approach of Mana is perfect. Therefore, it is recommended that the technique developed by Mana should be used in excavation problems.

7.3 EFFECT OF SOIL MODELING PROCEDURE

There are many methods for modeling stress-strain behavior of soils. Elastic, nonlinear elastic and elasto-plastic models have been employed in the studies of excavations.

The nonlinear elastic model allows the soil modulus to be adjusted consistently with the shear stress levels in each element. The form of the stress-strain curve is assumed to be hyperbolic up to failure, then, the shear modulus is reduced to near zero. The elasto-plastic model assumes plastic behavior until yielding; plastic deformation occurs thereafter upon further loading.

It has been shown that for practical problems, if appropriate soil parameters can be chosen, the type of soil modeling technique will not significantly influence predicted behavior.

However, it is important to note that the magnitudes of the elastic moduli needed for accurate modeling of observed behavior are significantly influenced by the soil modeling technique. Initial tangent modulus values are needed to define the initial slope of the stress-strain curves, if a nonlinear elastic model is used. On the other hand, the elasto-plastic model uses a single straight line stress-strain function until yielding is reached. Here, the stress-strain curve up to yielding can be represented by a secant modulus value. Clough has shown that in order to obtain agreement between observed and predicted wall deformations of San Francisco excavation shown in Figure 58, two different modulus values are needed to represent the two different soil modeling technique used in this problem. An initial tangent modulus value for the Bay Mud equal to $1200 s_u$ was used for the nonlinear elastic model while a secant modulus value of $360 s_u$ was used for the elasto-plastic model. It can be seen that, the magnitudes of the input modulus values for the two soil model were different by a factor of four. Therefore, depending upon the soil model employed, best modulus values must be choosed.

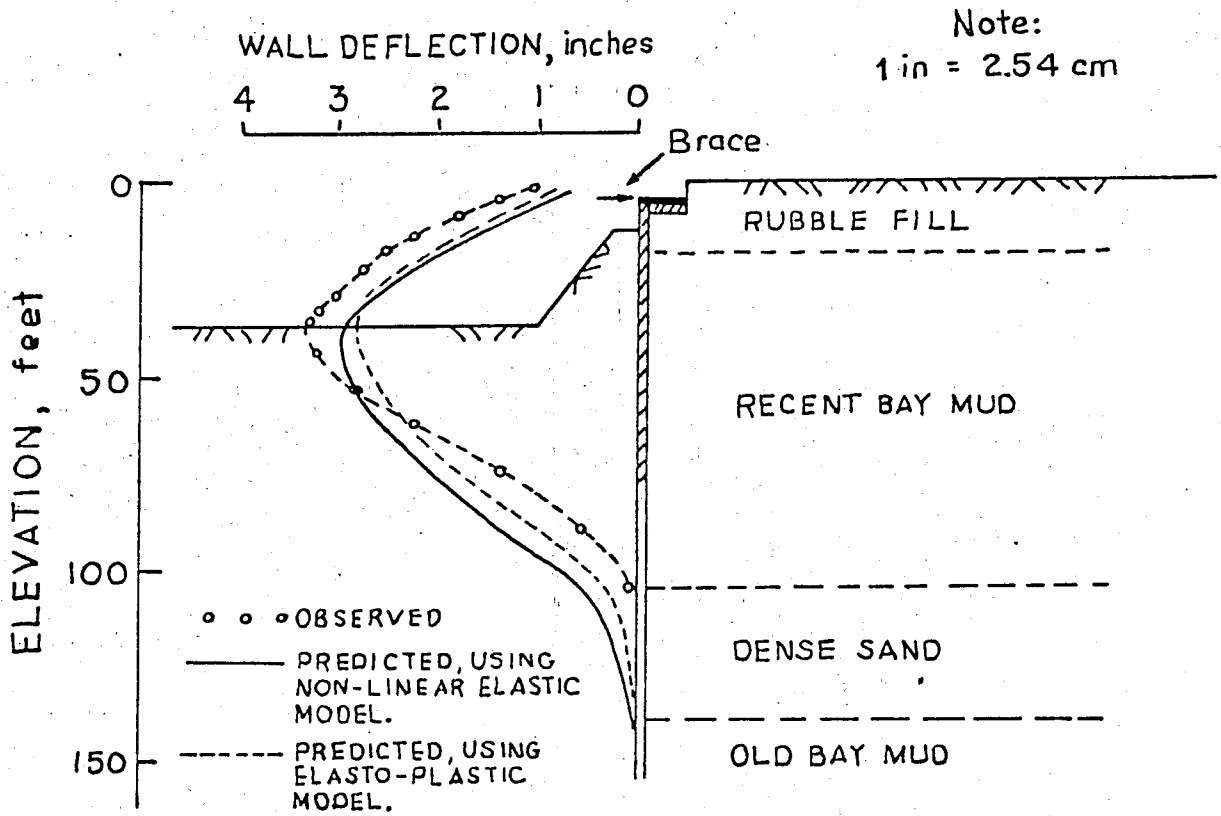


Figure 58. Comparison of Observed Excavation Deflections to Values Predicted Using a Nonlinear Elastic Model and an Elasto-Plastic Model (after Clough, 1975).

7.4 PROBLEMS IN SELECTING SOIL MODEL PARAMETERS FOR DESIGN

The number of parameters needed to describe a soil model is a function of the complexity of the model; the most desirable model is the one which needs a little number of parameters to be defined to simulate a reliable soil behavior.

The nonlinear elastic model requires the following parameters if it is the case of the undrained loading of soft, saturated clays;

K_0 - coefficient of lateral earth pressure

S_u - undrained shear strength

E_i - initial tangent modulus

E_{ur} - unload-reload modulus

R_f - curve fitting parameter

Because R_f usually is an easily defined constant and E_i and E_{ur} are typically about equal in undrained loading, the parameter selection problem reduces to three values K_0 , S_u and E_i . If the clay is near normally consolidated, K_0 is a relatively easy defined constant. The determination of S_u and E_i is the most difficult part of the soil parameter identification.

The design shear strength has a significant influence on predicted behavior. The difficulties in choosing the appropriate value of S_u come from two main reasons. The first one is the scatter in test results. The scatter is likely in part due to natural causes as well as experimental related problems. The second difficulty is in evaluation whether or not allowance should be made for disturbance effects which would lead to selection of higher values than indicated by data.

The determination of the initial tangent modulus is more difficult than the shear strength, since data scatter is typically greater and disturbance effects more substantial. The increase of the modulus with increasing value of shear strength might be expected based on fundamental concepts. For soft clays, the initial tangent values determined from laboratory test results are too low because of disturbance effects. This determined values must be corrected. The wrong assumed variations of modulus values can lead to large differences in predicted results. Reported studies and results of many laboratory tests point out that laboratory based modulus values and shear strengths are far too low.

Bowline Point and Hartford excavations in soft clays prove that this assumption is correct. Obviously, it is possible to adjust the modulus values obtained from standard undrained triaxial testing. But then the question becomes, "how much higher?", and the answer must depend upon many factors, such as type of clay, amount of over-consolidation of the clay, sensitivity of the clay and quality of test procedures. A modulus value based on 600 to 800 s_u seems to give representative predicted movements. This value is highly based on case history studies, but how general this finding is remains to be seen.

Thus, to feel fully confident in finite element predictions, may not be satisfactory for an engineer without additional means of corroborating the results.

7.5 PROBLEMS INTRODUCED BY CONSTRUCTION VARIABLES

Construction variables represent unanticipated construction problems or changes which affect excavation behavior. These events are relatively common due to nature of the temporary excavations. These are;

1-The contractor falls behind schedule or finds a particular concept unworkable and changes the sequence of construction and even the shoring system.

2-Surcharge loads are placed in locations not expected.

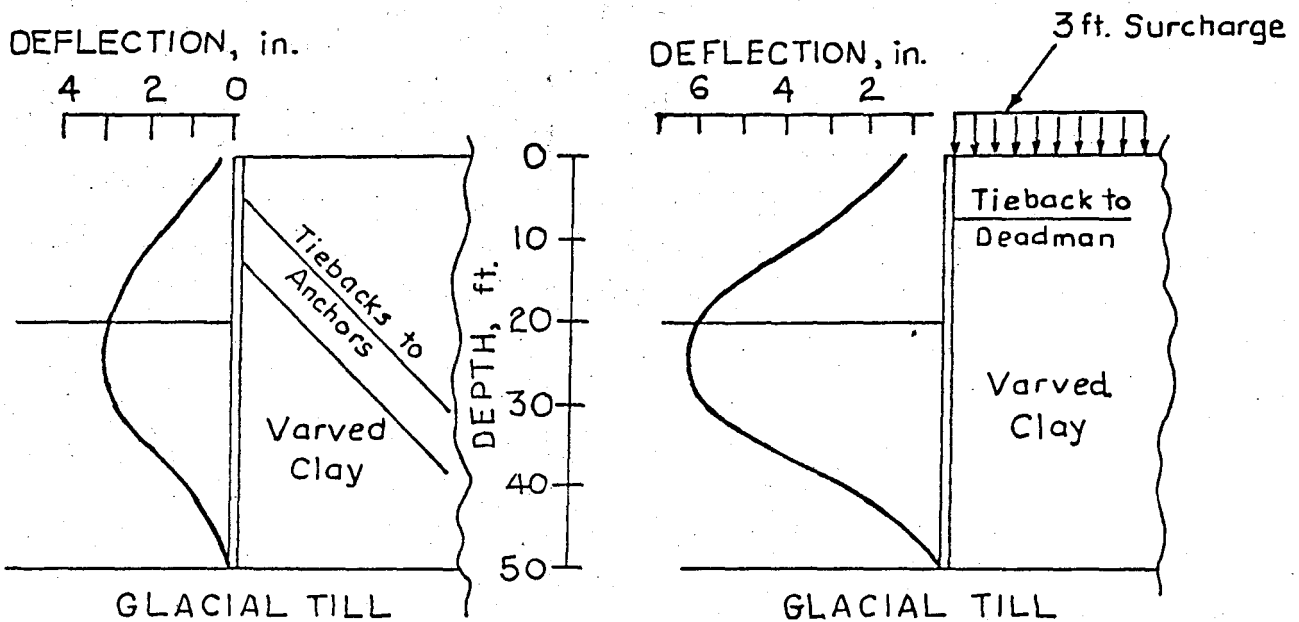
3-The temporary excavation platform is overexcavated before brace installation.

4-Improper installation of anchors.

These and many other sometimes seemingly small details have been known to modify excavation performance drastically.

An example showing the effects of one such incident on finite element predictions occurred in Hartford, Connecticut. It has been reported that during the excavation which was to be made into soft varved clay, the support system was originally intended to be a soldier pile and lagging wall. The wall is tied-back with two levels of inclined tie-backs anchored into an underlying till layer. However, early into the project, the contractor sought and was granted two changes. The first one was the placement of a surcharge loads of up to one meter of fill. The second one was the change in anchorage system such as a single deadman anchor system could be used

Note: 1 in = 2.54cm



(a) Original Prediction, Intended Design, $S_u = 400$ psf

(b) Predicted Behavior Changed Construction Conditions, $S_u = 400$ psf

Figure 59. Predicted Wall Deflections, Hartford Excavation, Showing Effect of Construction Changes on Prediction (after Clough, Murphy and Woolworth, 1975).

in lieu of the dual inclined anchor system. Clough has reported that by repeating the finite element analyses and accommodating the changed construction conditions, the predicted maximum wall deflection, as shown in Figure 59, is 15 cm, a 100 percent increase over the original prediction. Thus, construction variables contribute an additional unknown element whose effects on behavior can lead to inaccurate conclusions from finite element predictions.

7.6 SUMMARY

In this chapter, factors affecting temporary excavations in soft clay were described; these are, the method of excavation simulation, the type of soil modeling, soil parameters and construction sequences.

It must be noted that the above mentioned factors are to be considered as controlling parameters of primary importance during the analyses of excavations; and every small change on them must be reflected to predicted results. Improvements or reanalyses must be made, if necessary.

CHAPTER 8

CONCLUSION

As has been illustrated thus far, excavation in soft clays requires a detailed investigation program in order to be solved by using a finite element analysis. The experience and reported case history studies have been found to be very useful to obtain reasonable predictions in excavation problems. Since the state-of-the-art is not well established in this area, additional care must be given to obtain a satisfactory and complete analysis.

Also, the problems involved in defining soil parameters and construction sequences make "pure prediction" of the behavior of temporary excavations by finite element analysis very difficult. In certain instances it may be possible, but in general this will not be the case. (Lough and Mana provide an observational approach which obviates many of the questions shrouding the "pure prediction" technique. The proposed method consists of the following steps:

1-The project is studied carefully so as to produce reasonable estimates for soil profile and ground water table location. Laboratory tests are performed on representative soil samples. An expected construction sequence is established.

2-Using the best available information and a relatively simple model, an incremental finite element analysis is performed. Acceptably conservative soil parameters are employed in the analysis. The results of the analysis are viewed as preliminary and subject to modification.

3-The project is instrumented so that deflections of the wall system and soil mass can be measured. Initial excavation is made and at this stage soil conditions and construction sequences are examined to determine if any changes exist relative to those assumed in the analyses.

4-Following step 3, a reanalysis of the problem is undertaken if:

a-Soil conditions or construction sequences are different from

those assumed in the original analysis.

b-The observed soil and wall deflections are different from those predicted.

5-In the reanalysis, any changed conditions are accommodated and soil parameters are adjusted consistent with the comparison of predicted and observed behavior, e.g., if initial predicted deflections are too large, soil stiffness and/or strength is increased. Adjustments in the parameters are made until an analysis yields agreement with the early observed behavior, and when agreement is obtained in the early stages, the predictions for the final stages should represent accurate values.

6-Careful control is maintained during subsequent construction to insure that no further deviations occur in assumed soil conditions and construction sequences.

The above described procedure if properly used should lead to accurate and reliable predictions of excavation behavior, by using a finite element method.

The following conclusions can be drawn from the results of case history studies and the laboratory tests on "full-scaled" specimens.

It has been shown that, the simulation of excavation in a finite element analysis can be done by a number of different, but satisfactory procedures. To be accurate, in the calculation of excavation forces, direct calculation technique using higher order elements seems to be the best one but also a four node isoparametric element should be also satisfactory but it requires more data to specify the excavation sequences.

Using either a nonlinear elastic or elasto-plastic soil model the temporary excavation behavior in soft clays can be reasonably simulated. With the appropriate soil parameters, either model can be made to lead to the same predicted excavation behavior.

In general, for soft clays, the values of shear strength and tangent modulus are difficult to predict. For finite element studies these factors have a primary importance in the predicted movements. These parameters are particularly crucial to temporary excavation studies because of the direct variation of critical soil settlements with them.

Disturbance effects in laboratory testing apparently lead to significant reductions in measured soil modulus values. This, in turn leads to significant overpredictions of excavation movements by finite element analyses relying solely on laboratory test results. An adjustment of these parameters should be made based on the results of case history studies.

It has been found that the predicted results of case history studies could be obtained by using a mesh composed of smaller number of elements than those of the original analyses. But in design stage, great care must be given to the selected element configuration.

Changes in excavation sequences or support system design often take place during construction, this lead to unanticipated performance. A continuous contact should be maintained between the contractor and the designer in order to control the progress of the excavation. Isolation of the finite element analysis from the actual stages of construction can lead to false predictions.

By considering all the above mentioned parameters, it must be stated that the program used in this thesis closely predicts the results obtained by previous studies: thus, it is possible to use this program to predict behaviors of future similar excavations in clays.

Because of difficulties in selecting soil parameters and anticipating construction changes, the finite element analysis should be incorporated into an observational procedure. This allows for reanalyses to be performed so as to accomodate better soil parameter estimates and construction changes.

When properly utilized, a finite element analysis can be expected to give useful design information and reliable performance predictions for temporary excavations in soft clays.

REFERENCES

- 1-Browzin, B.S., "Anchored Bulkheads: Horizontal and Sloping Anchors", *Journal of Geotechnical Division, ASCE*, Vol. 107, No. GT 5, May, 1981, pp. 629-644.
- 2-Clough, G.W. and Duncan, J.M., "Finite Element Analyses of Port Allen and Old River Locks", "Contract Report S-69-6, U.S. Army Engineer Waterways Experiment Station, Corps of Engineers, Vicksburg, Mississippi, September, 1969.
- 3-Clough, G.W., Weber, P.R. and Lamont, J., "Design and Observation of a Tied-Back Wall," *Proceedings of the Specialty Conference on Performance of Earth and Earth-Supported Structures, Purdue Univ.*, Vol. 1, Pt. 2, June, 1972, pp. 1367-1390.
- 4-Clough, G.W. and Reed, M.W., "Measured Behavior of Braced Wall in Very Soft Clay," *Journal of the Geotechnical Division, ASCE*, Vol. 110, Jan., 1984, pp 1-18.
- 5-Clough, G.W. and Hansen, L.A., "Effects of Clay Anisotropy on Braced Wall Behavior," *Journal of the Geotechnical Division, ASCE*, Vol. 107, No. GT 7, July, 1981, pp. 893-914.
- 6-Clough, G.W., Murphy, D.J. and Woolworth, R.S., "Temporary Excavation in Varved Clay," *Journal of the Geotechnical Division, ASCE*, Vol. 101, No. GT 3, March, 1975, pp 279-295.
- 7-D'Appolonia, D.J., Poulos, H.G. and Ladd, C.C., "Initial Settlement of Structures on Clay," *Journal of the Geotechnical Division, ASCE*, Vol. 97, October, 1971, pp 1359-1377.
- 8-Duncan, J.M. and Chang, C.Y., "Nonlinear Analysis of Stress and Strain in Soils," *Journal of the Soil Mechanics and Foundations Division, ASCE*, Vol. 96, No. SM5, Proc. Paper 7513, September, 1970, pp 1629-1653.
- 9-Peck, R.B., Hanson, W.E. and Thornburn, T.H., *Foundation Engineering*, 2nd ed., John Wiley and Sons, Inc., New York, N.Y. 1974.
- 10-Schroeder, W.L., and Roumillac, P., "Anchored Bulkheads with Sloping Dredge Lines," *Journal of Geotechnical Division, ASCE*, Vol. 109, No. GT6, June, 1983, pp. 845-851.
- 11-Stroh, D., "Discussion-Performance of Tied-Back Walls in Clay," *Journal of Geotechnical Division, ASCE*, Vol. 101, No. GT8 August, 1975, pp 833-836.
- 12-Tsinker, G.P., "Anchored Sheet Pile Bulkheads: Design Practice" *Journal of Geotechnical Division, ASCE*, Vol. 109, No. GT8, Aug. 1983.

APPENDIX A

FINITE ELEMENT MESH DESIGN

In the incremental analyses of excavation problems, the geometry of the problem was continually changing with each increment: however, only one finite element mesh was employed for each problem by designing the mesh to account for the initial geometry, excavation geometry and geometry during anchor installation. Alterations to the mesh for each increment were accomplished by changes of material properties for the appropriate elements, e.g., excavated elements were assigned very low values of modulus to represent air, and reassigned concrete modulus values to simulate placement of concrete.

In addition to the geometry of the mesh, there are a number of other considerations in designing the finite element mesh for an excavation study, including the following:

- 1-Number of elements required to appropriately represent the excavation for the purposes of obtaining satisfactory values of deflections.

- 2-Location of lateral boundaries

- 3-Accounting for the presence of interface elements during initial and excavation phases.

These considerations are discussed in subsequent sections of this appendix.

Number of Elements

In order to minimize the amount of computer time required for the analyses, it was desirable to minimize the number of elements employed for the problem; however, it was also desired to use a suitable number of elements so that an acceptable degree of accuracy could be attained in the structural deflections and stresses. The degree of accuracy that may be obtained in simulating a particular mode of behavior with a given number of finite elements of a particular type depends upon how closely the displacement pattern assumed in developing the element stiffness corresponds to the particular mode of behavior desired.

Locations of Lateral Boundaries

In cases of excavation problems, it was desirable to locate lateral boundaries so that they would have a negligible effect on the excavation behavior. Because in most cases the centerline of the excavation was a line of symmetry along which deflections would be vertical, this line of symmetry was taken as one of the lateral boundaries and was represented by a line of rollers which prevented horizontal movements but allowed vertical movements. However, the other boundary had to be located a sufficient distance away from the excavation so that its influence on the behavior of the wall was negligible.

Interface Elements

Because the finite element mesh was designed to account for the completed geometry of the excavation as well as the initial and intermediate geometries, provisions had to be made to include the interface elements for all of these conditions. However, for initial and excavation conditions, the interface elements had to behave as if they were not present.

Before excavation, an interface element between any two two-dimensional elements should have been "inactive" and merely served to maintain nodal point compatibility, i. e., not to allow any relative movement between adjacent elements. To satisfy this requirement, the normal and shearing stiffnesses were assigned very large values, as shown in Table 8.

After excavation of an interface element and the adjacent two-dimensional elements, the interface element should not induce any interaction with the newly placed materials until the adjacent two-dimensional elements are placed. For this condition the very low stiffnesses shown in Table 8 were employed.

Upon and after activation, the interface elements may have four additional possible sets of stiffness values, as shown in Table 8. These stiffness values represent the following conditions:

- 1-The interface between the rigid concrete and the newly placed "liquid" backfill layer.
- 2-The interface under normal conditions.
- 3-The interface upon shear failure.

Table 8. Stiffness Values For Interface Element Under Inactive and Active Conditions. (after Clough, 1969).

Condition	Status	k_s lb./cu. ft.	k_n lb./cu. ft.
Inactive	Between Solid Elements	1×10^{11}	1×10^{11}
	Between Excavated Elements	1×10^{-3}	1×10^{-3}
Active	Between Concrete and Newly Placed Layer	1×10^{-3}	1×10^9
	Normal Operation	As Calculated	1×10^9
	Shear Failure	1×10^{-3}	1×10^9
	Tension Failure	1×10^{-3}	1×10^{-3}

-125-

4-The interface upon tension failure.

Shear failure of the interface element usually occurred only during the placement of the few layers immediately above the element. In fact, it has been found that every interface failed upon the placement of the first layers immediately above, and that for this condition the "overshoot" of the allowable shear stress was very large. This indicated that the full friction was being developed under these initial conditions.

It is economical to extend the vertical interface elements through the whole mesh. This allows the numbering of the nodal points in the vertical direction would be continuous, resulting in a smaller set of equations to be solved for each analysis and thereby resulting in a savings in computer time. The interface elements which were located between adjacent two-dimensional elements of the same material were kept in an inactive condition throughout the analysis.